Theory for dynamical self arrest and gelation in microemulsions and the block copolymer systems

by

Sangwook Wu

A dissertation submitted to the graduate committee

in partial fulfillment of the requirements for the degree of

DOCTOR OF PHILOSOPHY

Major: Condensed Matter Physics

Program of Study Committee:
Joerg Schmalian, Major Professor
Paul Canfield
James Evans
Kai-Ming Ho
Janwei Qiu

Iowa State University

Ames, Iowa

2005

Graduate College
Iowa State University

This is to certify that the doctoral dissertation of

Sangwook Wu

has met the dissertation requirements of Iowa State University

_____

Major Professor

_____

For the Major Program

DEDICATION

I would like to dedicate this thesis to my wife Annie Moon and to my two sons Hyunjun and Hyunsung without whose support I would not have been able to complete this work. I would also like to thank my friends and family for their loving guidance and financial assistance during the writing of this work.

TABLE OF CONTENTS

LIST OF FIGURES

CHAPTER 1. INTRODUCTION

In case of many supercooled liquids, when the temperature is decreased rapidly from the liquid state, a glass rather than the crystalline solid forms. When the temperature approaches the glass transition temperature T_g, the viscosity of the system reaches an extremely large value($\sim 10^{13}$ Poise). Traditionally, two different approaches are adapted for explaining this nonequilibrium glassy behavior, a thermodynamic approach and a kinetic approach.

In the thermodynamic approach, the glass transition temperature is determined by analyzing thermodynamic variables such as the specific volume,the specific heat or the entropy. Fig. 1.1 shows the entropy versus temperature. Below the melting temperature T_M, rapid quenching leads to a supercooled liquid instead of a crystal. The limit of supercooling of a liquid is attained when the entropy of the liquid becomes equal to the entropy of the crystal. For a typical glass forming liquid, below this limit, we encounter an "entropy crisis": the entropy of the liquid becomes lower than the entropy of the crystal. (1) This limit temperature of supercooling, T_K, is called "Kauzmann temperature". In other words, the Kauzmann temperature T_K is a thermodynamic limit for the glass transition. The actual glass transition, where the viscosity becomes extremely large(typically 10^{13} Poise), happens before T_K.

One of the prevailing kinetic approach to glassy behavior is the mode coupling theory (MCT). (2) (4) In MCT, the glassy behavior emerges from ergodicity breaking. In ergodic phases such as an equilibrium liquid, the system can explore the entire phase space. However, in nonergodic phases such as a glass, the system is trapped in one of the local minima. Ergodicity breaks down. When we define the Fourier transform of the correlation function of density fluctuations $F_{\mathbf{q}}(t) = \lim_{t\to\infty} \frac{1}{T} \langle \rho_{\mathbf{q}}(t)\rho_{-\mathbf{q}}(0)\rangle$, the criterion for glassiness is

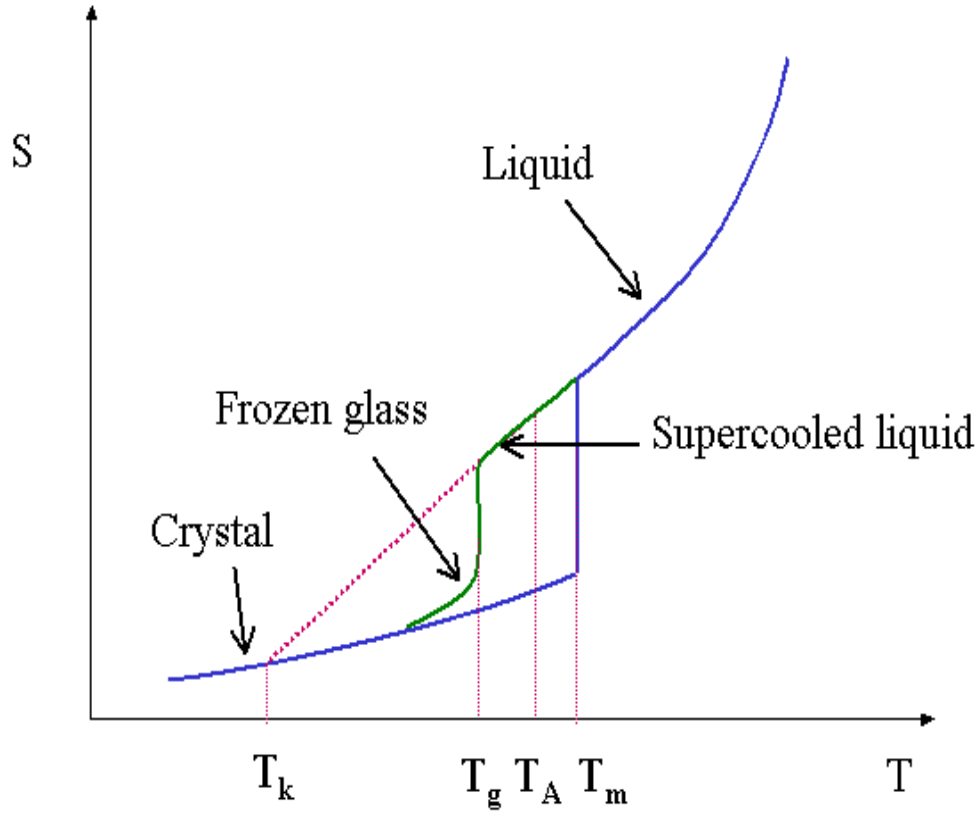

Figure 1.1 Entropy versus temperature. T_K and T_m are Kauzmann temperature and melting temperature respectively. Below T_K, we encounter an "entropy crisis", the so called "Kauzmann paradox".

$$\lim_{t\to\infty} F_{\mathbf{q}}(t) = 0, \text{ liquid}$$
$$\lim_{t\to\infty} F_{\mathbf{q}}(t) \neq 0, \text{ glass} \tag{1.1}$$

MCT theory predicts the temperature T_A, at which dynamical self arrest sets in. At the temperature T_A, the viscosity η has a power law of divergency $\eta \sim |T - T_A|^{-\gamma}$ and the barrier between local minima diverges. (3) In general, the temperature T_A is not identical to the actual glass temperature T_g. Rather it is known that $T_A > T_g$, which means below T_A, activated relaxation, ignored in the MCT, still continues and the system finally falls out of equilibrium at T_g.

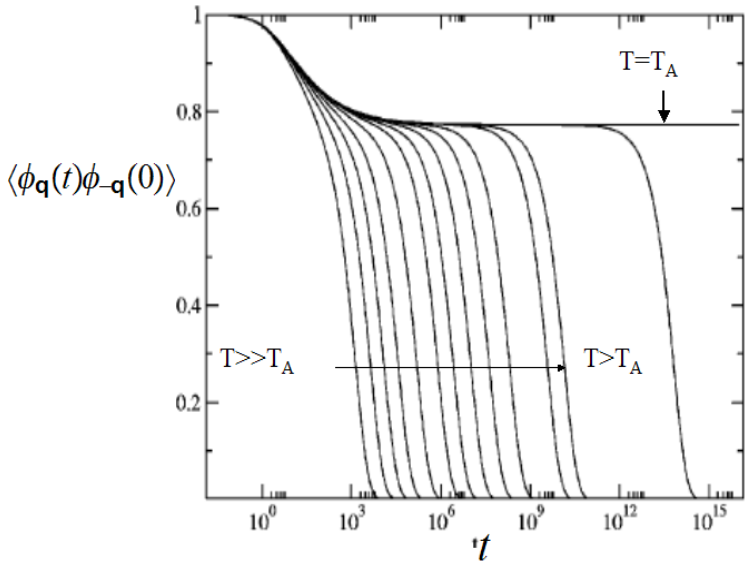

Figure 1.2 Time dependence of the correlation function obtained using mode coupling theory for a 3-dimensional Coulomb frustrated Ising ferromagnet (5)

Fig. 1.2 shows density fluctuation function $F_{\mathbf{q}}(t)$ versus time. At higher temperature, $T >> T_A$, the correlation function $F_{\mathbf{q}}(t)$ shows a simple exponential decay. At $T > T_A$, the correlation function $F_{\mathbf{q}}(t)$ shows a slow decay to make a plateau, which demonstrates the slow

dynamics of particles trapped in the cage of its nearest neighbors. As time increases, the trapped particles finally escape from the cage and decay to zero. At $T = T_A$, the density fluctuation function $F_{\mathbf{q}}(t)$ does not decay to zero and saturates into a non-zero value at our laboratory time scale. The particles are arrested kinetically in the cage of nearest neighbors. In the viewpoint of statistical mechanics, ergodicity break down at $T = T_A$. In MCT, the glass transition is a dynamical transition from ergodic phase into nonergodic phase. (5) (4) (3) The dynamic and thermodynamic descriptions of glasses are not contradictory description of glassy physics. It has been shown that the MCT temperature T_A is precisely the same temperature, where an exponentially large number of metastable states emerges, leading to an extensive configurational entropy. Thus, the self arrest at T_A has a clear meaning in terms of the thermodynamic description of glass.

The problem in the theory of glass is that the theoretical description of classical liquids with strong hard core repulsion leads to major difficulties to perform controlled calculation for either the liquid and glassy state of these systems. However, a number of "soft materials" also show glassy behavior but allow a more controlled theoretical description. For example, major progress of the equilibrium theory of microemulsions and block copolymers has been made during last decade. Based on these results, a theory for glassy behavior of such system will be developed in this thesis.

A microemulsuion consist of oils, waters and surfactants. Oil and water phase separate at low temperatures, an effect which can be altered by adding amphiphilic surfactant molecules like soap or lipids. Depending on the nature of the surfactant and its volume fraction, complex inhomogeneous structures occur. (8) These are caused by the competition between short-ranged forces between oil and water, favoring the separation of uniformly condensed phases, and stoichiometric constraints due to the surfactant which energetically frustrate this separation. Examples of such structures are emulsions, which are non-equilibrium colloidal suspensions, and microemulsions in which oil and water are intertwined in complex structures but are at equilibrium with respect to overall phase separation. The former consist of macroscopically large droplets or bicontinuous networks of oil and water separated by monolayer interfaces of

amphiphiles. Microemulsions, on the other hand, are composed of self-organized mesoscopic structures often in form of lamellae. These strongly correlated fluids are of great scientific and technological interest: they present extreme materials properties, like ultra-small surface tensions. Related phases are essential for the stability of cell membranes, formed by phospholipid molecules; applications of range from medicine to biomolecular assemblies such as the Golgi apparatus, to food science in the preparation of sauces, and to petroleum industry, just to name a few prominent examples. Many of the mesoscale structures found in these amphiphilic systems are extremely long lived while the macroscopic mechanical properties may resemble those of a soft solid, as in "stiff mayonnaise". Sometimes this may arise from phases with true broken translation symmetry, like smectics. In other cases the system may not exhibit any clear broken symmetry. The latter would then be analogous to a glass. Light and neutron scattering reveal the hallmarks of glassy motions also on the mesoscopic scale of a variety of amphiphilic assemblies. (9) (10) (11)

Block copolymer systems, i.e. macromolecules built of sequences of chemically distinct repeat units so called monomers, are of particular interest due to the phenomenon of microphase separation and the resulting formation of complex ordered structures and change in their macroscopic mechanical properties. (13) (12) (30) (16) For example, a diblock copolymer melts consisting of blocks of A and B monomers are chiefly characterized by the Flory-Huggins parameter

$$\chi = v_{\mathrm{AB}} - \frac{1}{2}\left(v_{\mathrm{AA}} + v_{\mathrm{BB}}\right), \tag{1.2}$$

which characterizes the segregation strength between A and B monomers and is inversely proportional to the temperature. Here, $v_{ss'}$ is a measure for the short distance repulsion between s and s' monomers ($s, s' =$ A or B) in units of $k_{\mathrm{B}}T$. For large enough χ, i.e. at low temperature, phase separation into A-rich and B-rich regions occurs. (12) These regions are limited in size due to the covalent bond between the blocks resulting in the phenomena of microphase separation. Another parameter which determines the behavior of a diblock copolymer is the total degree of polymerization S. For large S, the reduction of the contacts between A and B monomers leads to phase separation due to a loss of entropy. (29) The phase state of a

block copolymer depends on the product of χ and S. (12) In particular, in case of equal length of the A and B blocks, the system develops lamellar order with a period. The transition between the mixed and microphase separated state (lamellar phase) is via a fluctuation induced first order transition originally proposed by Brazovskii. (14) (13) The observation of this transition in poly(ethylene-propylene)-poly(ethylethylene) diblock copolymers of approximately equal persistence length is probably the most convincing experimental verification of the Brazovskii scenario of weak crystallization. (16) Complex inhomogeneous structures in block copolymer system are caused by the competition between short-ranged repulsive forces between monomers, favoring macroscopic phase separation, and long range interaction between different blocks due to a chemical bond which energetically frustrate this macroscopic phase separation. (30)

Telechelic polymer is one of the simple example of associating polymers. Telechelic polymers are comprised of the water soluble chains with hydrophobic end groups. The association between the end groups is due to weak interactions such as hydrogen bonding. (31) (32) The thermoreversible association between hydrophobic end groups leads to aggregates and physical networks. Associating telechelic polymers are of technological importance in cosmetics, and oil recovery and applied to peptide synthesis, enzyme modification and solid rocket propellant. (33) The structure of telechelic polymers has a form of symmetric ABA triblock copolymer with extremely small volume fraction of f. In this telechelic polymer, there is an additional competition between phase separation and molecular association at end groups. (34) Small angel neutron scattering (SANS)and rheological investigation reveals the glassy behaviors in diblock copolymers (16) and in gels. (17) (18) (19)

In the next chapter, the electrostatic model for microemulsions and the density functional theory for block copolymers in equilibrium state will be reviewed. In chapter 3, replica approach for nonrandomness and self-generated glass of Brazovskii model will be discussed. In chapter 4, the nonequilibrium physics of microemulsion and block copolymers, the main result of this thesis, will be discussed.

CHAPTER 2. EQUILIBRIUM THEORY OF MICROEMULSION AND BLOCK COPOLYMER SYSTEMS

2.1 Charge frustrated Ising model for microemulsions

Water and oil are immiscible. They are thermodynamically unstable. When we add a sufficient amount of surfactant, oil and water becomes miscible and forms a thermodynamical stable phase. The surfactant is comprised of a polar head group(soluble in water) and hydrophobic tail group(soluble in oil). The role of the surfactant is to reduce the interfacial energy between water and oil molecules to stabilize two different phases. (8) Water-oil-surfactant systems are called a microemulsions, in which small droplets of water is dispersed in a continuous phase of oil. (20) The various types of microstructure (lamellar, bicontinous and more complex structure) depends on the temperature, the volume fraction and the chemical component of the surfactant f and the pressure, which is shown by low angle X-ray crystallography and small angel neutron scattering experiment. (21) (20)

In this chapter, we will review the charge frustrated Ising model to describe the various phases of a microemulsion. The charge frustrated Ising model is based on the Landau-Ginzburg functional motivated by Stillinger's density functional approach. (22) (24) (23) (25) Also, the Landau-Ginzburg density functional of a charge frustrated Ising model can be derived by local gauge theory. (26) By analyzing the Landau-Ginzburg functional, the various phases of a microemulsion will be investigated as a function of the volume fraction of surfactant f, water-oil size a and the temperature.

The oil-water-surfactant system is described by the charge frustrated Ising model. (23). The frustrated Ising model in zero external field is applied to water-oil-surfactant system with

the same concentration of oil and water molecule. The model Hamiltonian for a microemulsion system is given by

$$H = -\frac{1}{2}\sum_{ij} J_{ij} S_i S_j - \mu \sum_i t_i + \frac{q^2}{2}\sum_{i\neq j} V_{ij} S_i S_j t_i t_j. \tag{2.1}$$

$S_i = \pm 1$ indicates whether a lattice site i is occupied by a polar or hydrophobic species and $t_i = 1, 0$ indicates whether this species belongs to the surfactant molecule. In analogy to the Coulomb interaction, a fictitious positive (negative) charge is assigned to hydrophobic(polar) species of the system. V_{ij} is Coulomb interaction induced by surfactant. The frustrating charge q is given by

$$q = (3/4\pi\beta\rho_s r_s^2)^{1/2}, \tag{2.2}$$

where $\beta = 1/kT$ and ρ_s is the number density of surfactants. r_s is the typical distance between hydrophobic and hydrophilic groups within surfactant. (25) (22) μ controls the relative amount of surfactant. The nearest neighbor interaction J_{ij} is defined as

$$\begin{aligned} J_{ij} &= J \quad \text{for } r_{ij} = a \\ &= 0 \quad \text{otherwise.} \end{aligned} \tag{2.3}$$

a corresponds to a lattice spacing, i.e. the typical size of water or oil molecules, which we assume to be similar. In real system, a corresponds to approximately $3\mathring{A}$. (8) Fig. 2.1 shows the charge frustrated Ising model on the lattice.

The t_i fields can be traced out by using a Hubbard-Stratonovich transformation, which yields

$$Z \sim \sum_{S_i} e^{\frac{\beta}{2}\sum_{ij} J_{ij} S_i S_j} \int D\Phi e^{-S_I[\Phi_i, S_i]}, \tag{2.4}$$

where

$$S_I[\Phi_i, S_i] = \frac{1}{2}\sum_{jk} \Phi_j \left(\beta q^2 V\right)^{-1}_{jk} \Phi_k - \sum_j \ln\left[1 + z e^{i\Phi_j S_j}\right]. \tag{2.5}$$

In Eqn. 2.5, the fugacity z, is defined as $z = e^{\beta\mu}$. Making a Gaussian approximation on $S_I[\Phi_i, S_i]$ and integrating out the Φ_i degree of freedom we get

$$Z \sim \sum_{S_i} e^{\frac{\beta}{2}\sum_{ij} U_{ij} S_i S_j}, \tag{2.6}$$

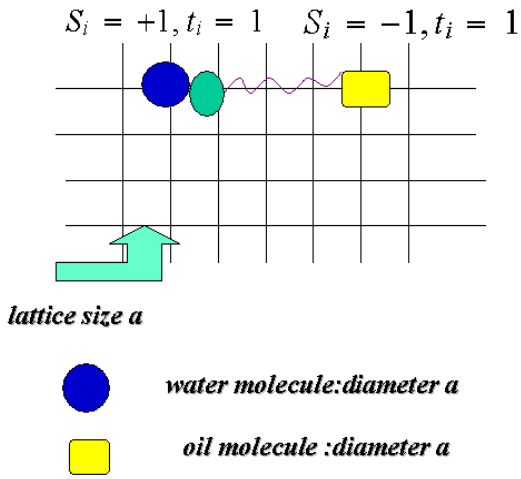

Figure 2.1 Illustration of the charge frustrated Ising model for water-oil-surfactant

where

$$U_{ij} = J_{ij} - \frac{6faT}{r_s^3} \int \frac{d^d k}{(2\pi)^d} e^{i\mathbf{k}\cdot\mathbf{r}_{ij}} \left(\frac{4\pi q^2}{q_D^2 + k^2} \right) \tag{2.7}$$

with $q_D = \dfrac{\sqrt{6}}{r_s}$. f is the volume fraction of surfactant. q_D is Debye wave vector with screening length. The long range interaction has Coulombic character, since the chemical binding between head group and tail group of the surfactant can be regarded as a local electroneutrality condition. (22) The effective problem corresponds to a competition between a short range ferromagnetic interaction and long range antiferromagnetic ordering. This frustration will play a critical role to form the glass in a microemulsion, which will be discussed in chapter 4. The

partition function is calculated as

$$\begin{aligned} Z &= \sum_{S_i} e^{\frac{\beta}{2}\sum_{ij} U_{ij} S_i S_j} \\ &\sim \mathcal{N}^{-1} \int \prod_i d\phi_i e^{-\frac{\beta}{2}\sum_{ij} U_{ij}^{-1}\phi_i\phi_j} \left(\sum_{S_j=\pm 1} e^{\beta \sum_j \phi_j S_j} \right) \\ &\sim \int \prod_i d\phi_i e^{-\beta S(\phi_i)}, \end{aligned} \tag{2.8}$$

where $\beta S(\phi_i)$ is given by

$$\begin{aligned} \beta S(\phi_i) &= \frac{\beta}{2}\sum_{ij} U_{ij}^{-1}\phi_i\phi_j - \sum_i \ln\left(\sum_{S=\pm 1} e^{\beta\phi_i S} \right) \\ &= \frac{\beta}{2}\sum_{ij} U_{ij}^{-1}\phi_i\phi_j - \sum_i \ln\left(2\cosh\phi_i\right). \end{aligned} \tag{2.9}$$

Using $-\ln(2\cosh x) \sim (-\ln 2) - \frac{1}{2}x^2 + \frac{1}{12}x^4$, it follows:

$$\beta S(\phi_i) = \frac{\beta}{2}\sum_{ij} U_{ij}^{-1}\phi_i\phi_j - \frac{\beta^2}{2}\sum_i \phi_i^2 + \frac{\beta^4}{12}\sum_i \phi_i^4 \tag{2.10}$$

Within a mean field theory, the order parameter is given by

$$m_i = \tanh(\beta\overline{\phi}_i), \tag{2.11}$$

where $\partial S(\phi_i)/\partial\phi_i|_{\overline{\phi}_i} = 0$. The free energy can now be expressed as a functional of m_i.

$$\begin{aligned} F[m_i] &= \frac{1}{2}\sum_i \left[(1+m_i)\ln(1+m_i) + (1-m_i)\ln(1-m_i)\right] - \frac{1}{2}\sum_{ij} U_{ij} m_i m_j \\ &= \frac{1}{2}(T - T_c^0)\sum_i m_i^2 + \frac{T}{12}\sum_i m_i^4 - \frac{1}{2}\frac{6faT}{r_s^3}\int \frac{d^dk}{(2\pi)^d}\sum_{ij} e^{i\mathbf{k}\cdot\mathbf{r}_{ij}}\left(\frac{4\pi q^2}{q_D^2 + k^2}\right) m_i m_j \end{aligned} \tag{2.12}$$

Here, $T_c^0 (= 3\sigma a^2)$ is oil-water demixing temperature in case of $f = 0$, i.e. without surfactant. It can be expressed as a function of the oil-water surface tension σ. In the continuum limit, Eqn. 3.28 is written as

$$F[\rho(x)] = \frac{1}{2}\int d^dx\{r_0\rho^2 + [\nabla\rho]^2 + \frac{u}{2}\rho^4\} + \frac{Q}{8\pi}\int d^dx \int d^dx' \frac{\rho(x)\rho(x')}{|\overrightarrow{x} - \overrightarrow{x}'|} e^{|\overrightarrow{x} - \overrightarrow{x}'|q_D}, \tag{2.13}$$

where we used a rescaled field $\rho = \sqrt{\frac{\sigma a}{2}} m$. $\rho(x)$ characterizes pesudo-charge degree of freedom with $\rho(x) > 0$ in a water, $\rho(x) < 0$ in a oil region and $\langle \rho(x) \rangle = 0$ on the average. Since we deal with the same amount of the oil and water molecules, only the quartic term is relevant to the free energy. The bare mass r_0 and the frustration strength Q are given by

$$\begin{aligned} r_0 &= -\frac{6}{a^2} \\ Q &= \frac{36ft}{r_s^3 a}. \end{aligned} \tag{2.14}$$

t is a reduced temperature ($t = \frac{T}{T_c^0}$). This is the Landau-Ginzburg density functional for a microemulsion.

2.2 Gauge theory for microemulsions

There exists an interesting analogy between the energy functional for a microemulsion and a local gauge theory. Inorder to demonstrate this, we start from:

$$F = \frac{1}{2}\int d^dx[\Big((\partial_\mu + \frac{g}{2}\tau A_\mu)\varphi_\alpha\Big)^2 + r_0\varphi_\alpha^2 + \frac{1}{2}u\varphi_\alpha^4 + (-\frac{1}{2}F_{\mu\nu}F^{\mu\nu})], \tag{2.15}$$

where α is index for to water and oil molecules which runs from 1 to 2. μ runs form 1 to 3. $(= x, y, z)$ The field φ is defined as $\varphi(\mathbf{x}) = (\varphi_1(x), \varphi_2(x))$, which corresponds to the density fields of water oil molecules in a microemulsion. And the vector potential A_μ in QED corresponds to an effective interaction between the surfactant and water-oil molecules. (26). g is a coupling constant for the interaction. τ is the generator of SO(2) and given as

$$\tau = \begin{pmatrix} 0 & -1 \\ 1 & 0 \end{pmatrix}. \tag{2.16}$$

r_0 and u are the bare mass and the coupling constant in the ordinary φ^4 theory. The SO(2) transformation is a rotations around the average density fields $(\varphi_1^0, \varphi_2^0)$ in 2 dimension. The partition function is given as

$$Z = \int \mathcal{D}A\mathcal{D}\varphi \exp\left\{-\frac{1}{2}\int d^dx[((\partial_\mu + g\tau A_\mu)\varphi_\alpha)^2 + r_0\varphi_\alpha^2 + \frac{1}{2}u\varphi_\alpha^4 + (\frac{1}{2}F_{\mu\nu}F^{\mu\nu})]\right\}. \tag{2.17}$$

Introducing the current field $j_\mu(x)$, the partition function is given as

$$\begin{aligned} Z &= \int \mathcal{D}A\mathcal{D}\varphi \exp\{-\frac{1}{2}\int d^dx \left[S_0 + A_\mu(x)(-\partial^2 g^{\mu\nu} + \partial^\mu\partial^\nu \right. \\ &\quad \left. +2g^2 g^{\mu\nu}\varphi_\alpha(x)\varphi_\alpha(x))A_\nu(x) - j_\mu(x)A_\mu(x))\right]\}, \end{aligned} \tag{2.18}$$

where the current $j_\mu(x)$ is defined as $-g[(\partial_\mu\varphi_\alpha)\,\tau\varphi_\alpha]$ and $g^{\mu\nu}$ is delta function $\delta_{\mu\nu}$. Among the four component of vector field, two are fixed: $A^0 = 0$, and, using Coulomb gauge, $\overrightarrow{\nabla}\cdot\overrightarrow{A} = 0$. Then we have only two degree of freedom and it corresponds to transverse component. The partition function reads

$$\begin{aligned} &\int \mathcal{D}A\mathcal{D}\varphi \exp\left\{-\frac{1}{2}\int d^dx \left[S_0 + A_\mu(x)(-\partial^2 + \frac{g^2}{4}\varphi_\alpha(x)\varphi_\alpha(x))A_\nu(x) - j_\mu(x)A_\mu(x)\right]\right\} \\ &\sim \int \mathcal{D}A \exp\left\{-\frac{1}{2}\int d^dx \left[A_\mu(x)(-\partial^2 + \frac{g^2}{4} < \varphi_\alpha^2(x) >)A_\nu(x) - j_\mu(x)A_\mu(x)\right]\right\} \end{aligned} \tag{2.19}$$

where we used $\varphi^*_\alpha(x)\varphi_\alpha(x)$ as average value $\left\langle\varphi^2_\alpha(x)\right\rangle = \left[\varphi^0_1(x)\right]^2 + \left[\varphi^0_2(x)\right]^2$.

For the effective interaction between water and oil molecules which is mediated by the surfactant, the surfactant field(A_μ) is integrated out. Using the Gaussian integral,

$$\int \mathcal{D}x e^{-\frac{1}{2}\ (x_i A_{ij} x_j)+j_i x_i} = \exp(\frac{1}{2}[j(A)^{-1}_{ij} j]), \tag{2.20}$$

the integral over the gauge field is straightforward and yields:

$$\begin{aligned}&\int \mathcal{D}A \exp\left\{-\frac{1}{2}\int d^dx\ \left[A_\mu(x)(-\partial^2 + \frac{g^2}{4} < \varphi^2_\alpha(x) >)A_\nu(x) - j_\mu(x)A_\mu(x)\right]\right\}\\ &= \exp[-\frac{1}{2}Tr\ln(-\partial^2 + \frac{g^2}{4}\left\langle\varphi^2_\alpha(x)\right\rangle)].\end{aligned} \tag{2.21}$$

This leads to the partition function.

$$Z(j) = Z(0)\exp\int d^dx\ d^dx'\ \frac{1}{2}[j(x)G(x-x')j(x')]. \tag{2.22}$$

The two point correlation function is then determined by the functional derivative

$$\frac{1}{Z(0)}\frac{\delta^2 Z(j)}{\delta j(x)\delta j(x')} = G(x-x') \tag{2.23}$$

and is given as

$$G(x-x') = \int \frac{d^3q}{(2\pi)^3}\frac{1}{(q^2 + \frac{g^2}{4}\left\langle\varphi^2_\alpha(x)\right\rangle)}e^{iq(x-x')} \tag{2.24}$$

$$= \frac{1}{4\pi(x-x')}e^{-m(x-x')}, \tag{2.25}$$

where m is given as $\frac{g^2}{4}\left\langle\varphi^2_\alpha(x)\right\rangle = m^2$. Using this result, we finally obtain the partition function

$$Z = \int \mathcal{D}\varphi e^{-\frac{1}{2}\int d^dx[S_0]}\exp\left\{\int d^dx\ d^dx'\ \frac{1}{2}[j(x)\frac{1}{4\pi(x-x')}e^{-m(x-x')}j(x')]\right\}. \tag{2.26}$$

When we consider the fluctuation field $\psi(x)$ as $\varphi^0(x) + \psi(x)$, then $j(x)j(x')$ can be expressed as 2×2 matrix form of $\frac{g^2}{4}\psi_\alpha\ (x)W\psi_\alpha(x)$. W is given by

$$W = \begin{pmatrix} \left[\varphi^0_1(x)\right]^2 & -\varphi^0_1(x)\varphi^0_2(x) \\ -\varphi^0_1(x)\varphi^0_2(x) & \left[\varphi^0_2(x)\right]^2 \end{pmatrix}. \tag{2.27}$$

It follows, $\psi_1^2(x) + \psi_2^2(x) = 0$. This condition is what we used for water and oil density field. Also, this condition is found for block copolymer as incompressibility condition. Then, the partition function is given as

$$Z = \int D\varphi exp\left[-\frac{1}{2}\int d^dx[S_0] - \frac{Q}{8\pi}\int d^dx d^dx' \frac{e^{-m(x-x')}}{(x-x')}\varphi_\alpha(x')\varphi_\alpha(x)\right] \tag{2.28}$$

with $Q = g^2\frac{g}{2}(\left[\varphi_1^0(x)\right]^2 + \left[\varphi_2^0(x)\right]^2)$. This result is the same with Eqn. 2.13. The mass acquirement in particle physics is expressed as Debye-Hückel theory in the chemistry. (26)

2.3 Phase diagrams in equilibrium state

To analyze the equilibrium phases of a microemulsion, we should investigate the correlation function of the system. Within mean field theory, the density-density correlation function of the model, $G(\mathbf{q}) = T^{-1} \langle \rho_{\mathbf{q}} \rho_{-\mathbf{q}} \rangle$ is given by

$$G(q) = \frac{1}{r + q^2 + \dfrac{Q}{q^2 + q_D^2}}. \tag{2.29}$$

where r, $r_0 + u \langle \rho \rangle^2$, is the renormalized "mass" of the theory. $G(q)$ can alternatively written as

$$G(q) \ = \frac{q_D^{-2}}{\alpha_+^2 - \alpha_-^2} \left(\frac{\alpha_+^2 - 1}{\left(\frac{q}{q_D}\right)^2 + \alpha_+^2} - \frac{\alpha_-^2 - 1}{\left(\frac{q}{q_D}\right)^2 + \alpha_-^2} \right), \tag{2.30}$$

where

$$\alpha_\pm^2 = \frac{1}{2}(\frac{r}{q_D^2} + 1) \mp \sqrt{\frac{1}{4}\left(\frac{r}{q_D^2} - 1\right)^2 - \frac{Q}{q_D^4}}. \tag{2.31}$$

After some algebra, Eqn. 2.30 can be written as

$$G(q) \ = \frac{q^2 + q_D^2}{(q^2 - q_m^2)^2 + (2q_m/\xi)^2}, \tag{2.32}$$

where the modulation length $l_m = \frac{2\pi}{q_m}$ and the correlation length ξ are defined as $l_m = \frac{1}{\alpha_-}$, $\xi = \frac{1}{\alpha_+}$. The Fourier transform of Eqn. 2.32 gives a correlation function in a real space. If we approximate $q \sim q_m$ in the nominator in Eqn. 2.32, we find:

$$G\,(x) = \frac{q_m^2 + q_D^2}{8\pi q_m x/\xi} e^{-x/\xi} \sin(\frac{2\pi x}{l_m}). \tag{2.33}$$

Eqn. 2.33 explains why l_m is the modulation length and ξ the correlation length of the microemulsion. Depending on the ratio of two length scales, a modulated state, a homogeneously mixed state and, a state with macroscopic phase separation occur.

In what follows we analyze the mean field equation $r(T) = r_0 + uT \int \frac{d^3q}{(2\pi)^3} G(q)$ self consistently and determine α_+ and α_-. This enables us to determine the phase boundaries between the various phases. The phase diagram of model Hamiltonian 2.13 for different values of r_s/a in the equilibrium state are plotted in Fig. 2.2 and Fig. 2.3 respectively. In the emulsion

phase, oil and water are macroscopically separated. And in the microemulsion phase, oil and water are intertwined with each other to form bicontinuous phase or lamellar phase. On the other hand, in the homogeneously mixed or disordered phase, there is no definite structure. Each transition lines in Fig. 2.2 and Fig. 2.3 are obtained by solving the mean field equation,

$$r(T) = r_0 + uT \int \frac{d^3q}{(2\pi)^3} G(q), \tag{2.34}$$

where $u = -\frac{2\pi^2 r_0}{T_c^0 \Lambda}$ and Λ is cut off momentum. $G(q)$ is defined as Eqn. 2.30. The line 3 in Fig. 2.2 and Fig. 2.3, the macroscopic separation of oil and water, is obtained by $\alpha_-^2 = 0$ and positive real α_+^2, which means the modulation length, l_m, goes to infinity with the finite correlation length ξ in real space. From the Eqn. 2.31, the transition into uniformly ordered state is fulfilled when $r(T) = -\frac{Q}{q_D^2}$ from Eqn. 2.31. Then, the mean field equation leads to

$$-\frac{Q}{q_D^2} = r_0 - \frac{2\pi^2 r_0}{\Lambda} \frac{T}{T_c^0} \int \frac{d^3q}{(2\pi)^3} \frac{q_D^{-2}}{\alpha_+^2 - \alpha_-^2} \left(\frac{\alpha_+^2 - 1}{\left(\frac{q}{q_D}\right)^2 + \alpha_+^2} - \frac{\alpha_-^2 - 1}{\left(\frac{q}{q_D}\right)^2 + \alpha_-^2} \right). \tag{2.35}$$

Changing the integral variable $\frac{q}{q_D} = x$, $q^2 = q_D^2 x^2$ and $dq = q_D dx$,

$$-\frac{Q}{q_D^2} = r_0 - r_0 \frac{T}{T_c^0} \frac{q_D}{\alpha_+^2 - \alpha_-^2} \int_0^{\Lambda/q_D} ds s^2 \left(\frac{\alpha_+^2 - 1}{s^2 + \alpha_+^2} - \frac{\alpha_-^2 - 1}{s^2 + \alpha_-^2} \right). \tag{2.36}$$

When we define the integral

$$F(z) = \frac{q_D}{\Lambda} \int_0^{\Lambda/q_D} dx \frac{x^2}{x^2 + z^2} = 1 - \frac{q_D z}{\Lambda} \tan^{-1}\left(\frac{\Lambda}{q_D z}\right), \tag{2.37}$$

Eqn. 2.35 can be written as

$$-\frac{Q}{q_D^2} = r_0 - r_0 \frac{T}{T_c^0} \frac{1}{1 - \frac{Q}{q_D^4}} \left(F(\alpha_+^2) \left(\alpha_+^2 - 1\right) + 1 \right), \tag{2.38}$$

where we set $\Lambda = 1$ and $\alpha_-^2 = 0$ and $\alpha_+^2 = 1 - \frac{Q}{q_D^4}$. Defining $G(x) = F(x)(x-1)$, the mean field equation is written as

$$\frac{T_c}{T_c^0} = \frac{r_0 + \frac{Q}{q_D^2}}{r_0} \frac{1 - \frac{Q}{q_D^4}}{G(\sqrt{1 - \frac{Q}{q_D^4}}) + 1}. \tag{2.39}$$

The reduced temperature t_c is defined as $t_c = T_c/T_c^0$. We can solve the Eqn. 2.39 self consistently for the reduced temperature t_c as a function of f, r_s and a. with Eqn. 2.14. In a

similar way, the line 1 and line 2 can be obtained by complex α_-^2 and α_+^2 in a homogeneous mixed state. In this state, the modulation length l_m goes to infinity and the correlation length ξ goes to zero. The condition of complex α_-^2 and α_+^2 is fulfilled at $\frac{r(T)}{q_D^2} = 1 - 2\sqrt{\frac{Q}{q_D^4}}$ and $\frac{r(T)}{q_D^2} = 1 + 2\sqrt{\frac{Q}{q_D^4}}$ respectively from Eqn. 2.31. Introducing the dimensionless parameter ε,

$$\varepsilon = \frac{r - q_D^2}{r + q_D^2}\sqrt{\frac{4Q}{\left(r - q_D^2\right)^2} - 1}. \tag{2.40}$$

$\alpha_\pm^2$ can be expressed as

$$\begin{aligned} \alpha_\pm^2 &= \lim_{\varepsilon\to 0}(\frac{r}{q_D^2} + 1)(1 \mp \varepsilon i) \\ &= \lim_{\varepsilon\to 0}\left(1 - \sqrt{\frac{Q}{q_D^4}}\right)(1 \mp \varepsilon i) \\ &= \lim_{\varepsilon\to 0}\Gamma(1 \mp \varepsilon i), \end{aligned} \tag{2.41}$$

where we set $\left(1 - \sqrt{\frac{Q}{q_D^4}}\right)$ as Γ. Then, $\alpha_+^2 - \alpha_-^2$ is given by

$$\alpha_+^2 - \alpha_-^2 = -\lim_{\varepsilon\to 0} 2\Gamma\varepsilon i. \tag{2.42}$$

For the transition line 2, the mean field equation can be written as

$$\begin{aligned} 1 - 2\sqrt{\frac{Q}{q_D^4}} &= \frac{r_0}{q_D^2} + \lim_{\varepsilon\to 0}\frac{r_0}{q_D^2}\frac{T}{T_c^0\Lambda}\int_0^\Lambda dqq^2\frac{q_D^{-2}}{2\Gamma\varepsilon i}\left(\frac{\alpha_+^2 - 1}{\left(\frac{q}{q_D}\right)^2 + \alpha_+^2} - \frac{\alpha_-^2 - 1}{\left(\frac{q}{q_D}\right)^2 + \alpha_-^2}\right) \\ &= \frac{r_0}{q_D^2} + \lim_{\varepsilon\to 0}\frac{r_0}{q_D^2}\frac{T}{T_c^0}\frac{G(\Gamma - \Gamma\varepsilon i) - G(\Gamma + \Gamma\varepsilon i)}{2\Gamma\varepsilon i} \\ &= \frac{r_0}{q_D^2} - \frac{r_0}{q_D^2}\frac{T}{T_c^0}G'(\Gamma), \end{aligned} \tag{2.43}$$

where $G'(\Gamma)$ denotes $\frac{d}{dx}\left(1 - q_D\sqrt{x}\tan^{-1}\left(\frac{1}{q_D\sqrt{x}}\right)(x-1)\right)$. The mean field equation is written as

$$\frac{T}{T_c^0} = \frac{-q_D^2 + 2\sqrt{Q} + r_0}{r_0 G'(\Gamma)}. \tag{2.44}$$

In a same way, the transition line 1 from the microemulsion state into the homogeneous mixed state at higher temperature is given as

$$\frac{T}{T_c^0} = \frac{-q_D^2 - 2\sqrt{Q} + r_0}{r_0 G'(\Delta)}, \tag{2.45}$$

where $\Delta = 1 + \sqrt{\frac{Q}{q_D^4}}$. The remarkable aspect of the phase diagram is the expansion of the microemulsion region with the increase of the surfactant length. The surfactant plays a role as catalyst of mixing water and oil molecules to form the intertwined structures. The uniformly ordered phase emerges at relatively low temperature in the presence of the enlarged surfactant.

The first term of model Hamiltonian, Eqn. 2.13 describes a short range interaction in the analogy of Ising model, which favors the uniform phase. However, the second term is a long range interaction to disturb the uniform phase. The competition between these two opposite interactions supplies the microemulsion system with a mechanism for frustration. This will lead to glassy behavior under certain conditions. This glassy behavior of a microemulsion will be discussed in chapter 4.

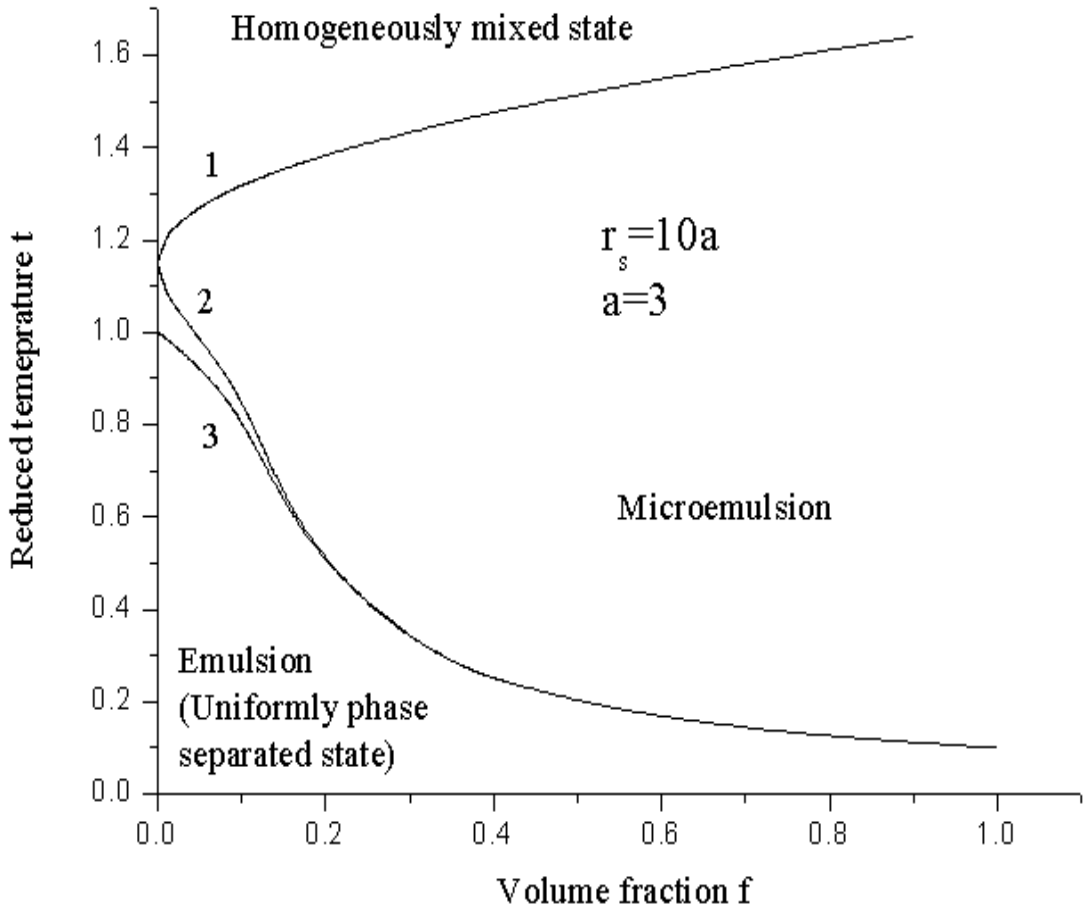

Figure 2.2 The phase diagram of the model Hamiltonian 2.13 with $r_s/a = 10$ in equilibrium state.

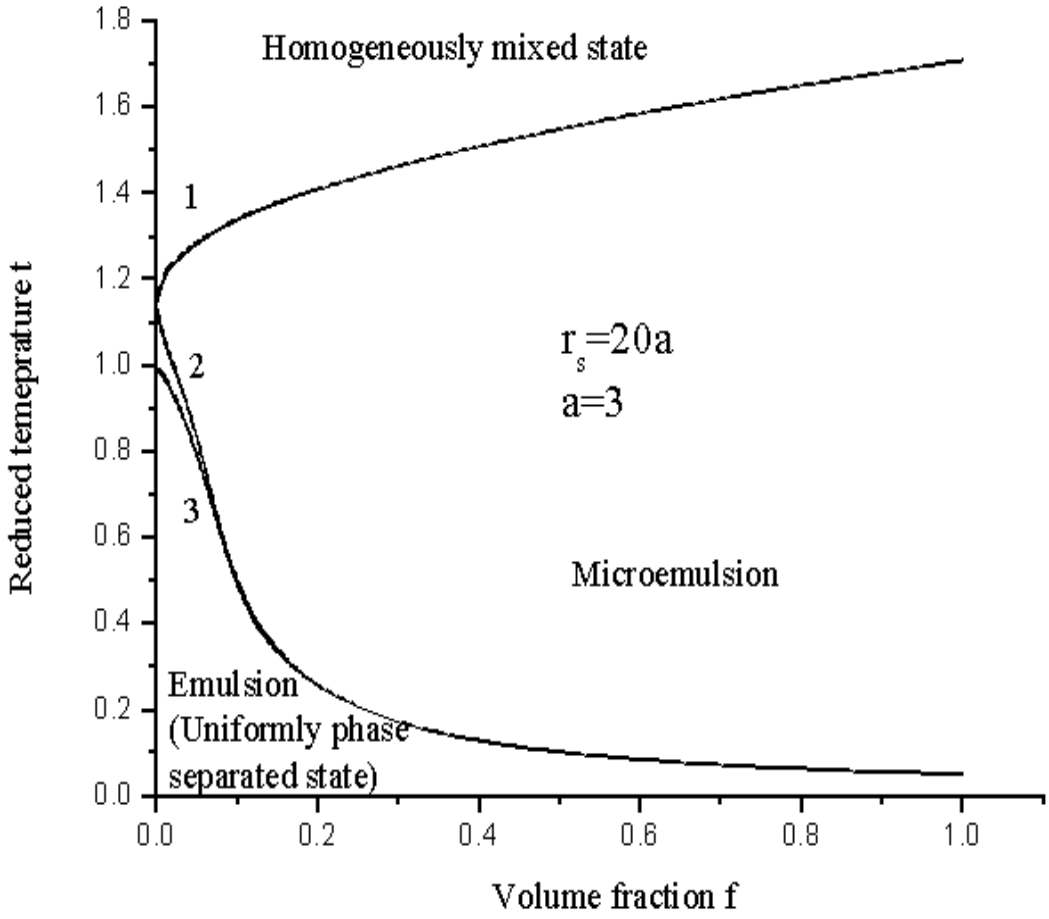

Figure 2.3 The phase diagram of the model Hamiltonian 2.13 with $r_s/a = 20$ in equilibrium state.

2.4 Density functional theory of block copolymers

In this section, we will review of density functional theory for block copolymer. Block copolymer are made by the covalent bonding of two(diblock) or more polymer chains. (29). Block copolymers show various morphologies(lamellar, bcc, hexagonal phase$\cdots$) depending on three physical parameters: the Flory-Huggins parameter, χ, the degree of polymerization, S, and the volume fraction f in bulk or in solution. The microstructures of block copolymers are explained successfully by Leibler's density functional theory in the weak segregation limit. Leibler obtained the universal value $(\chi S)_{MST} \sim 10.5$ for microphase separation for symmetric diblock copolymer. (12) According to his mean field theory, for symmetric diblock copolymer $f = 0.5$, a lamellar mesophase undergoes a second order transition from the disordered state. However, experimentally for the symmetric diblock copolymers, the lamellar mesophase is known to undergo a first-order transition by the experiment. (15) This contradiction was solved by Fredrickson and Helfand. (13) They made the composition fluctuation correction to Leibler's result and obtained $(\chi S)_{MST} \sim 10.5 + 41\overline{S}^{-1/3}$, which was more consistent with the experiment. In addition, it was shown in Ref. (13) that the transition is fluctuation induced first order transition predicted by Brazovskii. (14) (12) In what follows, we summarize the approach used in Ref. (12) (13), needed to develop a theory of glassiness in such systems.

We consider N polymer chains ($n = 1, ..., N$) of asymmetric type ABC triblock copolymers, each consisting of S segments ($n = 1, ..., S$). The relevant degrees of freedom of the polymer are the positions (in d-dimensional space) of the segments $\mathbf{R}_{n,s}$. We define the composition values of A block polymer and C block copolymer as $f = \frac{S_A}{S}$ and $g = \frac{S_B}{S}$, respectively. The geometries of the diblock copolymer ($g \to 0$) and symmetric ABA triblock copolymer($g \to f$) are special cases of the asymmetric ABC triblock copolymer as Fig. 2.4.

The polymers are characterized by a Gaussian statistical weight and an additional excluded volume pseudo-potential

$$H^{\mathrm{E}} = \frac{d}{2} \sum_{n,s} \left(\frac{\mathbf{R}_{n,s+1} - \mathbf{R}_{n,s}}{b} \right)^2 + \frac{1}{2} \sum_{s,s';n,n'} \upsilon_{s,s'} \delta \left(\mathbf{R}_{n,s} - \mathbf{R}_{n',s'} \right). \tag{2.46}$$

b is the characteristic persistence length of the polymer and υ the strength parameter of the

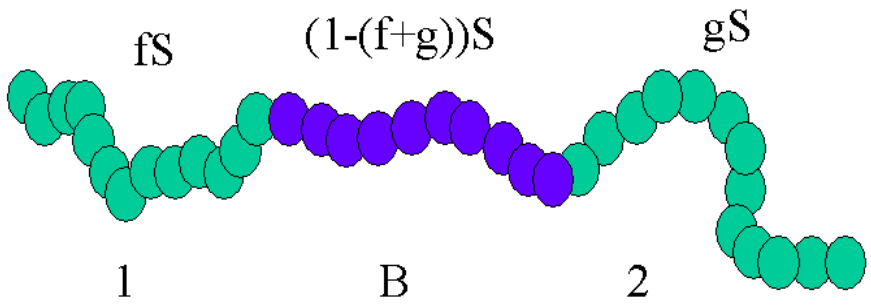

Figure 2.4 The geometry of triblock copolymers. When $g \to f$, it reduces to a symmetric ABA triblock copolymer. Also when $g \to 0$, it reduces to a diblock copolymer. 1, 2 are labels for monomers in A block and B for monomers in B block.

excluded volume interaction (with dimension of a volume).

To solve the Edward Hamiltonian for block copolymers, it is useful to analyze the conditional partition function

$$Z\left[\phi_A,\phi_B\right]=\left\langle \prod_{\gamma=A,B}\delta\left(\phi_\gamma\left(\mathbf{q}\right)-\rho_\gamma\left(\mathbf{q}\right)\right)\right\rangle^{\mathrm{E}}, \tag{2.47}$$

where $\rho_\gamma\left(\mathbf{r}\right)=\sum_{n,s}^{\gamma}\delta\left(\mathbf{r}-\mathbf{R}_{n,s}\right)$ is the particle density of the block A and of block B. The particle density field $\rho_\gamma\left(\mathbf{r}\right)$ is replaced by collective field variables $\phi_\gamma\left(\mathbf{r}\right)$. The average with respect to this Hamiltonian is given by $\left\langle ...\right\rangle^{\mathrm{E}}=\frac{\int D\mathbf{R}_{...}\exp\left(-H^{\mathrm{E}}\right)}{\int D\mathbf{R}\exp(-H^{\mathrm{E}})}$. Averages with respect to the purely Gaussian distribution with $\upsilon=0$ are denoted as $\left\langle ...\right\rangle^{\mathrm{W}}$ where $H^{\mathrm{W}}=H^{\mathrm{E}}\left(\upsilon=0\right)$ refers to a pure Wiener measure.

Next we assume that the system is incompressible in the sense that the total density of the system does not vary in space:

$$\rho_{\mathrm{A}}\left(\mathbf{r}\right)+\rho_{\mathrm{B}}\left(\mathbf{r}\right)=\rho_0=\frac{SN}{V}. \tag{2.48}$$

In our calculation, we assume equal persistence lengths of A and B polymers. ρ_0 has a dimension of $\sim b^{-3}$. The incompressible condition enables us to express the density variation of the A-block in terms of the density variation of the B-block $\Psi_\gamma\left(\mathbf{r}\right)=\phi_\gamma\left(\mathbf{r}\right)-\left\langle\rho_\gamma\left(\mathbf{r}\right)\right\rangle^{\mathrm{W}}$. By an incompressible condition, we have $\Psi\left(\mathbf{r}\right)=\Psi_{\mathrm{A}}\left(\mathbf{r}\right)=-\Psi_{\mathrm{B}}\left(\mathbf{r}\right)$. Then $\Psi\left(\mathbf{r}\right)>0$ corresponds to an excess of A-monomers whereas $\Psi\left(\mathbf{r}\right)<0$ refers to an excess of B-monomers. In particular one obtains very simple expression for the excluded volume interaction in terms of the field Ψ:

$$V_{\mathrm{ev}}\left[\Psi\right]=-\chi\int d^dr\Psi\left(\mathbf{r}\right)^2, \tag{2.49}$$

where Flory-Huggins parameter χ is defined as $2\upsilon_{\mathrm{AB}}-\left(\upsilon_{\mathrm{AA}}+\upsilon_{\mathrm{BB}}\right)$.

2.4.1 Tranformation to collective coordinate

The partition function of the system is defined by $Z = \int D\phi_A D\phi_A \exp\left(-S\left[\phi_A, \phi_B\right]\right)$, the effective action of these density fields $S\left[\phi_A, \phi_B\right] = -\log Z\left[\phi_A, \phi_B\right]$.

$$Z\left[\phi_A, \phi_B\right] = \exp\left(-V_{\text{eff}}\left[\phi_A, \phi_B\right]\right) \left\langle \prod_{\mathbf{q},\gamma=A,B} \delta\left(\phi_{\gamma,\mathbf{q}} - \rho_{\gamma,\mathbf{q}}\right) \right\rangle^{\text{W}}, \tag{2.50}$$

where the average need only be performed with respect to the bare Wiener measure. $V_{\text{eff}}\left[\phi_A, \phi_B\right]$ is an interaction term between two different polymer chains. By introducing the integral representation of the delta function, the partition function can be expanded in powers of ρ^γ

$$\begin{aligned} Z\left[\phi_A, \phi_B\right] = \exp\left(-V_{\text{eff}}\left[\phi_A, \phi_B\right]\right) \prod_{\gamma=A,B} \int Dj_\gamma \exp\left(i \int \frac{d^d q}{(2\pi)^d} \phi_{\mathbf{q}} j_{\gamma,-\mathbf{q}}\right) \\ \times \sum_{n=0}^{\infty} \frac{(-i)^n}{n!} \sum_{\gamma_1} ... \sum_{\gamma_n} \int \frac{d^d q_1}{(2\pi)^d} ... \int \frac{d^d q_n}{(2\pi)^d} S_n^{\gamma_1 ... \gamma_n}\left(\mathbf{q}_1 ... \mathbf{q}_n\right) j_{\gamma_1,-\mathbf{q}_1} ... j_{\gamma_n,-\mathbf{q}_n}. \end{aligned} \tag{2.51}$$

The integrals over j goes from $-i\infty$ to $i\infty$ and $S_n^\gamma\left(\mathbf{q}_1 ... \mathbf{q}_n\right)$ denotes the n-the moment of the density field with respect to the Wiener measure $S_n^\gamma\left(\mathbf{q}_1 ... \mathbf{q}_n\right) = \langle \rho_{\mathbf{q}_1}^{\gamma_1} ... \rho_{\mathbf{q}_n}^{\gamma_n} \rangle^{\text{W}}$. The logarithm of the moments corresponds to the cumulant expansion allowing us to rewrite

$$\begin{aligned} W\left[j_A, j_B\right] &= \log \sum_{n=0}^{\infty} \frac{1}{n!} \sum_{\gamma_1} ... \sum_{\gamma_n} \int \frac{d^d q_1}{(2\pi)^d} ... \int \frac{d^d q_n}{(2\pi)^d} S_n^{\gamma_1 ... \gamma_n}\left(\mathbf{q}_1 ... \mathbf{q}_n\right) j_{\gamma_1,-\mathbf{q}_1} ... j_{\gamma_n,-\mathbf{q}_n} \\ &= \sum_{n=0}^{\infty} \frac{1}{n!} \sum_{\gamma_1} ... \sum_{\gamma_1} \int \frac{d^d q_1}{(2\pi)^d} ... \int \frac{d^d q_n}{(2\pi)^d} S_{c,n}^{\gamma_1 ... \gamma_n}\left(\mathbf{q}_1 ... \mathbf{q}_n\right) j_{\gamma_1,-\mathbf{q}_1} ... j_{\gamma_n,-\mathbf{q}_n}, \end{aligned} \tag{2.52}$$

where $S_{c,n}^{\gamma_1 ... \gamma_n}\left(\mathbf{q}_1 ... \mathbf{q}_n\right)$ are the connected correlation with

$$S_{2,c}^{\gamma_1 \gamma_2}\left(\mathbf{q}_1, \mathbf{q}_2\right) = S_2^{\gamma_1 \gamma_2}\left(\mathbf{q}_1, \mathbf{q}_2\right) - S_1^{\gamma_1}\left(\mathbf{q}_1\right) S_1^{\gamma_2}\left(\mathbf{q}_2\right). \tag{2.53}$$

The partition function is given as

$$Z\left[\phi_A, \phi_B\right] = \exp\left(-V_{\text{eff}}\left[\phi_A, \phi_B\right]\right) \prod_{\gamma=A,B} \int Dj_\gamma \exp\left(W\left[j_A, j_B\right] + i \int \frac{d^d q}{(2\pi)^d} \phi_{\gamma,\mathbf{q}} j_{\gamma,-\mathbf{q}}\right). \tag{2.54}$$

By introducing a density fluctuation field

$$\Psi_\gamma\left(\mathbf{r}\right) = \phi_\gamma\left(\mathbf{r}\right) - \left\langle \rho_\gamma\left(\mathbf{r}\right) \right\rangle^{\text{W}}, \tag{2.55}$$

we obtain the effective potential $\Gamma[\Psi_A, \Psi_B]$ as

$$\Gamma[\Psi_A, \Psi_B] = \sum_{n=0}^{\infty} \frac{-1}{n!} \sum_{\gamma_1} ... \sum_{\gamma_n} \int \frac{d^d q_1}{(2\pi)^d} ... \int \frac{d^d q_n}{(2\pi)^d} \Gamma_n^{\gamma_1 ... \gamma_n}(\mathbf{q}_1 ... \mathbf{q}_n) \Psi_{\gamma_1, -\mathbf{q}_1} ... \Psi_{\gamma_n, -\mathbf{q}_n}, \quad (2.56)$$

where $\Gamma[\phi_A, \phi_B]$ is transformed via Legendre transformation:

$$\Gamma[\phi_A, \phi_B] = W[j_A, j_B] + i \int \frac{d^d q}{(2\pi)^d} \phi_{\gamma, \mathbf{q}} j_{\gamma, -\mathbf{q}}. \quad (2.57)$$

Using the fact that $\Psi_\gamma(\mathbf{r}) = \xi_\gamma \Psi(\mathbf{r})$ with $\xi_\mathrm{A} = 1$ and $\xi_\mathrm{B} = -1$ it follows

$$\begin{aligned}\Gamma[\Psi] &= \sum_{n=0}^{\infty} \frac{-1}{n!} \int \frac{d^d q_1}{(2\pi)^d} ... \int \frac{d^d q_n}{(2\pi)^d} \Gamma_n(\mathbf{q}_1 ... \mathbf{q}_n) \Psi_{\gamma_1, -\mathbf{q}_1} ... \Psi_{\gamma_n, -\mathbf{q}_n} \\ &= \sum_{n=0}^{\infty} \sum_{\gamma_1} ... \sum_{\gamma_n} \frac{-1}{n!} \int \frac{d^d q_1}{(2\pi)^d} ... \int \frac{d^d q_n}{(2\pi)^d} \Gamma_n^{\gamma_1 ... \gamma_n}(\mathbf{q}_1 ... \mathbf{q}_n) \xi_{\gamma_1} ... \xi_{\gamma_n} \Psi_{-\mathbf{q}_1} ... \Psi_{-\mathbf{q}_n}. \quad (2.58)\end{aligned}$$

We obtain only one field variable, Ψ, but nevertheless have to evaluate a set of matrix propagators in order to determine the correlation function of this single field. The two point correlation functions for a noninteracting asymmetric triblock copolymer chain is given by

$$\begin{aligned}S_{\mathbf{k}}^{\mathrm{AA}} &= \frac{2S}{x^4}(e^{-gx^2} + e^{-fx^2} + e^{-x^2} - e^{-(1-f)x^2} - e^{-(1-g)x^2} + e^{-(1-f-g)x^2} - (2 - fx^2 - gx^2) \\ S_{\mathbf{k}}^{\mathrm{BB}} &= \frac{2S}{x^4}(e^{-(1-f-g)x^2} - x^2 + (1-f-g)x^2) \\ S_{\mathbf{k}}^{\mathrm{AB}} &= \frac{S}{x^4} e^{-(2+f)x^2}(e^{-(1+f)x^2} - e^{-(2-g)x^2})(2e^{(1+f)x^2} - e^{-x^2} - e^{(1+f-g)x^2}). \quad (2.59)\end{aligned}$$

The two point correlation functions for noninteracting diblock copolymer chains($g \to 0$) are given as (12)

$$\begin{aligned}S_{\mathbf{k}}^{\mathrm{AA}} &= \frac{2S}{x^4}[e^{-fx^2} + fx^2 - 1] \\ S_{\mathbf{k}}^{\mathrm{BB}} &= \frac{2S}{x^4}[e^{-(1-f)x^2} + x^2(1-f) - 1] \\ S_{\mathbf{k}}^{\mathrm{AB}} &= \frac{S}{x^4}[1 + e^{-x^2} - e^{-(1-f)x^2} - e^{-fx^2}]. \quad (2.60)\end{aligned}$$

The two point correlation functions for a noninteracting symmetric ABA triblock copolymer chains ($g \to f$) are given as (37)

$$\begin{aligned}S_{\mathbf{k}}^{\mathrm{AA}} &= \frac{2S}{x^4}[2(e^{-fx^2} + fx^2 - 1) + e^{-(1-2f)x^2} - 2e^{-(1-f)x^2} + e^{-x^2}] \\ S_{\mathbf{k}}^{\mathrm{BB}} &= \frac{2S}{x^4}[e^{-(1-2f)x^2} + x^2(1-2f) - 1] \\ S_{\mathbf{k}}^{\mathrm{AB}} &= \frac{2S}{x^4}[1 - e^{-fx^2} + e^{-(1-f)x^2} - e^{-(1-2f)x^2}], \quad (2.61)\end{aligned}$$

where $x^2 = q_0^2 R_0^2$. R_0 is a total gyration length of the block copolymer. In Fig. 2.5, we show the correlation function $\mathcal{G}_{\mathbf{q}}$ for $f = 0.25$ and different χS.

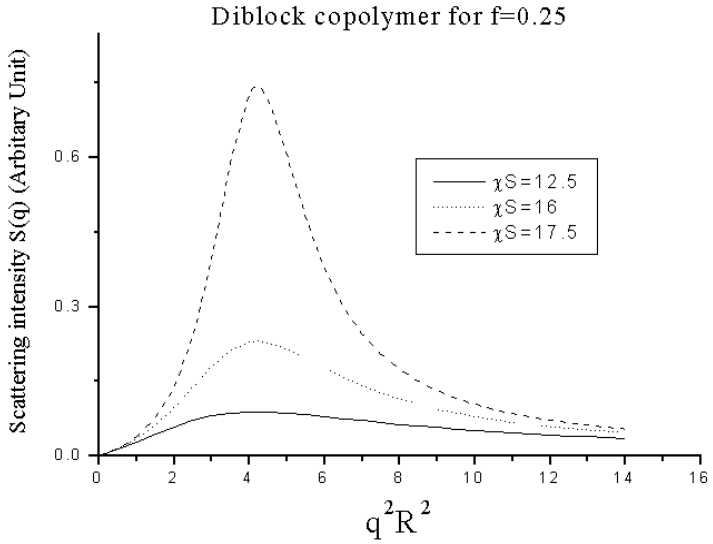

Figure 2.5 Scattering intensity of diblock copolymer for $f = 0.25$ is plotted as a function of q^2R^2 for three different values of χS. (12)

If χS grows, the correlation function is sharply peaked at $\sim 1/R_0$. Then, the correlation function of block copolymer can be expanded around peak position of scattering function.

$$\begin{aligned} \mathcal{G}_{\mathbf{q}} &= \left(\frac{S_{\mathbf{k}}^{\mathrm{BB}} + S_{\mathbf{k}}^{\mathrm{AA}} + 2S_{\mathbf{k}}^{\mathrm{AB}}}{S_{\mathbf{k}}^{\mathrm{AA}} S_{\mathbf{k}}^{\mathrm{BB}} - \left(S_{\mathbf{k}}^{\mathrm{AB}}\right)^2} - 2\chi\right)^{-1} \\ &= \frac{N}{F^* - 2\chi S + F^{**}(qR_0 - x^*)^2}, \end{aligned} \tag{2.62}$$

where $F^* = F\left(x^*, f\right)$ and $F^{**} = \frac{1}{2}\left.\frac{\partial^2 F(x,f)}{\partial x^2}\right|_{x=x^*}$. For example for $f = 0.5$ it holds $x^* \simeq 1.945$ with $\frac{1}{2}F\left(x^*, \frac{1}{2}\right) \simeq 10.5$ and $\frac{1}{2}\left.\frac{\partial^2 F\left(x,\frac{1}{2}\right)}{\partial x^2}\right|_{x=x^*} \simeq 7.29$ for diblock copolymer. In the case of symmetric ABA triblock copolymer $f = 0.25$, $x^* \simeq 2.633$ with $\frac{1}{2}F\left(x^*, \frac{1}{2}\right) \simeq 17.99$ and $\frac{1}{2}\left.\frac{\partial^2 F\left(x,\frac{1}{2}\right)}{\partial x^2}\right|_{x=x^*} \simeq 8.18$.

Since the Flory-Huggins parameter is inversely proportional to the temperature, the interaction parameter $\chi S = 17.5$ corresponds to a lower temperature than $\chi S = 16$ or $\chi S = 12.5$

for fixed degree of polymerization S. When we decrease temperature, the scattering intensity increases and finally diverges at $\chi S = 17.6$ within mean field theory. The critical value $\chi S = 17.6$ is spinodal point and denoted as $(\chi S)_{spinodal}$.

Fig. 2.6 shows the spinodal line of diblock copolymer for different volume fraction f.

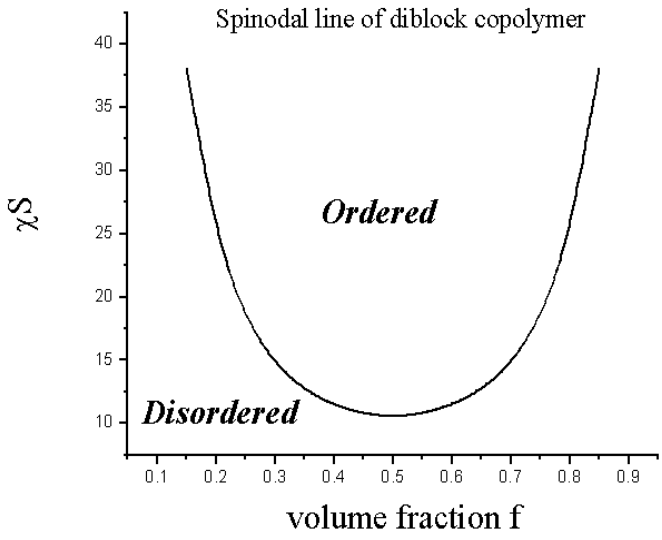

Figure 2.6 The spinodal line of a diblock copolymer for different volume fraction f

Even though we can predict the borderline for ordered state and disordered state as a function of the interaction parameter χS and the volume fraction f, more information is required for the prediction of a variety of microstructure of diblock copolymer. The information lies in the higher order terms. By constructing Landau density functional with the higher order terms, we can predict the specific phases of diblock copolymer by energy minimization. In the next section, we will review how to calculate the higher order terms in Landau density functional.

2.4.2 The derivation of higher order vertex functions

The higher vertex terms $\Gamma_{\mathbf{3}}$ and $\Gamma_{\mathbf{4}}$ can be obtained directly from an effective potential approach. (35) The free energy in the presence of external source field J is written as

$$F[J] = -\log Z[J], \tag{2.63}$$

where the partition function of the system is given by

$$Z[J] = \int D\varphi \exp[-H - J\varphi]. \tag{2.64}$$

Using Legendre transformation, we can define a new function as $\Gamma[\overline{\varphi}(x)]$, which corresponds to Gibbs free energy of the system.

$$\Gamma[\overline{\varphi}(x)] = F[J] - \int J(y)\overline{\varphi}(x). \tag{2.65}$$

$\overline{\varphi}(x)$ is a field value at the saddle point. We find there is a relation between the second derivative of $F[J]$ with respect to external source fields and the second derivative of Legendre transformed function $\Gamma[\overline{\varphi}(x)]$ with respect to $\overline{\varphi}(x)$:

$$\left(\frac{\delta^2 F[J]}{\delta J(x)\delta J(y)}\right) = \left(\frac{\delta^2 \Gamma[\overline{\varphi}(x)]}{\delta\overline{\varphi}(x)\delta\overline{\varphi}(y)}\right)^{-1} = S(x,y), \tag{2.66a}$$

where $S(x,y)$ is two point correlation function between two points x, y in real space. By simple algebra, the third derivative of $F[J]$ with respect to external source fields gives us a relation

$$-G_{ijk} = \sum_{lmn} S_{il}S_{jm}S_{kn}\Gamma_{lmn}, \tag{2.67}$$

where G_{ijk} is a three point correlation function and defined as $\frac{\delta^3 F[J]}{\delta J(x)\delta J(y)\delta J(z)}$ and Γ_{lmn} is given by $\frac{\delta^3 \Gamma[\overline{\varphi}(x)]}{\delta\overline{\varphi}(l)\delta\overline{\varphi}(m)\delta\overline{\varphi}(n)}$. The expansion coefficients in Landau free energy correspond to amputated diagrams(cutting the external legs in diagram). The amputation is carried by multiplying $S_{il}^{-1}S_{jm}^{-1}S_{kn}^{-1}$ on both sides of Eqn. 2.7 and summing over the indices l, m, and n. Fig. 2.7 shows the diagrammatic method to calculate the third order vertex function.

The fourth order vertex function is obtained by fourth derivative of $F[J]$ and Γ with same amputation procedure. Fig.2.8 shows the diagrams for 4th order vertex function.

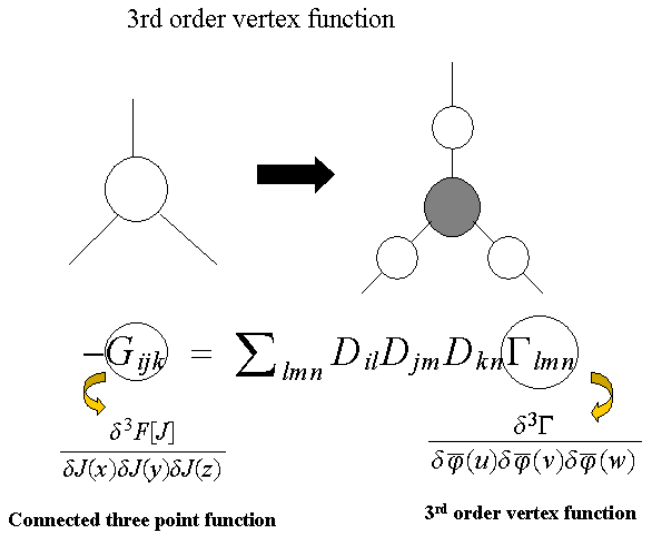

Figure 2.7 3rd order vertex function. The coefficient of the Landau free energy is the gray diagram without any external line. This is done by an amputation procedure. (35)

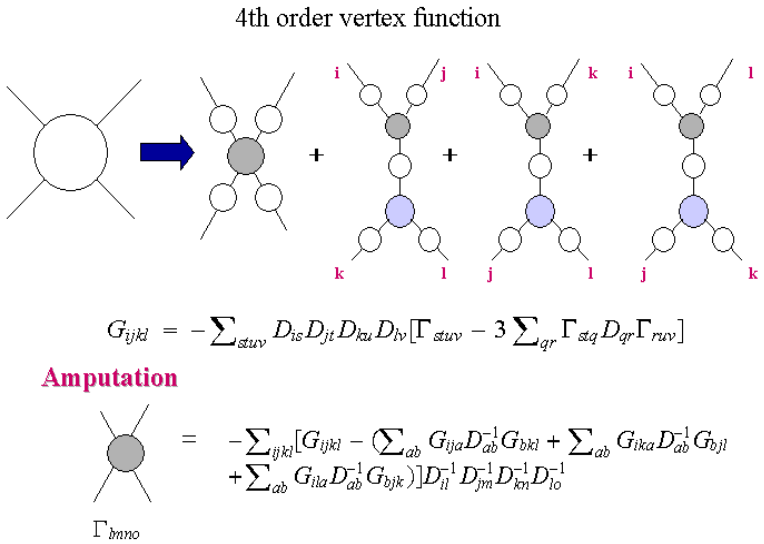

Figure 2.8 Diagramms for the 4th order vertex function (35)

The results show that

$$\Gamma^{(3)}(\mathbf{q}_1,\mathbf{q}_2,\mathbf{q}_3) = -\sum_{ijk} G^{(3)}_{ijk}(\mathbf{q}_1,\mathbf{q}_2,\mathbf{q}_3)[S^{-1}_{iA}(\mathbf{q}_1) - S^{-1}_{iB}(\mathbf{q}_1)]\times \\ [S^{-1}_{jA}(\mathbf{q}_1) - S^{-1}_{jB}(\mathbf{q}_1)][S^{-1}_{jA}(\mathbf{q}_1) - S^{-1}_{jB}(\mathbf{q}_1)]. \tag{2.68}$$

$$\Gamma^{(4)}(\mathbf{q}_1,\mathbf{q}_2,\mathbf{q}_3,\mathbf{q}_4) = \sum_{ijkl} \gamma_{ijkl}[S^{-1}_{iA}(\mathbf{q}_1) - S^{-1}_{iB}(\mathbf{q}_1)][S^{-1}_{jA}(\mathbf{q}_1) - S^{-1}_{jB}(\mathbf{q}_1)]\times \\ [S^{-1}_{kA}(\mathbf{q}_1) - S^{-1}_{kB}(\mathbf{q}_1)][S^{-1}_{lA}(\mathbf{q}_1) - S^{-1}_{lB}(\mathbf{q}_1)] \tag{2.69}$$

with

$$\begin{aligned}\gamma_{ijkl} = \sum_{\mathbf{q}',mn}[&G_{ijm}(\mathbf{q}_1,\mathbf{q}_2,\mathbf{q}')S^{-1}_{mn}(\mathbf{q}')G_{nkl}(-\mathbf{q}',\mathbf{q}_3,\mathbf{q}_4) \\ &+ G_{ikm}(\mathbf{q}_1,\mathbf{q}_3,\mathbf{q}')S^{-1}_{mn}(\mathbf{q}')G_{njl}(-\mathbf{q}',\mathbf{q}_2,\mathbf{q}_4) \\ &+ G_{ilm}(\mathbf{q}_1,\mathbf{q}_4,\mathbf{q}')S^{-1}_{mn}(\mathbf{q}')G_{njk}(-\mathbf{q}',\mathbf{q}_2,\mathbf{q}_3)] - G_{ijkl}(\mathbf{q}_1,\mathbf{q}_2,\mathbf{q}_3,\mathbf{q}_4),\end{aligned} \tag{2.70}$$

where $S^{-1}_{iA}(\mathbf{q}_1)$ is inverse two point correlation function. The calculation for the three and four point correlation functions are explained in Appendix A. Fig.2.9 shows the third and fourth order vertex functions as a function of the volume fraction f.

After these considerations, we are ready to construct the Landau free energy for block copolymers. The Hamiltonian for block copolymer can be written as

$$F_{block} = \frac{1}{2}\int_{\mathbf{q}} \Psi_{\mathbf{q}}\mathcal{G}^{-1}_{\mathbf{q}}\Psi_{\mathbf{q}} + \frac{W}{3}\int_{\mathbf{q},\mathbf{q}'} \Psi_{\mathbf{q}}\Psi_{\mathbf{q}'}\Psi_{-\mathbf{q}-\mathbf{q}'} + \frac{U}{4}\int_{\mathbf{q},\mathbf{q}',\mathbf{q}''} \Psi_{\mathbf{q}}\Psi_{\mathbf{q}'}\Psi_{\mathbf{q}"}\Psi_{-\mathbf{q}-\mathbf{q}'-\mathbf{q}"}, \tag{2.71}$$

where $\int_{\mathbf{q}}$ denotes $\int \frac{d^dq}{(2\pi)^d}$ and the integration is performed over momentum space and W and U are defined as $\frac{1}{2}\Gamma_3$, $\frac{1}{6}\Gamma_4$. In the vicinity of critical point, $10.5 < \chi S < 12$, the composition profile of A and B components in block copolymer is sinusoidal. In this weak segregation regime, we calculate the higher order vertex functions at $|\mathbf{q}| = q_0$. Fig. 2.10 shows a composition profile of block copolymer in the WSL regime.

Fig. 2.11 shows sets of wave vector in the hpc(parallelogram) and bcc(octahedron) struc-

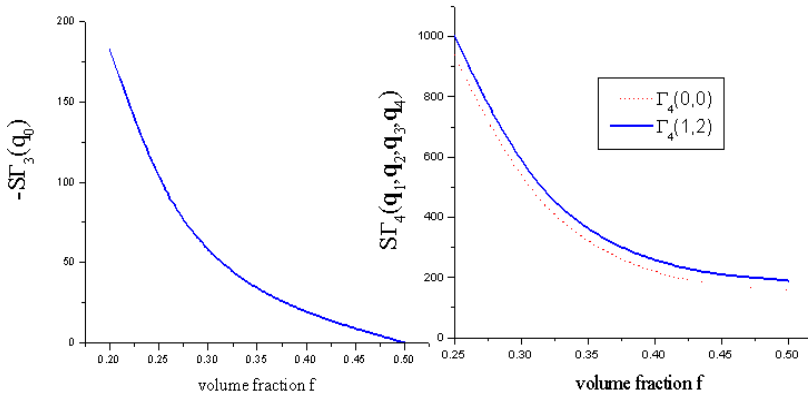

Figure 2.9 The third and fourth order vertex functions as a function of the volume fraction f (12)

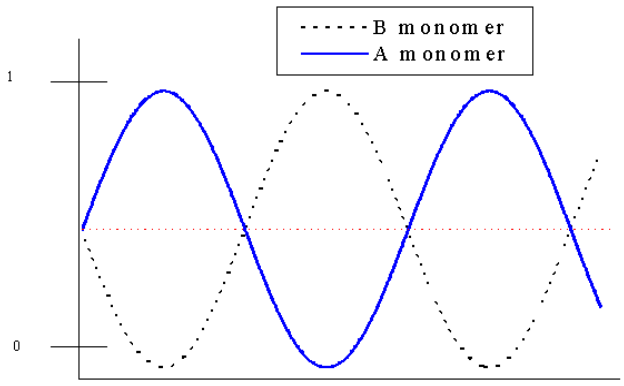

Figure 2.10 A composition profile of block copolymer in WSL regime (36)

ture. For hpc and bcc structure in Fig. 2.11, higher order vertex terms are given by

$$\Gamma_4^{hpc}(\mathbf{q}_1,\mathbf{q}_2,\mathbf{q}_3,\mathbf{q}_4) \sim 18[\Gamma_4(0,0)+4\Gamma_4(0,1)]$$
$$\Gamma_4^{bcc}(\mathbf{q}_1,\mathbf{q}_2,\mathbf{q}_3,\mathbf{q}_4) \sim 36[\Gamma_4(0,0)+8\Gamma_4(0,1)+2\Gamma_4(0,2)+4\Gamma_4(1,2)]. \quad (2.72)$$

For lamellar phase, higher order vertex functions are given by

$$\Gamma_3(\mathbf{q}_1,\mathbf{q}_2,\mathbf{q}_3) \sim \Gamma_3(q_0)$$
$$\Gamma_4(\mathbf{q}_1,\mathbf{q}_2,\mathbf{q}_3,\mathbf{q}_4) \sim 6\Gamma_4(0,0). \quad (2.73)$$

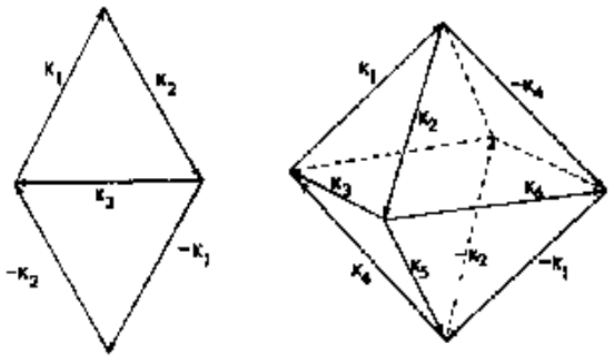

Figure 2.11 Wave vector sets in hpc and bcc structure. This structure determines the higher order vertex function. (37)

The Landau free energy for each structure is minimized in $\Psi_{\mathbf{q}}$ giving $\Psi_{\mathbf{q}} = 0$ in the disordered state and $\Psi_{\mathbf{q}} = \overline{\Psi}_{\mathbf{q}} \neq 0$ in the microphases. (37) The correlation function of block copolymer can be transformed into Brazovskii type correlation function.

$$\mathcal{G}_{\mathbf{q}} = \frac{Z}{\varepsilon_0^2 q_0^2 + (q-q_0)^2} \quad (2.74)$$

with the bare mass $\varepsilon_0^2 = \dfrac{F^* - 2\chi S}{F^{**}x^{*2}}$, $q_0 R_0 = x^*$ and $Z = \dfrac{S}{F^{**}R_0^2} = \dfrac{6}{F^{**}b^2}$. Fig. 2.12 shows the phase diagram of diblock copolymer for different volume fraction within mean field calculation. The higher order vertex functions are calculated from Eqn. 2.72.

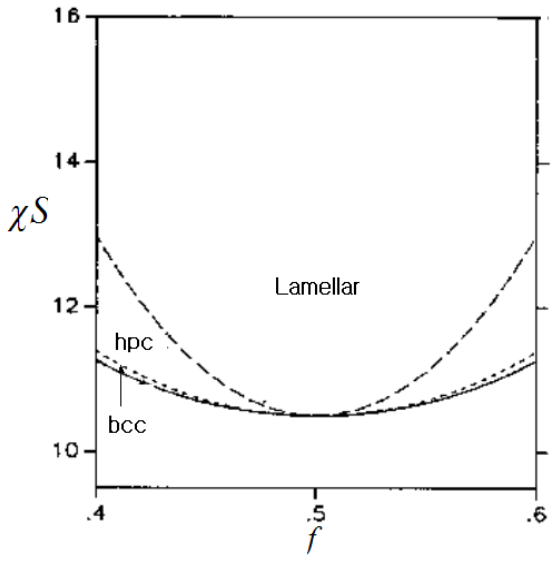

Figure 2.12 The phase diagram of a diblock copolymer for different volume fraction within the mean field calculation (37)

Especially, the mean field solution predicts that the order-disorder transition of a lamellar mesophase for $f = 0.5$ is second order(disorder→bcc→hexagonal→lamellar). When the temperature approaches to order-disorder transition region, the composition fluctuation with $|\mathbf{q}| \neq q_0$ plays an important role. (12) It was known that the fluctuation induces a first order transition for the symmetric case $f = 0.5$. (14). The Fredrickson-Helfand analysis with the fluctuation effect demonstrates order-disorder transition of lamellar phase for $f = 0.5$ undergoes a first order transition(Disorder→Lamellar), which is quite consistent with the experimental result. Fig. 2.13 shows the order-disorder phase transition of lamellar phase for the volume fraction f by mean field calculation and the fluctuation effect correction to the mean field solution.

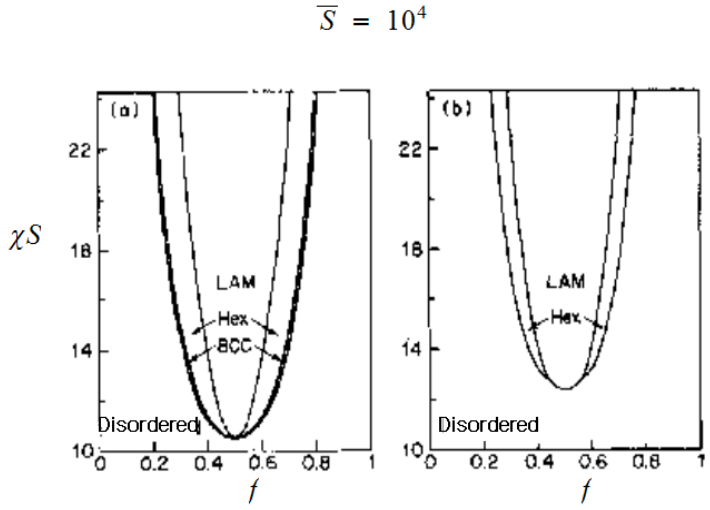

Figure 2.13 The phase diagram of a diblock copolymer by mean field calculation and fluctuation correction to the mean field solution. (16)

Qualitatively, the first order transition behavior can be understood using Fig. 2.14. Fig. 2.14 shows the free energy density in Hartree approximation as a function of the amplitude of lamellar phase. The Hartree free energy density is given by $f_H(A) = \tau_R A^2 + \frac{u_R}{4} A^4 + \frac{w_R}{36} A^4$. τ_R,u_R and w_R are temperature dependent renormalized parameter. (13) (a) in Fig. 2.14 shows a disordered state with the minimum $A = 0$. (b) shows a metastable state and (c) shows the fluctuation induced first order transition with the minimum $A = 0$ and $A \neq 0$ at $(\chi S)_t$. (d) shows a stable lamellar phase with $A \neq 0$ below $(\chi S)_t$. (38)

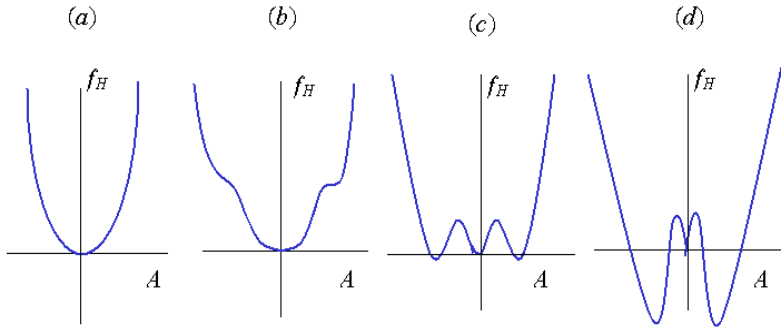

Figure 2.14 The fluctuation induced first order transition (38)

Quantitatively, the mean field solution is modified by the fluctuation effect as

$$\mathcal{G}_{\mathbf{q}}{}^{-1} = \frac{1}{S}\left[F(x,f) - 2\chi S + \frac{c^3 d\lambda}{\overline{S}^{1/2}} \frac{\mathcal{G}_{q_0}}{\sqrt{S}}\right], \tag{2.75}$$

where $\overline{S} = Sb^6/v^2$ and b, v are persistence length and volume. (13) $d = 3x^*/2\pi$, c, and λ are composition dependent coefficients. (13) $F(x,f)$ is defined in Eqn. 2.62. For example, $c = 1.10195$, $d = 1.8073$, and $\lambda = 106.18$ for symmetric block copolymer($f = 0.5$). (38) From

the nonlinear equation, $(\chi S)_t$ is given by

$$(\chi S)_t \sim 10.5 + 41\overline{S}^{-1/3}. \tag{2.76}$$

When we set $b = 1$ and $v = 1$=1, $(\chi S)_t \sim 10.5 + 41S^{-1/3}$. Fig. 2.9 shows the vertex functions are inversely proportional to the degree of polymerization number S. Longer polymeric chains in block copolymer imply the smaller vertex terms, which means that the validity of the perturbative treatment to block copolymer depends on the chain length of the block copolymer. This perturbative correction to the mean field theory is safe only for large $S(\ S > 10^4)$. (13) The equilibrium physics of block copolymer is well described by the Brazovskii model, which motivates to analyze the nonequilibrium properties of it. We expect the nonequilibrium physics of block copolymers to be deeply relevant to the nonequilibrium properties of Brazovskii model. In chapter 3, the glassy behavior of Brazovskii model will be discussed.

2.5 Model for a physically reversible associating polymer

In this section, we consider a physically reversible associating polymer, in which there exists an attractive hydrophobic interactions between the end segments of ABA type symmetric triblock copolymer chains. There are two types interactions, the excluded volume interaction between monomers and the attractive interaction at end segments, which causes a frustration in a physically reversible associating polymer.

There are two kinds of gels, *chemical gel and physical gel*. A strong bond such as covalent bond is involved in a chemical gel, an effect of great importance to vulcanization phenomena. Destruction of the chemical bonds leads to the denaturation of polymer chains. On the other hand, the weak chemical bonds such as van der Waals or hydrogen interactions are involved in making physical gels. Since the bonding interaction is weak (order of kT), the gelation in the physical gel is thermoreversible. (39)

The two point correlation functions of symmetric ABA triblock copolymer are adapted in this associating polymer problem. The number of associations in the system is controlled by an interaction strength Q. In equilibrium, the partition function is characterized in addition to excluded interaction term,

$$Z_{asscoation} = \langle \exp(-V_P) \rangle^E$$

$$V_P = -\sum_{n_1,\cdots,n_p} \sum_{s_1,\cdots,s_p} U(\mathbf{R}_{n_1,s_1},\cdots,\mathbf{R}_{n_p,s_p}) \prod_{i,j(i>j)} (1-\delta_{n_i,n_j}\delta_{\widehat{s}_i,\widehat{s}_j}), \tag{2.77}$$

where V_P is the potential energy causing the aggregations and The label of the end point segments $\widehat{s}$ is defined as $\widehat{s} = 1 \cdots fS$ and $S - fS \cdots S.P$ is the number of segments which are joining at a given association. From the definition of interaction energy for the association, we exclude the self interaction for the same end segments within the same polymer chains ($\delta_{n_i,n_j}\delta_{\widehat{s}_i,\widehat{s}_j} = 1$). However, for even the same polymer chains, we allow the association between a different end segments within the same polymer chain. ($\delta_{n_i,n_j} = 1$ & $\delta_{\widehat{s}_i,\widehat{s}_j} = 0$). Fig. 2.15 shows the dumbbell and backfolding structure of the end to end looping.

As the composition value f of the end point segments increases, we should consider a backfolding structure despite the entropy penalty comes along with it. (41) (40) In what

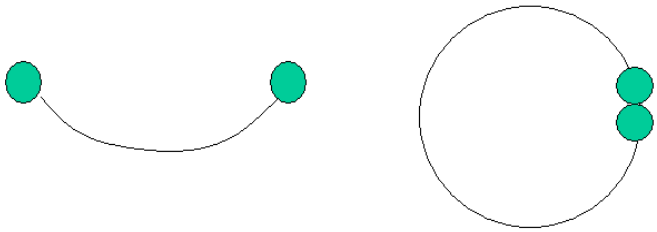

Figure 2.15 The dumbbell and backfolding structure.

follows we consider $P = 3$ and $P = 4$. It holds

$$V_3 = -\sum_{n_1,\cdots,n_3}\sum_{s_1,\cdots,s_3} U(\mathbf{R}_{n_1,s_1},\mathbf{R}_{n_2,s_2},\mathbf{R}_{n_3,s_3})\prod_{i,j(i>j)}(1-\delta_{n_i,n_j}\delta_{\widehat{s}_i,\widehat{s}_j})$$
$$V_4 = -\sum_{n_1,\cdots,n_4}\sum_{s_1,\cdots,s_4} U(\mathbf{R}_{n_1,s_1},\mathbf{R}_{n_2,s_2},\mathbf{R}_{n_3,s_3},\mathbf{R}_{n_4,s_4})\prod_{i,j(i>j)}(1-\delta_{n_i,n_j}\delta_{\widehat{s}_i,\widehat{s}_j}), \qquad (2.78)$$

where we assumed the form of the three and four body interaction causing the associated interaction between end segments. We express V_3 and V_4 in terms of these collective coordinates:density of end segments. We assume that the three body and four body interaction as

$$U(\mathbf{R},\mathbf{R},\mathbf{R}'') = u(\mathbf{R}-\mathbf{R}')u(\mathbf{R}-\mathbf{R}'')$$
$$U(\mathbf{R},\mathbf{R}',\mathbf{R}'',\mathbf{R}''') = u(\mathbf{R}-\mathbf{R}')u(\mathbf{R}-\mathbf{R}'')u(\mathbf{R}-\mathbf{R}''') \qquad (2.79)$$

and the finite range potential $u(\mathbf{r})$ can be characterized by a strength

$$Q^{1/2} = \int d^3r u(\mathbf{r}). \qquad (2.80)$$

Typical length scale a_1(for example, $u(\mathbf{r}) = \frac{Q^{1/2}}{a_1^3}\exp\left(-(8\pi)^{1/3}r/a_1\right)$). In the limit $a_1 \to 0$, we obtain $u(\mathbf{r}) = Q^{1/2}\delta(\mathbf{0})$.In case, we obtain $u(\mathbf{0})$ at some point, this has then to be understood as $Q^{1/2}\delta(\mathbf{0}) = Q^{1/2}a_1^{-3}$. The typical size of a single end segment ,l_{end}, has a range of $\left(\frac{1}{6}fS\right)^{1/2} b < l_{end} < fSb$. Clearly, the characteristic length a_1 should be larger than l_{end} for an actual association. We demand $a_1/l_{end} = M > 1$. Especially, the attractive interaction between the end segments is originated from a hydrophobic polymers such as poly(styrene) or HEUR (hydrophobic ethoxylated urethane). (42) The stiffness of the end segments will be an important factor for the association. In our calculation, we increase M for an effective interaction between the end segments of polymer chains instead of changing the persistence length b of the end point segment. Using the lower estimate for l_{end},which is the more conservative constraint on a_1, we find

$$a_1 = Mb\left(\frac{1}{6}fS\right)^{1/2}. \tag{2.81}$$

The particle density of the end point segments are given as

$$\begin{aligned}\rho_c(\mathbf{r}) &= \sum_{n,s}{}' \delta\left(\mathbf{r} - \mathbf{R}_{n,s}\right)\\ \rho_e(\mathbf{r}) &= \sum_{n,s}{}'' \delta\left(\mathbf{r} - \mathbf{R}_{n,s}\right).\end{aligned} \tag{2.82}$$

The $\sum''_{n,s}$ summation over only the end point segments $s = 1\cdots fS$ and $S - fS$. The end point segments corresponds to A polymer block region and the central part to B block region in a triblock copolyemr. In this section, we use a notation $\rho_e(\mathbf{r})$ rather than $\rho_A(\mathbf{r})$ to emphasize the end segments. As shown in Appendix C, V_3 and V_4 can be expressed in terms of $\rho_e(\mathbf{r})$. Introducing the density field fluctuation field, $\Psi(\mathbf{r}) = \rho_e(\mathbf{r}) - \overline{\rho_e}$ and using $\int d^dr\Psi(\mathbf{r}) = 0$, we obtain $V_3[\Psi(\mathbf{r})]$ and $V_4[\Psi(\mathbf{r})]$ as

$$\begin{aligned}V_3[\Psi(\mathbf{r})] &= -Q\int d^3r\Psi(\mathbf{r})^3 + 3Q(2fSa_1^{-3} - \overline{\rho_e})\int d^3r\Psi(\mathbf{r})^2 + const.\\ V_4[\Psi(\mathbf{r})] &= -Q^{3/2}\int d^3r\Psi(\mathbf{r})^4 + 4Q^{3/2}(3a_1^{-3}fS - \overline{\rho_e})\int d^3r\Psi(\mathbf{r})^3\\ &\quad + 6Q^{3/2}(6a_1^{-3}fS\overline{\rho_e} - \overline{\rho_e}^2 - 10f^2S^2a_1^{-6})\int d^3r\Psi(\mathbf{r})^2 + const.\end{aligned} \tag{2.83}$$

In Fig. 2.16 and Fig. 2.17, we show various types of diagrams and their contributions for V_3 and V_4 interactions.

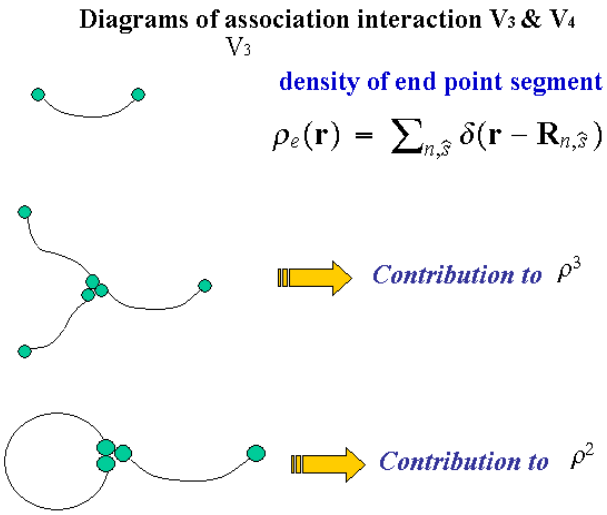

Figure 2.16 The diagrams for V_3 interaction

The rescaled free energy for associating polymer in terms of $\varphi(r)(= Z^{-1/2}\Psi(r))$ can be written as

$$F_{rescaled} = \frac{1}{2}\int_{\mathbf{q}} \varphi_{\mathbf{q}} \mathbf{G}_{\mathbf{q}}^{-1} \varphi_{\mathbf{q}} + \frac{\upsilon_{eff}}{3}\int_{\mathbf{q},\mathbf{q}'} \varphi_{\mathbf{q}}\varphi_{\mathbf{q}'}\varphi_{-\mathbf{q}-\mathbf{q}'} + \frac{u_{eff}}{4}\int_{\mathbf{q},\mathbf{q}',\mathbf{q}''} \varphi_{\mathbf{q}}\varphi_{\mathbf{q}'}\varphi_{\mathbf{q}"}\varphi_{-\mathbf{q}-\mathbf{q}'-\mathbf{q}"}, \tag{2.84}$$

where the rescaled correlation function $\mathbf{G}_{\mathbf{q}}^{-1}$ is defined as like block copolymer system

$$\mathbf{G}_{\mathbf{q}}^{-1} = \frac{1}{\varepsilon_0^2 q_0^2 + (q - q_0)^2} \tag{2.85}$$

with only the difference of rescaled vertex coefficients

$$\begin{aligned} u_{eff} &= Z^2 U = Z^2 \left(\frac{1}{6}\Gamma_4(q_0, q_0) - 4Q^{3/2}\right) \\ \upsilon_{eff} &= Z^{3/2} W = Z^{3/2}\left(\frac{1}{2}\Gamma_3(q_0) + 12Q^{3/2}(3a_0^{-3} f S - \overline{\rho_e}) - 3Q\right) \end{aligned} \tag{2.86}$$

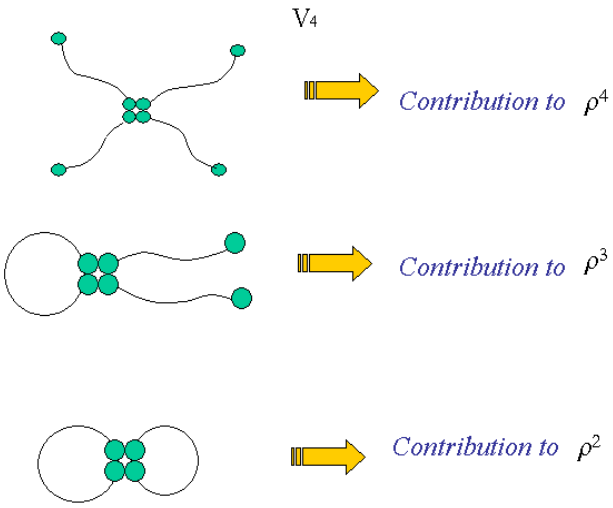

Figure 2.17 The diagrams for V_4 interaction

also with

$$\varepsilon_0^2 = \frac{F^* - 2\chi_{eff}S}{F^{**}x^{*2}}$$

$$\chi_{eff} = \chi - 3Q(2fSa_1^{-3} - \overline{\rho_e}) - 6Q^{3/2}(6a_1^{-3}fS\overline{\rho_e} - \overline{\rho_e}^2 - 10f^2S^2a_1^{-6}), \qquad (2.87)$$

where the average density of end segments is given by $\overline{\rho_e} = \frac{2fNS}{V}$. For a description of 3-dimensional network between the end segments, we choose $\Gamma_3(\mathbf{q}_1, \mathbf{q}_2, \mathbf{q}_3)$ and $\Gamma_4(\mathbf{q}_1, \mathbf{q}_2, \mathbf{q}_3, \mathbf{q}_4)$ as $\Gamma_3(q_0)$ and $\Gamma_4(q_0, q_0)$ since $\Gamma_4(q_0, q_0)$ makes nonplanar circuit. The effective interaction coefficients v_{eff}, u_{eff} are the net results of the repulsive excluded volume interaction between polymer chains and the attractive association between end segments.

CHAPTER 3. REPLICA APPROACH TO A GLASSY BEHAVIOR

3.1 Introduction

The purpose of this chapter is to discuss the replica approach for self generated glassiness, in which the glassiness is generated without quenched randomness. The replica approach is one of the prevailing method to deal with glassy behavior in glass forming materials. The replica approach has been applied first in the theory of spin glasses with quenched randomness. (43) Later on, the replica approach was developed to describe the self generated glassiness in systems without quenched randomness. (6) At first, the basic concept of the replica approach to glassiness in the systems with quenched randomness will be discussed. And then, the replica approach to the self generated glassiness will be explained in detail. The two replica approaches to glassy systems with and without quenched randomness share the similarity in that they introduce copies of the system(replicas) in calculating its free energy. Within the replica scheme for the self generated glassiness, the overlap between two different replicas is interpreted as long time correlation function. In obtaining long time correlation function, which is the order parameter of glassiness, two different mathematical techniques are used, an analytical and a numerical method. The analytical method is self consistent perturbation theory using Feynman diagrams called the SCSA(self consistent screening approximation). On the other hand, the numerical method is based on the dynamical mean field theory (DMFT), which was developed for strongly correlated electrons in transition metals. (52) At the end of this chapter, the analytical and numerical methods are compared for same model.

3.2 Replica approach for a system with quenched randomness

As an example of glassiness in case of quenched randomness, we will consider an Ising spin glass with infinite long range interaction known as Sherrington-Kirkpatrick (SK) model. (44) The Hamiltonian of the SK model is

$$H = -\frac{1}{2}\sum_{ij} J_{ij} S_i S_j - h\sum_i S_i, \tag{3.1}$$

where i, j includes all the site. J_{ij} is random interaction between the magnetic materials and h is external We assume J_{ij} has distribution as

$$P(J_{ij}) = \left(\frac{N}{2\pi J^2}\right)^{1/2} \exp\left[-\frac{N(J_{ij} - J_0/N)}{2J^2}\right], \tag{3.2}$$

where N is total number of spins and J_0 is a mean value. We are interested in the free energy of the system

$$F[J] = -T \ln Z[J]. \tag{3.3}$$

Since the free energy is an extensive quantity, the self averaging is satisfied. The average is performed over the distribution of J. Eqn. 3.3 is given as

$$F = -T \int dP[J] \ln Z[J]. \tag{3.4}$$

We have to evaluate the average $\ln Z[J]$. The mathematical trick is to perform this average based on the identity:

$$\ln Z = \lim_{m\to 0} \frac{Z^m - 1}{m}, \tag{3.5}$$

where m is a replica index. The average is performed over $Z^m[J]$. The replicated partition function for SK Ising model can be written as

$$[Z^m]_{av} = Tr_s \int \prod_{ij} dJ_{ij} \left(\frac{N}{2\pi J^2}\right)^{1/2} \exp\left[-\frac{N(J_{ij} - J_0/N)^2}{2J^2} + \frac{\beta}{2}\sum_{ij,a} J_{ij} S_i^\alpha S_j^\alpha + \beta h \sum_{i,a} S_i^\alpha\right].$$

After some algebra, $[Z^m]_{av}$ is written as

$$[Z^m]_{av} = Tr_s \exp\left[\frac{J^2\beta^2}{8N}\left(mN^2\right) + \sum_{\alpha\beta}\frac{J^2\beta^2}{8N}\left(\sum_i S_i^\alpha S_i^\beta\right)^2 + \frac{\beta J_0}{2N}\sum_\alpha\left(\sum_i S_i^\alpha\right)^2 + \beta h\sum_{i,a} S_i^\alpha\right], \tag{3.6}$$

where m is dimension of replica space and N is number of spins. We introduce Hubbard-Stratonovich transform, by which we can decouple a spin interaction at a different site. By penalty for the transform, we should calculate a spin coupling for a different replica space. we can express $[Z^m]_{av}$ in more simple form as

$$\begin{aligned}[Z^m]_{av} &= \exp[mN\frac{1}{2}(\beta J)^2]\times \\ &\int_{-\infty}^{\infty}\prod_{\alpha\beta}\frac{\beta J N^{1/2}}{\sqrt{2\pi}}dq^{\alpha\beta}\prod_{\alpha}\left(\frac{\beta J_0 N}{2\pi}\right)^{1/2}dx^{\alpha}\exp[-NG] \end{aligned} \tag{3.7}$$

with

$$\begin{aligned}G &\equiv \frac{1}{2}N(\beta J)^2\sum_{\alpha\beta}\left(q^{\alpha\beta}\right)^2+\frac{1}{2}N\beta J_0\sum_{\alpha}(x^{\alpha})^2 \\ &-\log Tr_s\exp\left[\frac{1}{2}(\beta J)^2\sum_{\alpha\beta}q^{\alpha\beta}S^{\alpha}S^{\beta}+\beta\sum_{\alpha}(J_0x^{\alpha}+h)S^{\alpha}\right]\end{aligned} \tag{3.8}$$

Applying the saddle point method to calculate 3.7, the condition at the saddle points$(q_0^{\alpha\beta}, x_0^{\alpha})$ $\frac{\partial G}{\partial q_0^{\alpha\beta}}=0$ and $\frac{\partial G}{\partial x_0^{\alpha}}=0$ leads to

$$\begin{aligned}q_0^{\alpha\beta} &= \left\langle S^{\alpha}S^{\beta}\right\rangle \equiv \widetilde{Z}^{-1}Tr_s\left[S^{\alpha}S^{\beta}\exp H_{eff}\right] \\ x_0^{\alpha} &= \langle S^{\alpha}\rangle \equiv \widetilde{Z}^{-1}Tr_s\left[S^{\alpha}\exp H_{eff}\right] \\ \widetilde{Z} &\equiv Tr_s\left[\exp H_{eff}\right]\end{aligned} \tag{3.9}$$

with the effective Hamiltonian $H_{eff}=\frac{1}{2}(\beta J)^2\sum_{\alpha\beta}q_0^{\alpha\beta}S^{\alpha}S^{\beta}+\beta\sum_{\alpha}(J_0x_0^{\alpha}+h)S^{\alpha}$. The free energy density$(f=F/N)$ with the saddle point ($\frac{\partial f}{\partial q_0^{\alpha\beta}}=0$ and $\frac{\partial f}{\partial x_0^{\alpha}}=0$) is given by

$$\begin{aligned}-\beta f &= \lim_{n\to 0}\left[\frac{1}{2}(\beta J)^2\left(1-\frac{1}{m}\sum_{\alpha\beta}\left(q_0^{\alpha\beta}\right)^2\right)\right. \\ &\left.-\frac{\beta J_0}{2m}\sum_{\alpha}(x_0^{\alpha})^2+\frac{1}{m}\log Tr_s\exp H_{eff}\right].\end{aligned} \tag{3.10}$$

The order parameters $q_0^{\alpha\beta}$ and x_0^{α} are relevant to glassiness and ferromagnetic ordering. The glass order parameter $q_0^{\alpha\beta}$ depends on the replica index α,β. The simple way of solving Eqn. 3.10 is to make $q_0^{\alpha\beta}$ replica independent q, which is so called replica symmetric solution

(RS). In the RS solution, $q_0^{\alpha\beta} = q$ and $x_0^{\alpha} = M$, the free energy density in the limit of $m \to 0$ leads to

$$-\beta f = \frac{1}{2}(\beta J)^2(1-q^2) - \frac{1}{2}\beta J_0 M^2 + \frac{1}{\sqrt{2\pi}}\int_{-\infty}^{\infty} dz e^{-\frac{1}{2}z^2} \log\cosh\eta(z), \tag{3.11}$$

where $\eta(z) = \beta(J\sqrt{q}z + J_0 M + h)$. From the condition for free energy density ($\frac{\partial f}{\partial q} = 0$ and $\frac{\partial f}{\partial M} = 0$), we can get the self consistent equation for two order parameters q and M such as

$$M(T,h) = \frac{1}{\sqrt{2\pi}}\int_{-\infty}^{\infty} dz e^{-\frac{1}{2}z^2} \tanh\eta(z) \tag{3.12}$$

$$q(T,h) = \frac{1}{\sqrt{2\pi}}\int_{-\infty}^{\infty} dz e^{-\frac{1}{2}z^2} \tanh^2\eta(z). \tag{3.13}$$

The phase diagram for Ising SK with infinite range interaction for $h = 0$ is shown in Fig.3.1.

The line 1 in Fig.3.1 is obtained from $q \to 0, M = 0$. By expanding Eqn. 3.13 with $\tanh^2 x \sim x^2 - \frac{2}{3}x^4$ near by the transition temperature T_f , we have

$$\begin{aligned} q &\sim (\beta J)^2 q - 2(\beta J)^4 q^2 \\ 1 &= (\beta J)^2 - 2(\beta J)^4 q. \end{aligned} \tag{3.14}$$

For small q, the glass transition temperature T_f is given as

$$T_f = kJ. \tag{3.15}$$

The line 3 in Fig. 3.1 is obtained from $q = 0, M \to 0$. By expanding Eqn.3.12 with $\tanh x \sim x - \frac{1}{3}x^3$ near by the magnetic transition temperature T_c, we have

$$\begin{aligned} M &\sim M\beta J_0 - \frac{2}{3}M^3\beta^3 J_0^3 \\ 1 &= \beta J_0 - \frac{2}{3}M^2\beta^3 J_0^3. \end{aligned} \tag{3.16}$$

For small M, the ferromagnetic transition temperature T_c is given as

$$T_c = kJ_0. \tag{3.17}$$

The line 3 in Fig. 3.1 is obtained from the condition of $q \neq 0, M = 0$ numerically. However, SK Ising model has two problems in that the solution is not stable below AT line(Almeida-Thouless line):eigenvalues of the Hessian matrix $A^{\alpha\beta,\gamma\delta} \equiv \frac{\partial^2 G}{\partial q^{\alpha\beta}\partial q^{\gamma\delta}}$ are not positive and entropy

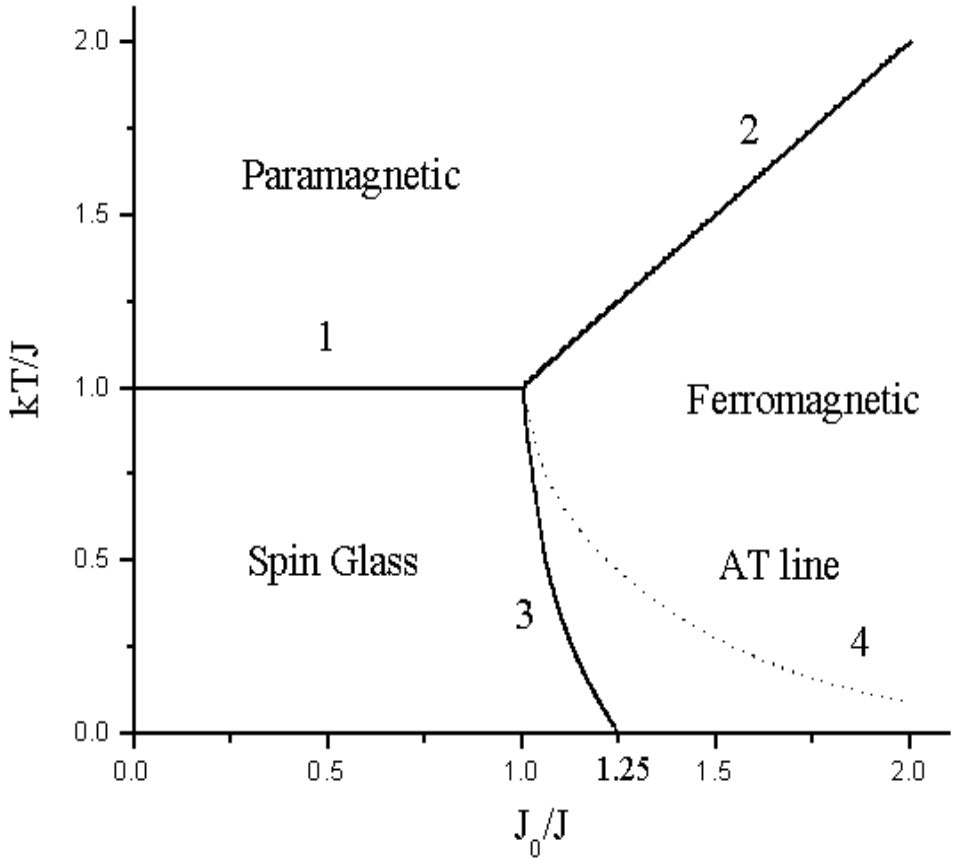

Figure 3.1 Phase diagram of the Ising SK model with infinite range interaction for $h = 0(27)(44)$

is negative, which requires us to find another solution beyond mean field calculation.(45) AT line is obtained from the inequality

$$\left(\frac{1}{J\beta}\right)^2 > \frac{1}{\sqrt{2\pi}}\int dz e^{-\frac{1}{2}z^2} Sech^4\left[\beta(J\sqrt{q}z + J_0 M + h)\right] \tag{3.18}$$

with Eqn. 3.12 and Eqn. 3.13. (45) More accurate solution is found by replica symmetry breaking (RSB) schemes. (46) The RSB solution is replica permutation breaking solution. In the replica symmetric solution(RS), the order parameter matrix $q_0^{\alpha\beta}$ in $m \times m$ replica space has all the same elements q_0. The RSB strategy is to divide $m \times m$ replica matrix into $m/m_1 \times m/m_1 (m/m_1$ is integer for $m \geq m_1 \geq 1)$ and replace q_0 by q_1 in the diagonal block in one step RSB. Fig. 3.2 shows one step and two step RSB schemes. q_0 in the block diagonal is replaced by q_1 and the elements of the off diagonal block are not changed in one step RSB. And the same procedure is repeated with $m_1 \times m_1$ block diagonal submatrix. In this case, $m_1 \times m_1$ replica matrix is broken into $m_1/m_2 \times m_1/m_2 (m_1/m_1$ is also integer for $m \geq m_1 \geq m_2 \geq 1)$ and replace q_1 by q_2 in the diagonal block in two step RSB.

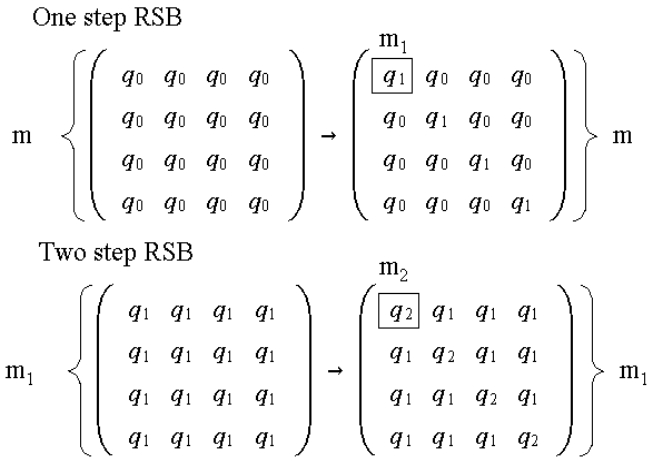

Figure 3.2 Iterative procedure for the construction of the matrix $q^{\alpha\beta}$ (47)

This iterative procedure can be repeated infinitely. Finally, in the limit $m \to 0$, we have

$0 \leq m_1 \leq m_2 \cdots \leq 1$. m_i become not integer but continuous value x_i by analytic continuation. The order parameter q_i also becomes a continuous function $q(x)$ for the interval $0 \leq x \leq 1$. The analysis of eigenvalues with RSB schemes show that there are no negative eigenvalues, which proves the Parisi solution is marginally stable for all the fluctuation (48). The instability below AT line and negative entropy problems in SK model for zero magnetic field are cured by RSB schemes. (27) Summarizing the replica steps to glassiness with quenched randomness, at first we calculate the replicated partition function $[Z^m]_{av}$ with saddle point method. And then one write down the saddle point equation $\frac{\partial G}{\partial q_0^{\alpha\beta}} = 0$ and Hessian matrix $\frac{\partial^2 G}{\partial q^{\alpha\beta} \partial q^{\gamma\delta}}$. In next step, we make an ansatz for $q^{\alpha\beta}$, for example, one step RSB as like Fig. 3.2, to plug this ansatz to saddle point equation and the Hessian matrix. The check of the stability of eigenvalues in the limit of $m \to 0$ becomes the final step of the replica calculation. (49) The above procedure for replica approach can be applied to the glassiness without quenched randomness with the main difference of $m \to 1$. In next section, we will discuss about the replica approach for the system without quenched randomness.

3.3 Replica approach for a system without quenched randomness

The theoretical approach to glassiness without and with quenched randomness is complwtely quite different. A widely accepted view is that the system gets trapped in local metastable states for very long time and can therefore not realize a considerable part of the entropy of the system, called the configurational entropy $S_{\rm c} = \log \mathcal{N}_{\rm ms}$, where $\mathcal{N}_{\rm ms}$ is the number of metastable states. (68) (69). If $\mathcal{N}_{\rm ms}$ is exponentially large with respect to the size of the system, $S_{\rm c}$ becomes extensive and equilibrium thermodynamics cannot be applied anymore. There are several theoretical approaches which offer a solution to this breakdown of equilibrium many body theory. On the one hand one can solve for the time evolution of correlation and response functions, an approach which explicitly reflects the dynamic character of the glassy state. Mostly because of its technical simplicity, an alternative (but in many senses equivalent) approach is based on a replica theory. (6)(7) Even though this approach does not allow to calculate for the complete time evolution, long time correlations as well as stationary response functions can be determined which are in agreement with the explicit dynamic theory. We will use the replica approach because of its relative simplicity. A simple example of ergodicity breaking occurs in ferromagnetism. As shown in Fig. 3.3, the spin up region and spin down region is separated by a large barrier that diverges with the system size. Ergodically averaging the magnetization for spin up and spin down region gives us zero. However, after applying an infinitesimal external field to the system to select only the spin up region like Fig. 3.3, we obtain finite magnetization. Thus, an external field can select one of the various states in the system. After the thermodynamic limit $N \to \infty$, one can then take the limit $h \to 0$ and the magnetization becomes finite.

The only half of the state, which is on one side from barrier, contributes to the physical observable. (28). Basically, the replica approach for the self generated glassiness adapts the similar scheme in the ergodicity breaking in ferromagnetic case. In this section, we will discuss the mathematical technique of this replica approach to the self generated glassiness.

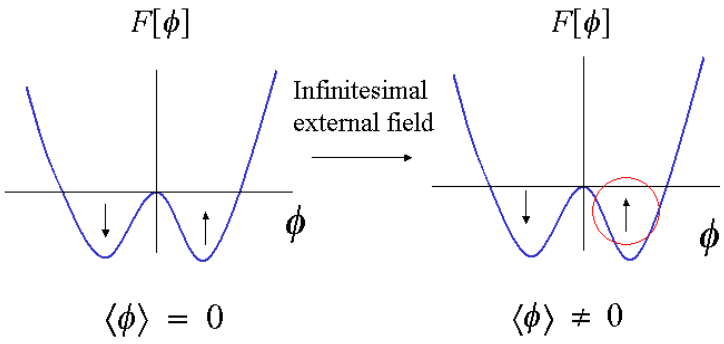

Figure 3.3 Ergodicity breaking in ferromagnetic system

The partition function in the presence of the ergodicity breaking field is given as

$$\widetilde{Z}[h] = \int d\phi e^{-\beta H[\phi,h]}. \tag{3.19}$$

And we choose the following form for this additional field:

$$H[\phi,h] = H[\phi] + \frac{g}{2\beta}\int dx\,[\phi(x)-h(x)]^2\,, \tag{3.20}$$

where $g > 0$ is a coupling constant. Usually, we have to take the limit $g \to 0$ after the thermodynamic limit. When the external field lies nearby the bottom of a well of the unperturbed free energy, the exponential term, $\frac{g}{2\beta}\int dx\,[\phi(x)-h(x)]^2$, becomes most dominant. Therefore we can find a useful information about the free energy landscape by scanning the entire space of the configurations of the external field $h(x)$. (6)

The free energy density for such a local metastable configuration is given by

$$\widetilde{f}[h] = -\frac{1}{\beta}\log\widetilde{Z}[h]. \tag{3.21}$$

The random external field leads to a number of ground states, which introduce the concept of probability for the configurations $\widetilde{p}[h]$. The probability $\widetilde{p}[h]$ has a form of Boltz-

man factor $\exp[-\beta\widetilde{f}[h]]$ which is justified from maximizing the configurational entropy $S_c(= -\int \mathcal{D}h\widetilde{p}[h]\log\widetilde{p}[h])$. The weight average of the free energy density is given as

$$\widetilde{F} = -\lim_{g\to 0}\frac{1}{\beta}\frac{\int \mathcal{D}h\widetilde{p}[h]\widetilde{f}[h]}{\int \mathcal{D}h\widetilde{p}[h]} \tag{3.22}$$

$$= -\lim_{g\to 0}\frac{1}{\beta}\frac{\int \mathcal{D}h\widetilde{Z}[h]\log\widetilde{Z}[h]}{\int \mathcal{D}h\widetilde{Z}[h]}. \tag{3.23}$$

The mathematical trick to integrate $\log\widetilde{Z}[h]$ is to use the following identity:

$$\frac{\partial}{\partial m}\log\left(\int \mathcal{D}h\widetilde{Z}^m[h]\right) = \frac{\int \mathcal{D}h\widetilde{Z}^m[h]\log\widetilde{Z}^m[h]}{\int \mathcal{D}h\widetilde{Z}^m[h]} \tag{3.24}$$

which leads to the result:

$$\begin{aligned}\widetilde{F} &= -\lim_{g\to 0}\frac{1}{\beta}\frac{\int \mathcal{D}h\widetilde{Z}[h]\log\widetilde{Z}[h]}{\int \mathcal{D}h\widetilde{Z}[h]} \\ &= -\lim_{g\to 0}\frac{1}{\beta}\frac{\partial}{\partial m}\log\left(\int \mathcal{D}h\widetilde{Z}^m[h]\right)\Big|_{m\to 1}.\end{aligned} \tag{3.25}$$

Defining $F(m)$ as

$$\begin{aligned}F(m) &= -\lim_{g\to 0}\frac{1}{m\beta}\log\left(\int \mathcal{D}h\widetilde{Z}^m[h]\right) \\ &= -\lim_{g\to 0}\frac{1}{m\beta}\log\left(\int \mathcal{D}h\exp[-m\beta\widetilde{f}[h]\right)\end{aligned} \tag{3.26}$$

with

$$\widetilde{Z}^m[h] = \int d^m\phi\exp\left[-\sum_{\alpha=1}^{m}H[\phi_\alpha,h]\right], \tag{3.27}$$

where α is replica index, the typical free energy of metastable state can be derived from

$$\widetilde{F} = \frac{\partial mF(m)}{\partial m}\Big|_{m=1}. \tag{3.28}$$

Also, the configurational entropy S_c can be calculated as

$$\begin{aligned}S_c &= -\int \mathcal{D}h\widetilde{p}[h]\log\widetilde{p}[h] \\ &= -\int \mathcal{D}h\widetilde{Z}[h]\log\widetilde{Z}[h].\end{aligned} \tag{3.29}$$

Using $\int \mathcal{D}h\widetilde{p}[h] = 1$, the configurational entropy S_c is given as

$$S_c = \frac{m^2}{T}\frac{\partial F(m)}{\partial m}\Big|_{m=1}. \tag{3.30}$$

The Eqn. 3.28 and 3.9 can be derived from *pseudo thermodynamics* by replacing β by $m\beta$. Defining $T_{eff} = T/m$, the configurational entropy can be expressed as

$$F = \widetilde{F}(T_{eff}) - T_{eff} S_c. \tag{3.31}$$

As the system is quenched, it is not equilibrated at T. Rather it is described by its own characteristic temperature T_{eff}. As an analogy with the ordinary thermodynamics, $\widetilde{F}(T_{eff})$ is considered as internal energy U. From the simple relation of thermodynamics, Eqn. 3.28 and Eqn. 3.9 are equivalent to

$$\widetilde{F} = -T_{eff}^2 \frac{\partial(\frac{F}{T_{eff}})}{\partial T_{eff}}, S_c = -\frac{\partial F}{\partial T_{eff}}. \tag{3.32}$$

The replicated integration $\int \mathcal{D}h \widetilde{Z}^m[h]$ in Eqn. 3.26 can be performed using Gaussian integral easily. We expand $[\phi_\alpha(x) - h(x)]^2$ and perform an integration over the ergodicity breaking field $h(x)$.

$$\begin{aligned} &\int d^m\phi \exp\left[-\sum_{\alpha=1}^{m} H[\phi_\alpha] - \frac{g}{2}\int dx \sum_{\alpha=1}^{m} \phi_\alpha^2(x)\right] \\ &\times \int \mathcal{D}h \exp\left[-\frac{g}{2}\int dx \sum_{\alpha=1}^{m} \left[h^2(x) - 2h(x)\phi_\alpha(x)\right]\right]. \end{aligned} \tag{3.33}$$

The integration over $h(x)$ leads to

$$\begin{aligned} &\int \mathcal{D}h \exp\left[-\frac{g}{2}\int dx \sum_{\alpha=1}^{m} \left[h^2(x) - 2h(x)\phi_\alpha(x)\right]\right] \\ &= \int \mathcal{D}h \exp\left[-\frac{gm}{2}\int dx h^2(x) + g\int dx \sum_{\alpha=1}^{m} h(x)\phi_\alpha(x)\right] \\ &= C \exp[\frac{g}{2m}\int dx \sum_{\alpha,\beta=1}^{m} \phi_\alpha(x)\phi_\beta(x)]. \end{aligned} \tag{3.34}$$

Finally, we have

$$\int \mathcal{D}h \widetilde{Z}^m[h] = \int d^m\phi \exp\left[-\sum_{\alpha=1}^{m} H[\phi_\alpha] - \frac{g}{2}\int dx \sum_{\alpha=1}^{m} \phi_\alpha^2(x) + \frac{g}{2m}\int dx \sum_{\alpha,\beta=1}^{m} \phi_\alpha(x)\phi_\beta(x)\right]. \tag{3.35}$$

Thus, the typical free energy of metastable state $F(m)$ up to an irrelevant constant is

$$F(m) = -\lim_{g\to 0}\frac{1}{m\beta}\log\int d^m\phi \exp\left[-\sum_{\alpha=1}^{m} H[\phi_\alpha] - \frac{g}{2}\int dx \sum_{\alpha=1}^{m}\phi_\alpha^2(x) + \frac{g}{2m}\int dx \sum_{\alpha=1}^{m}\phi_\alpha^2(x) + \frac{g}{2m}\int dx \sum_{\alpha,\beta\neq 1}^{m}\phi_\alpha(x)\phi_\beta(x)\right]. \tag{3.36}$$

In Eqn. 3.36, the overlap term between two different replica, $\frac{g}{2m}\int dx \sum_{\alpha,\beta\neq 1}^{m}\phi_\alpha(x)\phi_\beta(x)$, appears. As in case of the usual replica theory, we consider m to be an arbitrary integer numbers and perform the analytical continuation to arbitrary m at the end. To investigate the physical meaning of the replica coupling, we consider the correlation function in replica space $G_{\alpha\beta}(\mathbf{q}) = \langle\phi_\alpha(\mathbf{q})\phi_\beta(-\mathbf{q})\rangle$. The Dyson equation in replica space can be written as

$$G^{-1}_{\alpha\beta}(\mathbf{q}) = G_0^{-1}(\mathbf{q})\delta_{\alpha\beta} + \Sigma_{\alpha\beta}(\mathbf{q}) - \frac{g}{m} \tag{3.37}$$

where G_0^{-1} is bare propagator and includes $g - \frac{g}{m}$. $\Sigma_{\alpha\beta}(\mathbf{q})$ is a self energy in replica space and can be decomposed into a diagonal part and off diagonal part in replica space such as $\Sigma_{\alpha\beta}(\mathbf{q}) = \Sigma_K(\mathbf{q})\delta_{\alpha\beta} + \Sigma_F(\mathbf{q})$. We then construct the correlation function in replica space $G_{\alpha\beta}(\mathbf{q})$ with a diagonal part and off diagonal part such as

$$G_{\alpha\beta}(\mathbf{q}) = K(\mathbf{q})\delta_{\alpha\beta} + F(\mathbf{q}) \tag{3.38}$$

where $K(\mathbf{q})$ is a response function and is defined as $K(\mathbf{q}) \equiv G(\mathbf{q}) - F(\mathbf{q})$. This ansatz corresponds to one step RSB as mentioned in section 3.2. Eqn. 3.38 has an inverse relation of Eqn. 3.37. Using the inverse matrix in replica space, we have

$$\begin{aligned} G^{-1}(\mathbf{q}) &= G_0^{-1}(\mathbf{q}) + \Sigma_G(\mathbf{q}) \\ F(\mathbf{q}) &= G(\mathbf{q}) - \frac{1}{G^{-1}(\mathbf{q}) - m(\Sigma_F(\mathbf{q}) - \frac{g}{m})} \end{aligned} \tag{3.39}$$

with $\Sigma_G(\mathbf{q}) \equiv \Sigma_K(\mathbf{q}) + \Sigma_F(\mathbf{q})$. For example, in case of the microemulsion problem in chapter 2, the original Hamiltonian is given as Eqn. 2.13. The renormalized diagonal correlation function $G(\mathbf{q})$ is given as

$$G(\mathbf{q}) = \frac{1}{r + q^2 + \frac{Q}{q^2+q_D^2}} + g - \frac{g}{m}. \tag{3.40}$$

The replica scenario for self generated glass sets $m \to 1$ and $g \to 0$ at the end of calculation as like the ergodicity breaking in ferromagnetic case. In the limit of $m \to 1$ and $g \to 0$, the two correlation functions in replica space becomes

$$G(\mathbf{q}) = \frac{1}{r + q^2 + \frac{Q}{q^2+q_D^2}}$$
$$F(\mathbf{q}) = G(\mathbf{q}) - \frac{1}{G^{-1}(\mathbf{q}) - \Sigma_F(\mathbf{q})}. \tag{3.41}$$

When $\Sigma_F(\mathbf{q}) = 0$, the off diagonal function $F(\mathbf{q})$ goes to zero. However, despite of $g \to 0$, the nonzero $\Sigma_F(\mathbf{q})$ makes $F(\mathbf{q})$ nonzero, which signals self generated glassiness. The physical meaning of two correlation functions in replica space can be interpreted as

$$G(\mathbf{q}) = \langle \phi_{\mathbf{q}}(t)\phi_{-\mathbf{q}}(t)\rangle \ : \text{instant correlation function}$$
$$F(\mathbf{q}) = \lim_{t\to\infty} \langle \phi_{\mathbf{q}}(t)\phi_{-\mathbf{q}}(0)\rangle : \text{long time correlation function.} \tag{3.42}$$

The off diagonal correlation function can be obtained by analytical and numerical method. In next two sections, these two different methods will be discussed.

3.4 DMFT (Dynamical mean field theory) - numerical method

The major problem of the replica theory to self generated glassiness is the determination of the partition function $Z(m)$. Even for the liquid state (i.e. $m = 1$ and $g = 0$ at the outset) this is a very hard problem without known exact solution and we are forced to use computer simulations or to develop approximate analytical theories. In developing such an approximate theory we take advantage of the fact that glass forming systems are often driven by strong local correlations, as opposed to the pronounced long ranged correlations at a second order phase transition or the critical point of the liquid-vapor coexistence curve. This is probably most transparent in the mode coupling theory of undercooled liquids where a given molecule is locally caged by its environment built of other molecules.

Calling a physical system local does not necessarily imply that its correlation function is rapidly decaying in space. In the language of many body theory it only implies that the irreducible self energy $\Sigma(\mathbf{k}) \simeq \Sigma$ is independent of momentum. Here, Σ is related to the correlation function $G(\mathbf{k}) = \langle\phi(\mathbf{k})\phi(-\mathbf{k})\langle$ via Dyson equation

$$G(\mathbf{k})^{-1} = G_0(\mathbf{k})^{-1} - \Sigma. \tag{3.43}$$

If we consider the emergence of glassy states we have to use the replica theory and Eqn. 3.43 becomes an $(m \times m)$ matrix equation with $G_{\alpha\beta}(\mathbf{q}) = \langle\phi_\alpha(\mathbf{q})\phi_\beta(-\mathbf{q})\rangle$, $G^0_{\alpha\beta}(\mathbf{q}) = G^0(\mathbf{q})\delta_{\alpha\beta}$ as well as self energy matrix $\Sigma_{\alpha\beta}$.

Traditionally, the self energy is introduced because it has a comparatively simple structure within perturbation theory. However, in the theory of strongly correlated Fermi systems it has been recognized that a momentum independent self energy allows conceptually new, non-perturbative insight into the dynamics of many body systems. (51) (52) We will adopt the main strategy of this *dynamical mean field theory* to our problem.

3.4.1 DMFT theory

In a solid state physics, despite a good understanding of the weakly correlated electrons in a metal and the localized electrons in an insulators, it is hard to properly describe transition metals such as vanadium, iron and their oxides since the electrons on flat narrow d and f orbitals feel a strong Coulomb repulsion. (50) As one of the effective Hamiltonian to describe correlated electrons, the Hubbard Hamiltonian is widely used in a condensed matter physics. The Hubbard Hamiltonian is given by

$$H = -\sum_{\langle ij\rangle,\sigma} t_{ij}(c^{+}_{i\sigma}c_{j\sigma} + c^{+}_{j\sigma}c_{i\sigma}) + U\sum_{i} n_{i\uparrow}n_{i\downarrow}, \tag{3.44}$$

where t_{ij} and U represent electron hopping term between site i, j and on-site(local) Coulomb interaction respectively. σ is a spin index. The competing interaction between a kinetic hopping term and local repulsive Coulomb term controls the physical properties. Even though the Hubbard model has a simple and intuitive picture, the model is only solvable exactly in one dimension. To understand the physics in two and three dimension, it is inevitable to make proper assumptions even for numerical calculations such as exact diagonalization method and quantum Monte Carlo method, which leave some controversial problems. (52) The DMFT is one candidate method even for the nonperturbative region. In a classical spin model, for example, Ising model, the mean field solution becomes exact in the limit of large spatial dimension $d \to \infty$ or in the limit of large coordination number $Z \to \infty$. In this limit, the fluctuations in the "bath" of the surrounding neighbors become negligible, such that the Ising model reduces to a single-site problem. The surrounding of any site is completely is described by a single effective mean field parameter h_{MF} (Weiss field). The Ising Hamiltonian becomes purely local. (51) In DMFT, the spatial fluctuations *freeze out* by making the spatial dimension or coordination number large. However, in quantum system, we should consider the local quantum fluctuation, i.e. the fluctuation of neighboring spins as a "bath", which is not *frozen*. In the case of the quantum system, the Weiss field becomes a function of time instead of constant in a classical case. That is the main difference between the classical and quantum

case. The kinetic energy part of the Hubbard Hamiltonian is given as

$$E_{kinetic} = -t \sum_{\langle ij \rangle, \sigma} c^{+}_{i\sigma} c_{j\sigma} = \sum_{\mathbf{k}, \sigma} \epsilon_{\mathbf{k}} \widehat{n}_{\mathbf{k}\sigma}, \tag{3.45}$$

where $\widehat{n}_{\mathbf{k}\sigma} = c^{+}_{i\sigma} c_{i\sigma}$. The energy dispersion $\epsilon_{\mathbf{k}}$ is given as $\epsilon_{\mathbf{k}} = -2t \sum_{i=1}^{d} \cos k_i$. The density of state(DOS) $N_d(E) = \sum_k \delta(E - \epsilon_{\mathbf{k}})$ for $d \to \infty$ by central limit theorem is given by

$$N_d(E) \to \frac{1}{2t\sqrt{\pi d}} \exp\left[-\left(\frac{E}{2t\sqrt{d}} \right)^2 \right]. \tag{3.46}$$

The only nontrivial DOS is obtained by the proper scaling of

$$t \to \frac{t^*}{\sqrt{2d}}. \tag{3.47}$$

(53)

The transition nonvanishing amplitude between nearest neighbor $\left\langle c^{+}_{i\sigma} c_{j\sigma} \right\rangle \equiv g_{ij,\sigma}$, should take the form of $\mathcal{O}(\frac{1}{\sqrt{d}})$ since the order of the hopping term $t \sim \mathcal{O}(\frac{1}{\sqrt{d}})$ and $\mathcal{O}(d)$ for $\sum_{\langle ij \rangle, \sigma}$. This property gives us an interesting feature of the irreducible self energies in $d \to \infty$. As a simple example, Fig.3.4 shows the 2nd order irreducible self energy $\Sigma^{(2)}$ in Coulomb repulsive energy U. (51) Since the order of the transition amplitude has $\mathcal{O}(\frac{1}{\sqrt{d}}), \Sigma^{(2)}$ has a form of $\sum_{\langle ij \rangle, \sigma} \mathcal{O}(\frac{1}{d})^{3/2} \sim \mathcal{O}(\frac{1}{\sqrt{d}})$, which vanishes in $d \to \infty$. The diagrams comprised of more than two paths for $i \neq j$ collapsed to a single site and the diagrams survives only for $i = j$. (51) (52) (54) Since the irreducible self energy becomes a local quantity, we have an important result for the irreducible self energy.

The self energy becomes momentum independent.

$$\Sigma_{ij,\sigma}(\omega) = \Sigma_{ii,\sigma}(\omega) \text{ for } d \to \infty. \tag{3.48}$$

The Fourier transform reads

$$\Sigma_{\mathbf{k},\sigma}(\omega) = \Sigma_{\sigma}(\omega) \text{ for } d \to \infty. \tag{3.49}$$

In the case of classical problem, the self energy in $d \to \infty$ becomes a number. The purpose of this section is to combine DMFT with replica method for self generated glass.

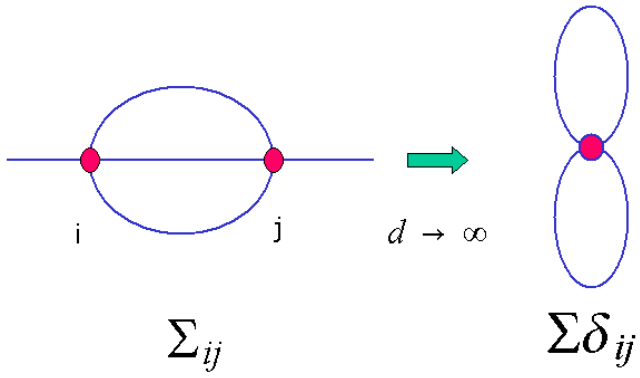

Figure 3.4 collapsed irreducible self energy in 2nd order in U. (51)

3.4.2 Application of the DMFT to glasses

Returning to the replica problem to self generated glassiness, $F(m)$ determines the configurational entropy and the average free energy of the system. We use the fact that the free energy $F(m)$ determined by Eqn. 3.36 can be written as (55) (56)

$$F(m) = \frac{1}{2}\mathrm{tr}\log\left(G_0^{-1} - \Sigma\right) + \frac{1}{2}\mathrm{tr}\left(\Sigma G\right) + \frac{1}{2}\Phi\left[G\right], \tag{3.50}$$

where the trace goes for each $\mathbf{q}$-point over the $(m \times m)$ matrix components together with a sum over $\mathbf{q}$. The latter can also be written as a matrix trace of real space functions $G(\mathbf{x}, \mathbf{x}')$ etc. The functional $\Phi[G]$ is well defined in terms of Feynman diagrams as the sum of skeleton diagrams of the free energy. In what follows we will not try to calculate Φ but merely use the fact that such a functional exists. From the definition of Φ it follows that it determines the self energy via functional derivative:

$$\Sigma_{\alpha\beta}\left(\mathbf{x}, \mathbf{x}'\right) = -\frac{\delta\Phi\left[G\right]}{\delta G_{\beta\alpha}\left(\mathbf{x}', \mathbf{x}\right)}. \tag{3.51}$$

Since we made the assumption that Σ is momentum independent, Fourier transformation yields $\Sigma_{\alpha\beta}(\mathbf{x},\mathbf{x}') = \Sigma_{\alpha\beta}\delta(\mathbf{x}-\mathbf{x}')$. Thus, the functional derivative, Eqn. 3.51, vanishes if $\mathbf{x} \neq \mathbf{x}'$, which implies that for a local theory, Φ solely depends on the local, momentum averaged, correlation function,

$$\overline{G}_{\alpha\beta} = \int \frac{d^d q}{(2\pi)^d} G_{\alpha\beta}(\mathbf{q}). \tag{3.52}$$

Since all our interactions, $V[\phi]$ are (by assumption) local as well, we conclude that there exists a local problem with Hamiltonian

$$H = \sum_{\alpha\beta} \phi_\alpha \mathcal{J}_{\alpha\beta} \phi_\beta + a_0^d \sum_\alpha V[\phi_a], \tag{3.53}$$

which has an identical functional $\Phi[G]$ of its own correlation function G, which is also a $(m \times m)$ matrix but does not depend on position or momentum. a_0 is a typical microscopic length scale, for example a hard core diameter and need be specified for each system. Even though, H has no spatial structure anymore, the perturbation theory up to arbitrary order is the same for both system. This holds for an arbitrary choice of the so called Weiss field, $\mathcal{J}$.

3.4.3 Derivation of Weiss field by cavity method

In the mapping the original lattice problem into local problem, we adapt a cavity method for fulfilling this purpose. The cavity method was developed for describing the short range interaction effect near T_c in a mean field theory by Onsager. We consider the action S_{loc} of local space in φ^4 model at first since this cavity method is easily extended to φ^3.

$$S_{loc} = \frac{1}{2}\varphi_o \mathcal{J} \varphi_o + \frac{u_{loc}}{4}\varphi_o^4, \tag{3.54}$$

where φ_o is a localized field at the origin and the u_{loc} is a local coupling constant for φ^4 theory. As mentioned in the previous section, the purpose of this procedure is to solve the local problem rather than the original lattice problem. In case of a block copolymer, we can assume that the monomers of polymer are located on the lattice. In the lattice problem, the action $S_{lattice}$ in the φ^4 continuum model is given as

$$S_{lattice} = \frac{1}{2}\int d^d x d^d x' \varphi(x) g(x-x')_0^{-1} \varphi(x') + \frac{u}{4}\int d^d x \varphi(x)^4, \tag{3.55}$$

where $g(x-x')_0$ is non-interacting Green's function and d is a dimension. And this action, $S_{lattice}$, of the lattice problem in the continuum model also can be written as

$$\begin{aligned} S_{lattice} &= \frac{a_0^{2d}}{2}\sum_{i,j}\varphi_i g_{ij,0}^{-1}\varphi_j + \frac{u a_0^d}{4}\sum_i \varphi_i^4 \\ &= \frac{1}{2}\sum_{i,j}\varphi_i G_{ij,0}^{-1}\varphi_j + \frac{u a_0^d}{4}\sum_i \varphi_i^4, \end{aligned} \tag{3.56}$$

where $G_{ij,0}^{-1}$ is defined as $a_0^{2d} g_{ij,0}^{-1}$. Within the cavity method, $S_{lattice}$ can be expressed as the sum of actions at o site and the environment.

$$S_{lattice} = S_o + \sum_{i \neq o} t_{oi}\varphi_o\varphi_i + S^{(o)}, \tag{3.57}$$

where S_o is the action at o site and $S^{(o)}$ is the action when the o site is removed. And t_{oi} is a coupling term between o site and the environment and given by

$$\begin{aligned} S_o &= \frac{1}{2}\varphi_o G^{0-1}_{oo}\varphi_o + \frac{ua_0^d}{4}\varphi_o^4 \\ S^{(o)} &= \frac{1}{2}\sum_{i,j\neq o}\varphi_i G^{0-1}_{ij}\varphi_j + \frac{ua_0^d}{4}\sum_{i\neq o}\varphi_i^4 \\ t_{oi} &\equiv G^{0-1}_{oi} \\ \Delta S &= \sum_{i\neq o} t_{oi}\varphi_o\varphi_i. \end{aligned} \tag{3.58}$$

The partition function $Z_{lattice}$ of the lattice problem is then given as

$$\begin{aligned} Z_{lattice} &= \int \mathcal{D}\varphi e^{-S_{lattice}} \\ &= \int \mathcal{D}\varphi_o \int \prod_{i\neq o}\mathcal{D}\varphi_i e^{-S_o-\Delta S-S^{(o)}} \\ &= \int \mathcal{D}\varphi_o e^{-S_o}\int \prod_{i\neq o}\mathcal{D}\varphi_i e^{-S^{(o)}-\Delta S} \\ &= Z^{(o)}\int \mathcal{D}\varphi_o \left\langle e^{-S_o-\Delta S}\right\rangle^{(o)}, \end{aligned} \tag{3.59}$$

where $\left\langle e^{-S_o-\Delta S}\right\rangle^{(o)}$is the average value when the o site is removed. Expanding $exp(-\Delta S)$ with respect to t_{oi}, we have

$$\left\langle e^{-S_o-\Delta S}\right\rangle^{(o)} \sim e^{-S_o}(1-\sum_{i\neq o} t_{oi}\varphi_o\left\langle\varphi_i\right\rangle^{(o)} + \frac{1}{2}\sum_{i,j\neq o} t_{oi}t_{oj}\varphi_o\varphi_o\left\langle\varphi_i\varphi_j\right\rangle^{(o)} + \cdots). \tag{3.60}$$

If the expectation value $\left\langle\varphi_i\right\rangle^{(o)} = 0$ for φ^4, it follows

$$\begin{aligned} \left\langle e^{-S_o-\Delta S}\right\rangle^{(o)} &\sim e^{-S_o}(1+\frac{1}{2}\sum_{i,j\neq o} t_{oi}t_{oj}\varphi_o\varphi_o\left\langle\varphi_i\varphi_j\right\rangle^{(o)} + \cdots) \\ &= e^{-S_o}(1+\frac{1}{2}\sum_{i,j\neq o} t_{oi}t_{oj}\varphi_o\varphi_o G^{(o)}_{ij} + \frac{1}{4!}\sum_{i,j,k,l\neq o} t_{oi}t_{oj}t_{ok}t_{ol}\varphi_o\varphi_o\varphi_o\varphi_o G^{(o)}_{ijkl} + \cdots), \end{aligned} \tag{3.61}$$

where $G^{(o)}_{ij}$ is the non interacting Green's function in the absence of o-site. In the case of φ^3 interaction, $\left\langle\varphi_i\right\rangle^{(o)} \neq 0$. In this case, we have extra terms in the expansion as like

$-\sum_{i\neq o} t_{oi}\varphi_o \langle\varphi_i\rangle$, $-\frac{1}{2}[\sum_{i\neq o} t_{oi}\langle\varphi_i\rangle]^2\varphi_o\varphi_o$. This extra term requires an introduction of new Weiss field $\mathcal{H}$, which is defined as $\sum_{i\neq o} t_{oi}\langle\varphi_i\rangle$. By power counting in $d\to\infty$ dimension, $\sum_{i,j,k} t_{oi}t_{oj}t_{ok}G^{(o)}_{ijk}$ (for $i=l$) and $\sum_{i,j,k,l} t_{oi}t_{oj}t_{ok}t_{ol}G^{(o)}_{ijkl}$ should vanishes. Based on the power counting,

$$\left\langle e^{-S_o-\Delta S}\right\rangle^{(o)} = e^{-S_o}(1+\frac{1}{2}\sum_{i,j\neq o} t_{oi}t_{oj}\varphi_o\varphi_o G^{(o)}_{ij}). \tag{3.62}$$

Reexponentiating Eqn. 3.62 (which is correct up to second order)

$$\left\langle e^{-S_o-\Delta S}\right\rangle^{(o)} = \exp(-S_o+\frac{1}{2}\sum_{i,j\neq o} t_{oi}t_{oj}\varphi_o\varphi_o G^{(o)}_{ij}). \tag{3.63}$$

We find the relation between S_{loc} and $S_{lattice}$

$$\begin{aligned} S_{loc} &= S_o - \sum_{i,j\neq o} t_{oi}t_{oj}G^{(o)}_{ij} \\ &= \frac{1}{2}\varphi_o\mathcal{J}\varphi_o + \frac{u_{loc}}{4}\varphi_o^4, \end{aligned} \tag{3.64}$$

where the Weiss field $\mathcal{J}$ is given as

$$\mathcal{J} = G^{0-1}_{oo} - \sum_{i,j\neq o} t_{oi}t_{oj}G^{(o)}_{ij}. \tag{3.65}$$

Since $G^{(o)}_{ij}$ is the non-interacting Green's function in the absence of site o , it's convenient to express $G^{(o)}_{ij}$ as the Green's function G_{ij} without the restriction of site o removed. This can be done by introducing a potential V on site $i=o$ and find the propagator $G_{ij}(V)$. And then we can exclude the site by taking the limit $V\to\infty$. $G_{ij}(V)$ is given as

$$G_{ij} = G_{ij} + G_{io}VG_{jo}, \tag{3.66}$$

where V is the repulsive potential at site o. When we analyze the paths which connect site i,j through site o, it follows.

$$\begin{aligned} G_{ij} &= G_{ij} + G_{io}VG_{jo} \\ &= G_{ij} + G_{io}VG_{jo} + G_{io}VG_{oo}VG_{jo} + G_{io}VG_{oo}VG_{oo}VG_{jo} + \cdots \\ &= G_{ij} + \frac{G_{io}VG_{jo}}{1-VG^0_{oo}}. \end{aligned} \tag{3.67}$$

By making the potential V at site o infinity, we can create the cavity at site o. Then, we can express $G_{ij}^{(o)}$ as the full Green's function.

$$G_{ij}^{(o)} = \lim_{V\to\infty} G_{ij}(V) = G_{ij} - \frac{G_{io}G_{jo}}{G_{oo}}. \tag{3.68}$$

Then, the Weiss field is now expressed in terms of the full Green's function which include the site $i = o$.

$$\mathcal{J} = G_{oo}^{0-1} - \sum_{i,j} t_{oi}t_{oj}(G_{ij} - \frac{G_{io}G_{jo}}{G_{oo}^0}), \tag{3.69}$$

where the sum over i, j does not need to be restricted, since the contributions either $i = o, j = o$ or both $i = j = o$ all vanish. Introducing the Fourier transform of G_{ij},

$$G_{ij} = \sum_q G(q)e^{iq(r_i - r_j)}, \tag{3.70}$$

we can write

$$\begin{aligned}\sum_{i,j} t_{oi}t_{oj}G_{ij}^0 &= \sum_q \sum_{i,j} t_{oi}t_{oj}e^{iq(r_i-r_j)}G(q) \\ &= \sum_q \epsilon_q^2 G(q),\end{aligned} \tag{3.71}$$

where $\epsilon_q = \sum_{i,j} t_{ij}e^{iq(r_i-r_j)}$. In a similar way, one finds

$$\begin{aligned}\sum_i t_{oi}G_{io} &= \sum_q \epsilon_q G(q) \\ G_{oo} &= \sum_q G(q).\end{aligned} \tag{3.72}$$

The Weiss field is given as

$$\begin{aligned}\mathcal{J} &= G_{oo}^{0-1} - \sum_{i,j} t_{oi}t_{oj}(G_{ij} - \frac{G_{io}G_{jo}}{G_{oo}}) \\ &= G_{oo}^{0-1} - \sum_q \epsilon_q^2 G(q) + \frac{\left(\sum_q \epsilon_q G(q)\right)^2}{\sum_q G(q)},\end{aligned} \tag{3.73}$$

where $\epsilon_q^{-1} = G^0(q)$. Defining $\rho(\omega) = \sum_q \delta(\omega - \epsilon_q)$, $\sum_q \epsilon_q G(q)$ is given by

$$\sum_q \epsilon_q G(q) = 1 + \Sigma G_{oo}. \tag{3.74}$$

In a similar way,

$$\sum_q \epsilon_q^2 G(q) = \sum_q \epsilon_q + a_0^d \Sigma (1 + \Sigma G_{oo}). \tag{3.75}$$

After some algebra, we can write

$$\mathcal{J} - G_{oo}^{0-1} = -\sum_q \epsilon_q + a_0^d \Sigma + G_{oo}^{-1}. \tag{3.76}$$

Since by definition $\sum_q \epsilon_q = G_{oo}^{0-1}$, it follows

$$\mathcal{J} = G_{oo}^{-1} + a_0^d \Sigma. \tag{3.77}$$

Eqn. 3.77 holds for φ^3 model. Thus, the bare propagator at the local site is given in terms of the full lattice propagator as well as the full self energy of the problem. Following Ref. (52), we use the freedom to chose $\mathcal{J}$ in order to guarantee that $\mathcal{G} = \overline{G}$. This implies that not only the functional Φ but also its argument is the same for the actual physical system and the auxiliary local one. It then follows that the self energy of the original system $\Sigma_{\alpha\beta}$ is, up to trivial prefactor, equal to the self energy of the auxiliary system, $a_0^d \Sigma_{\alpha\beta}$. We solely need to solve the much simpler problem, H, and determine for an assumed the Weiss field $\mathcal{J}$ the local self energy as well as the local propagator related by

$$\overline{G} = \left(\mathcal{J} - a_0^d \Sigma \right)^{-1}. \tag{3.78}$$

We made the right choice for $\mathcal{J}$ if simultaneously holds that self energy and averaged correlation function are related by

$$\overline{G} = \int \frac{d^d k}{(2\pi)^d} \left(G_0 \left(\mathbf{k} \right)^{-1} - \Sigma \right)^{-1}. \tag{3.79}$$

If this second equation is not fulfilled we need to improve the Weiss field $\mathcal{J}$ until Eqn. 3.78 and Eqn. 3.79 hold simultaneously, posing a self consistency problem. This is the most consistent way to determine the physical correlation functions under the assumption of a momentum independent self energy. It has been applied to a large class of problems in the field of strongly correlated Fermi systems, but is, as we have demonstrated here, very useful in a rather different context. The major task of the DMFT is therefore to solve H for given $\mathcal{J}$. This will be done for the specific choice of a replica symmetric correlation function

$$G_{\alpha\beta}(q) = K(q)\, \delta_{\alpha\beta} + F(q) \tag{3.80}$$

as well as the self energy

$$\Sigma_{\alpha\beta} = \Sigma_K \delta_{\alpha\beta} + \Sigma_F. \tag{3.81}$$

Below we will analyze the stability of this choice for a specific example.

3.4.4 The Brazovskii model of microphase separation

We are now in the position to apply our approach to a specific physical system. We consider a one component system ($L = 1$) governed by the three dimensional Brazovskii model (14),

$$H = \frac{1}{2}\int d^3x \left(\varepsilon_0^2 q_0^2 \phi^2 + \frac{2\upsilon}{3}\phi^3 + \frac{u}{2}\phi^4 + \frac{q_0^{-2}}{4}\left(\left[\nabla^2 + q_0^2\right]\phi\right)^2\right) \tag{3.82}$$

which has a broad range of applicability in systems with microphase separation like the theory of micro-emulsions (22) (57) (58), block copolymers (12) (13) or even doped transition metal oxides (59) (61). In Ref. (60) it was even argued that it might be used as a simple toy model for glass forming liquids. From Eqn. 3.82, it follows the dimensionless bare coupling constants are given by u/q_0 and $\upsilon/q_0^{3/2}$. The bare correlation function follows from Eqn. 3.82

$$\begin{aligned} G_0(q) &= \frac{1}{\varepsilon_0^2 q_0^2 + \frac{1}{4q_0^2}\left(q^2 - q_0^2\right)^2} \\ &\simeq \frac{1}{\varepsilon_0^2 q_0^2 + \left(q - q_0\right)^2}. \end{aligned} \tag{3.83}$$

The Brazovskii model is interesting because of the large phase space of low energy fluctuations as is evident from the gradient term, $\nabla^2 + q_0^2$, in the Hamiltonian. All fluctuations with momenta $|\mathbf{q}| = q_0$ can, independent of the direction of $\mathbf{q}$, be excited most easily. The wave number q_0 is related to various physical quantities in all these different systems. In microemulsions, q_0 is determined by the volume fraction of amphiphilic molecules whereas it is inversely proportional to the radius of gyration in block copolymers and to the strength of the Coulomb interaction in doped transition metal oxides. Clearly, the role played by the microscopic length scale a_0 of the previous section is q_0^{-1}. If the self energy is momentum independent the correlation function has a form like

$$G(q) = \frac{1}{\left(q - q_0\right)^2 + \varepsilon^2 q_0^2} \tag{3.84}$$

with $\varepsilon^2 = \varepsilon_0^2 - q_0^{-2}\Sigma > 0$, which yields $\overline{G} = \int \frac{d^3q}{(2\pi)^3} G(q) = \frac{q_0}{2\pi\varepsilon}$.

3.4.5 DMFT for the liquid state

Ignoring glassiness for the moment, the local Hamiltonian is given by

$$H = \frac{1}{2}\mathcal{J}\phi^2 + \frac{\upsilon q_0^{-3}}{3}\phi^3 + \frac{u q_0^{-3}}{4}\phi^4 + h\phi, \tag{3.85}$$

which leads to the partition sum $\mathcal{Z} = \int_{-\infty}^{\infty} d\phi e^{-H}$ and correlation function

$$\overline{G} = \frac{\int_{-\infty}^{\infty} d\phi \phi^2 e^{-H}}{\mathcal{Z}}. \tag{3.86}$$

$\mathcal{Z}$ and $\overline{G}$ are elementary integrals and can be expressed in terms of elliptic functions. The Weiss field which leads to the correct propagator can be obtained as $\mathcal{J} = \frac{\varepsilon_0^2 + 2\pi\varepsilon - \varepsilon^2}{q_0}$ which, together with Eqn. 3.85 and 3.86, leads to nonlinear algebraic equation for ε. In addition h is determined from the condition $\langle\phi\rangle = 0$. We have a self consistent nonlinear algebraic equation.

$$\begin{aligned} \frac{q_0}{2\pi\varepsilon} &= \frac{\int_{-\infty}^{\infty} d\phi \phi^2 e^{-H}}{\mathcal{Z}} \\ 0 &= \frac{\int_{-\infty}^{\infty} d\phi \phi e^{-H}}{\mathcal{Z}}. \end{aligned} \tag{3.87}$$

The solution of Eqn. 3.87 can be obtained numerically and the results are shown in Fig.3.5 for $\upsilon = 0$ and Fig. 3.6 for $\upsilon \neq 0$. In the limit of small ε one finds

$$|\varepsilon_0^2| = \frac{u/q_0}{2\pi\varepsilon} + 4\pi\varepsilon. \tag{3.88}$$

In equilibrium behavior, we have made the assumption that no phase transition to a state with a long range order of $\langle\phi\rangle \neq 0$ takes place despite that the Brazovskii Hamiltonain 3.82 undergoes a first-order phase transition to an ordered crystal in mean field for $\upsilon \neq 0$ and fluctuation induced first order transition for $\upsilon = 0$. The assumption implies that the fluid phase has been supercooled below the ordering temperature. In the laboratory this will likely be a kinetic issue that needs a nucleation theory for quantitative predictions. The results of Ref. (75), where the nucleation theory of the fluctuation induced Brazovskii transition at $\upsilon = 0$ was developed, demonstrate that the nucleation kinetics of the model is indeed very complex and supercooling is possible.

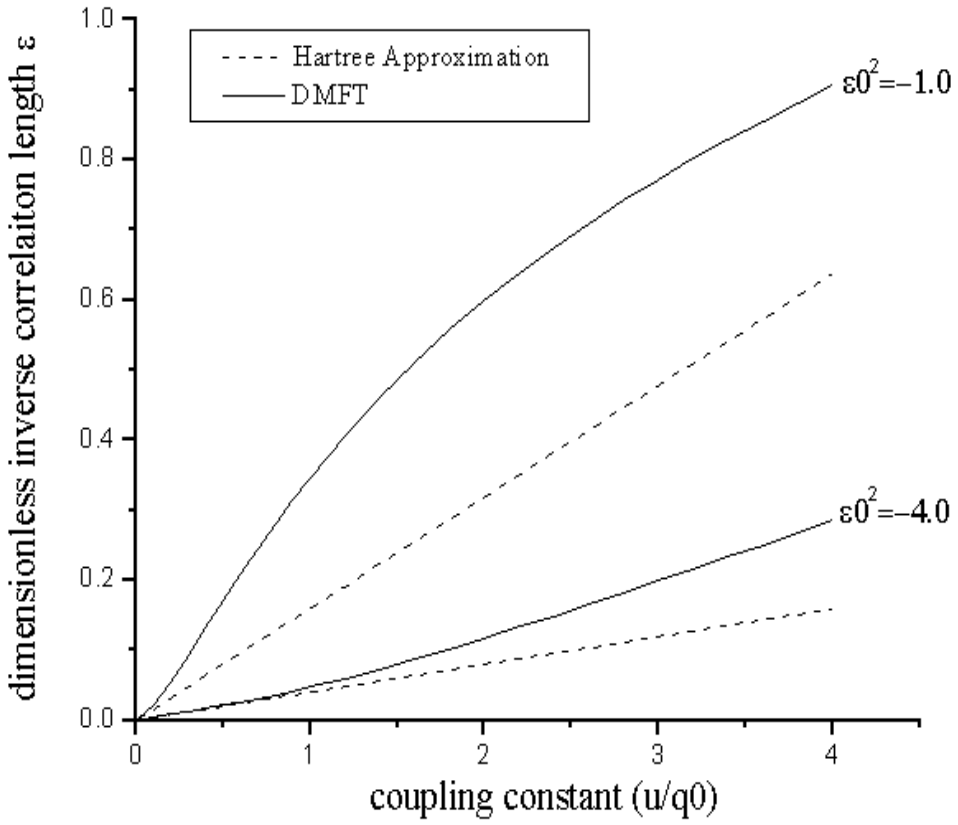

Figure 3.5 Inverse correlation length versus coupling constant u/q_0 for different bare segregation strength $\varepsilon_0^2 = -1$ and $\varepsilon_0^2 = -4$ for $\upsilon = 0$. The dashed line is for Hartree approximation.

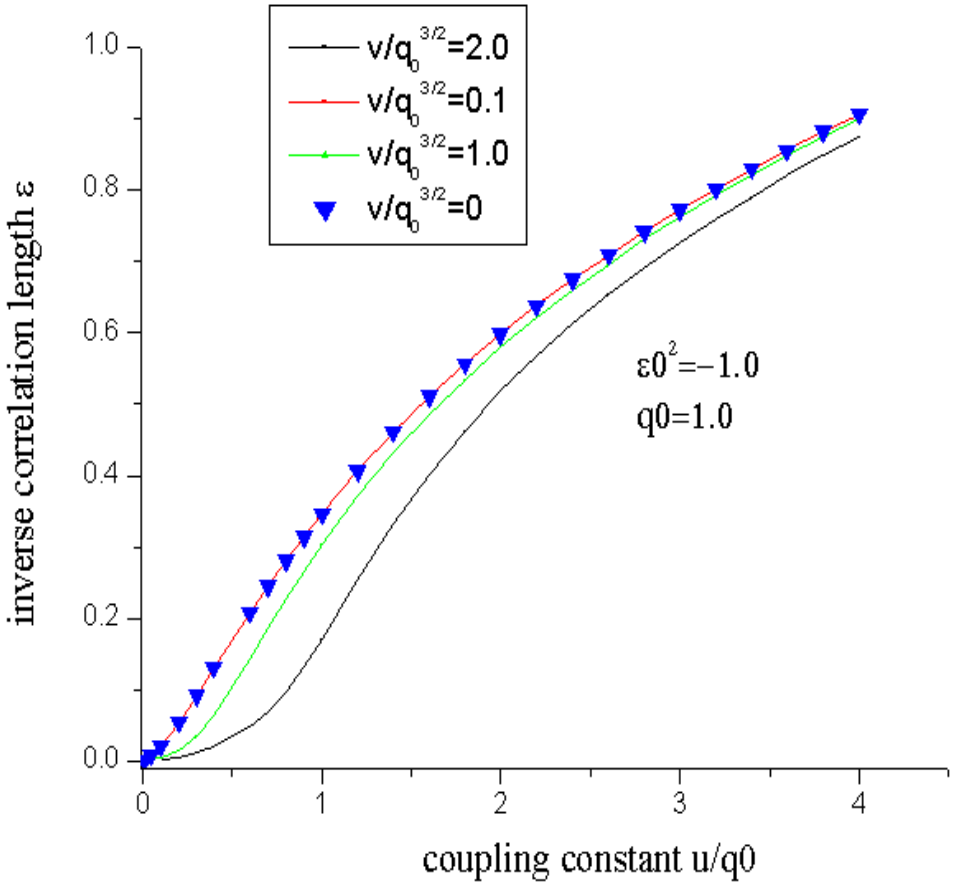

Figure 3.6 Inverse correlation length ε versus coupling constant u/q_0 for different cubic coupling constant $v/q_0^{3/2}$ in a liquid state.

3.4.6 DMFT in the glassy state

Within the replica theory of the glassy state we have to specify the replica structure of the correlation function for the original problem as well as for the auxiliary local one. We first chose a given structure and discuss its stability later. In replica space we start from the following structure of the propagators and self energies:

$$\begin{aligned} G_{\alpha\beta}(q) &= K(q)\,\delta_{\alpha\beta} + F(q) \\ \Sigma_{\alpha\beta} &= \Sigma_K \delta_{\alpha\beta} + \Sigma_F . \end{aligned} \tag{3.89}$$

Inverting the Dyson equation leads to:

$$\begin{aligned} K(q) &= \frac{1}{(q-q_0)^2 + \kappa^2 q_0^2} \\ mF(q) &= \frac{1}{(q-q_0)^2 + \varepsilon^2 q_0^2} - \frac{1}{(q-q_0)^2 + \kappa^2 q_0^2} \end{aligned} \tag{3.90}$$

with

$$\begin{aligned} \kappa^2 q_0^2 &= \varepsilon_0^2 q_0^2 - \Sigma_K(q) \\ \varepsilon^2 q_0^2 &= \varepsilon_0^2 q_0^2 - \Sigma_K(q) - m\Sigma_F(q) . \end{aligned} \tag{3.91}$$

The diagonal elements $K(q) + F(q)$ can be interpreted as the equilibrium, liquid state correlation function and is only determined by ε which can be related to the liquid state correlation length $\xi \simeq \frac{1}{\varepsilon q_0}$. On the other hand $F(q) = \lim_{t\to\infty} \lim_{t'\to\infty} \langle \phi_q(t)\, \phi_{-q}(t+t') \rangle$ characterizes long time correlations in analogy to the Edwards-Anderson parameter. Clearly, if $\Sigma_F \neq 0$, $\kappa > \varepsilon$ and $F(q) > 0$. Depending of whether one considers q values close to or away from q_0, $F(q)$ is governed by the correlation length ξ or the Lindemann length of the glass $\lambda_0 = q_0^{-1}\left(\kappa^2 - \varepsilon^2\right)^{-1}$, respectively. The physical significance of λ_0 as the length scale over which defects and imperfections of an crystalline state can wander after long time was discussed in Ref. (62). Finally, the correlation function $K(q)$ (which is solely determined by the short length $\frac{1}{\kappa q_0}$) is the response function of a local perturbation. Obviously, any response of the glassy system is confined to very small length scales even though the instantaneous correlation length

can be considerable. This is a clear reflection of the violation of the fluctuation dissipation relation within the replica approach. Averaging these functions over momenta gives:

$$\begin{aligned}\overline{K} &= \int \frac{d^3q}{(2\pi)^3} K(q) = \frac{q_0}{2\pi\kappa}. \\ \overline{F} &= \int \frac{d^3q}{(2\pi)^3} F(q) = \frac{q_0}{2\pi m}\left(\frac{1}{\varepsilon} - \frac{1}{\kappa}\right).\end{aligned} \tag{3.92}$$

The auxiliary local Hamiltonian is

$$H = \frac{1}{2}\sum_{ab} \mathcal{J}_{ab}\phi_a\phi_b + \sum_a \left(\frac{v q_0^{-3}}{3}\phi_a^3 + \frac{u q_0^{-3}}{4}\phi_a^4 + h\phi_a\right). \tag{3.93}$$

Within DMFT, we then find for its correlation function

$$\mathcal{G} = \overline{K}\delta_{ab} + \overline{F}. \tag{3.94}$$

In addition, the Weiss field is given by:

$$\mathcal{J}_{\alpha\beta} = \mathcal{J}\delta_{\alpha\beta} - \mathcal{C}. \tag{3.95}$$

These relations can be used to express the Weiss fields in terms of the ε and κ:

$$\begin{aligned}\mathcal{J} &= \frac{2\pi\kappa + \varepsilon_0^2 - \kappa^2}{q_0} \\ \mathcal{C} &= \frac{2\pi(\kappa - \varepsilon) + \varepsilon^2 - \kappa^2}{m q_0}.\end{aligned} \tag{3.96}$$

Thus, we have to determine $\overline{K}$ and $\overline{F}$ for given $\mathcal{J}$ and $\mathcal{C}$ and make sure that the latter are chosen such that $\overline{G} = \int \frac{d^3q}{(2\pi)^3} G(q) = \frac{q_0}{2\pi\varepsilon}$ is fulfilled. The partition sum of the local problem is given by

$$\mathcal{Z}(m) = \int d^m\phi e^{-\sum_{\alpha=1}^m H_0[\phi_\alpha] + \frac{1}{2}\mathcal{C}\left(\sum_\alpha \phi_\alpha\right)^2}, \tag{3.97}$$

where $H_0[\phi_\alpha] = \frac{1}{2}\mathcal{J}\phi_a^2 + \frac{v q_0^{-3}}{3}\phi_a^3 + \frac{u q_0^{-3}}{4}\phi_a^4 + h\phi_a$. $d^m\phi$ refers to the fact that ϕ is an m-component vector and the integral goes over an m-dimensional space with arbitrary m. The coupling between different replicas can be eliminated by performing a Hubbard-Stratonovich transformation, which leads to

$$\mathcal{Z}(m) = \int \frac{d\lambda}{\sqrt{2\pi\mathcal{C}}} e^{-\frac{\lambda^2}{2\mathcal{C}}} \Omega(\lambda)^m, \tag{3.98}$$

where

$$\Omega(\lambda) = \int d\phi e^{-(H_0[\phi]+\lambda\phi)} \tag{3.99}$$

is the equilibrium partition function however in an external field λ, with Gaussian distribution function. In order to determine the propagators of the local problem, we consider the sum of the diagonal elements

$$\sum_a \overline{G}_{aa} = m\left(\overline{K}+\overline{F}\right), \tag{3.100}$$

which is equal to $-2\frac{\partial \log \mathcal{Z}(m)}{\partial \mathcal{J}}$, yielding

$$\overline{K}+\overline{F} = -2\int \frac{d\lambda e^{-\frac{\lambda^2}{2\mathcal{C}}}\Omega(\lambda)^{m-1}}{\mathcal{Z}(m)\sqrt{2\pi\mathcal{C}}}\frac{\partial}{\partial\mathcal{J}}\Omega(\lambda). \tag{3.101}$$

The derivative with respect to $\mathcal{J}$ leads to

$$\frac{\partial}{\partial\mathcal{J}}\Omega(\lambda) = -\frac{1}{2}\int d\phi e^{-\left(\frac{1}{2}\mathcal{J}\phi^2+\frac{v q_0^{-3}}{3}\phi^3+\frac{u q_0^{-3}}{4}\phi^4+(h+\lambda)\phi\right)}\phi^2, \tag{3.102}$$

which gives the final expression for the diagonal element of the replica correlation function

$$\overline{K}+\overline{F} = \frac{\int \frac{d\lambda}{\sqrt{2\pi\mathcal{C}}}e^{-\frac{\lambda^2}{2\mathcal{C}}}\Omega(\lambda)^m\left\langle\phi^2\right\rangle_\lambda}{\mathcal{Z}(m)} \tag{3.103}$$

with

$$\left\langle\phi^2\right\rangle_\lambda = \frac{\int d\phi e^{-\left(\frac{1}{2}\mathcal{J}\phi^2+\frac{v q_0^{-3}}{3}\phi^3+\frac{u q_0^{-3}}{4}\phi^4+(h+\lambda)\phi\right)}\phi^2}{\Omega(\lambda)}. \tag{3.104}$$

In addition we also need to determine the off diagonal elements in replica space of the correlation function. We use

$$\sum_{a,b}\overline{G}_{ab} = m\overline{K}+m^2\overline{F}, \tag{3.105}$$

which equals to $2\frac{\partial \log \mathcal{Z}(m)}{\partial \mathcal{C}}$ and obtain an equation which can be used to determine the off diagonal elements $\overline{F}$

$$\overline{K}+m\overline{F} = -\frac{\int \frac{d\lambda}{\sqrt{2\pi\mathcal{C}}}e^{-\frac{\lambda^2}{2\mathcal{C}}}\Omega(\lambda)^m\mathcal{C}^{-1}\left\langle\phi\right\rangle_\lambda\lambda}{\mathcal{Z}(m)}. \tag{3.106}$$

Eqn. 3.103 and 3.106 are only independent equations if m differs from 1.

We next analyze these equations for small but finite $m-1$. This can be done by expanding Eqn. 3.103 and 3.106 into a Taylor series for small $m-1$ and comparing order by order. First

we consider the zeroth order term and find that both equations yield for $m = 1$, the results for the liquid state which determine ε. The next step is to consider the first corrections linear in $m - 1$. This can be used to check whether there are nontrivial solutions for $\kappa > \varepsilon$ and thus for the off diagonal self energy and long time correlation function. The difference between Eqn. 3.103 and 3.106 gives

$$\overline{F} = \frac{\int \frac{d\lambda}{\sqrt{2\pi\mathcal{C}}} e^{-\frac{\lambda^2}{2\mathcal{C}}} \Omega(\lambda)^m \left(\left\langle \phi^2 \right\rangle_\lambda + \mathcal{C}^{-1} \langle \phi \rangle_\lambda \lambda \right)}{(1-m)\, \mathcal{Z}(m)}. \tag{3.107}$$

Expanding the numerator for m close to 1 gives

$$\overline{F} = \frac{\delta I}{\mathcal{Z}(m=1)} \tag{3.108}$$

with

$$\delta I = -\int \frac{d\lambda \left(\mathcal{C}^{-1} \langle \phi \rangle_\lambda \lambda + \left\langle \phi^2 \right\rangle_\lambda \right) e^{-\frac{\lambda^2}{2\mathcal{C}}} \Omega(\lambda) \log \Omega(\lambda)}{\sqrt{2\pi\mathcal{C}}}. \tag{3.109}$$

As expected, it follows that $\overline{F} = 0$ if $\kappa = \varepsilon$, where $\mathcal{C} = 0$. This can be seen from the expansion $\langle \phi \rangle_\lambda \simeq -\left\langle \phi^2 \right\rangle_\lambda \lambda$, valid for small λ and by substituting $\mu = \lambda/\sqrt{\mathcal{C}}$. It follows

$$\overline{F}(\kappa = \varepsilon) \propto \int \frac{d\mu}{\sqrt{2\pi}} e^{-\frac{\mu^2}{2}} \left(1 - \mu^2\right) = 0. \tag{3.110}$$

In addition h is determined from the condition of $\langle \phi \rangle = 0$. In Fig. 3.7, we plot the dimensionless coupling constant u/q_0 where a solution with $\overline{F} \neq 0$ occurs for the first time. (i.e., at the dynamic transition to the glass) as a function of the bare phase segregation strength ε_0^2 for $v = 0$.

Depending on the interaction u, there will be some segregation strength beyond which the system develops nonergodic behavior. The emergence of a self-generated glassy state is therefore, not a consequence of the perturbation, but is a generic aspect of the mean field theory. In agreement with Refs. (61) (62), $\overline{F}$ jumps discontinuously from zero in the liquid state to a finite value in the glass. In Fig. 3.8, we show the result for the onset of a glassy solution with $\overline{F} \neq 0$. he interesting is the region of glassy behavior increases due to the additional interaction that destroys the perfect symmetry between ϕ and $-\phi$ in the Hamiltonian. A glassy state becomes possible already for $\varepsilon_0^2 > 0$, i.e., while the liquid is still stable even within the simplest mean field approach. The effects due to the ϕ^3 interaction are even more dramatic for the dimensionless inverse correlation length ε_A at the transition where $\overline{F} \neq 0$ for the first time. The corresponding result is shown in Fig. 3.8. In case of $\upsilon = 0$, the correlation length at the transition increases as the interaction between the modes decreases. Most importantly, we find that there is a nontrivial solution $\kappa > \varepsilon$. The emergence of a self generated glassy state was not a consequence of the perturbative solution used in Refs. (61) (62). The calculation is performed for a temperature $T = 1$. We can reintroduce the temperature into the calculation by substituting $u \to uT$. A critical value for u leads to a temperature $T_{\rm A}$ (for fixed u) where within mean field theory an exponential number of metastable states emerges. In addition we obtain that at the transition the ratio $\kappa_{\rm A}/\varepsilon_{\rm A} \simeq 3.5$ for $\upsilon = 0$, which is close to the result $\kappa_{\rm A}/\varepsilon_{\rm A} = 3$, obtained within perturbation theory. However, for $\upsilon \neq 0, \kappa_{\rm A}/\varepsilon_{\rm A}$ decreases. In case of a finite $\upsilon/q_0^{3/2}$ the transition for $u/q_0 \to 0$ remains at a finite value for $\varepsilon_{\rm A}$, including a finite value for $\kappa_{\rm A}$. Thus, in case of only a moderate additional cubic interaction is the glassy state strongly stabilized. As $\upsilon/q_0^{3/2}$ increases, the behavior changes and the correlation length at the glass transition has an upper limit (minimum of $\varepsilon_{\rm A}$), which is reached if $u/q_0 \sim \upsilon/q_0^{3/2}$. In the limit of strong interaction $u/q_0 \to \infty$, we find a limiting value $\varepsilon_{\rm A} \simeq 0.45$. This behavior is in qualitative agreement with the result obtained with perturbation theory.

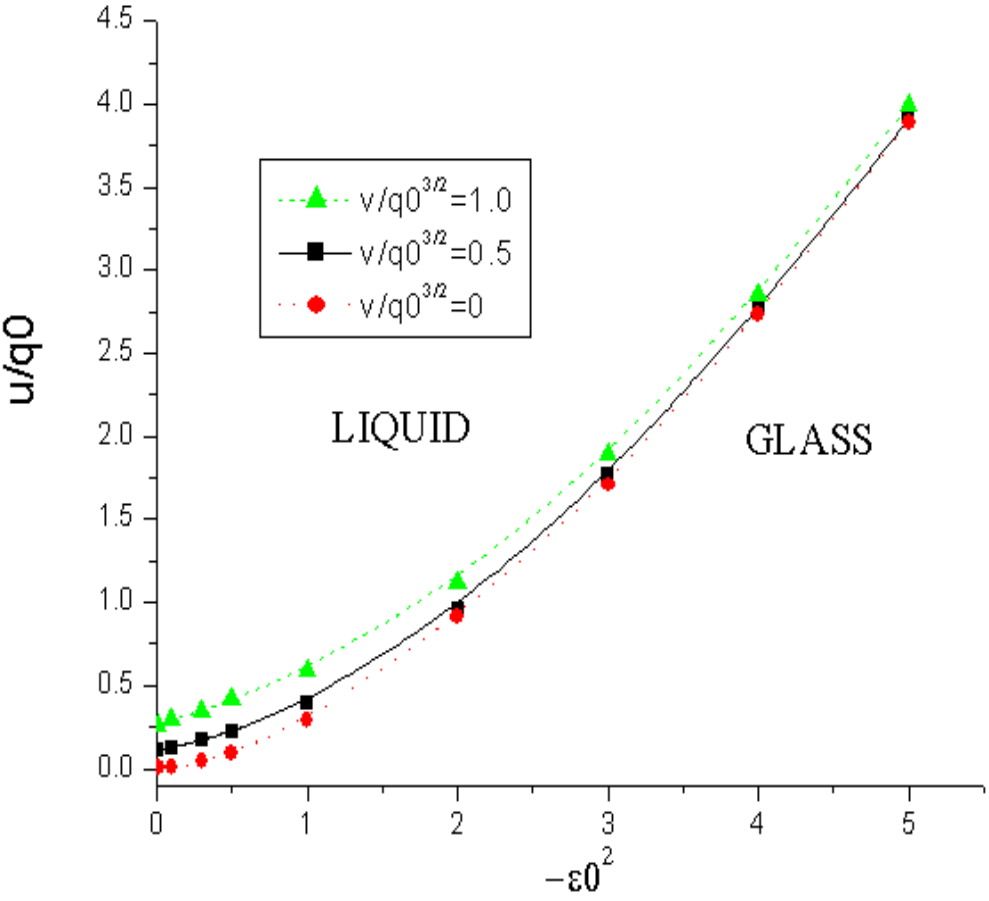

Figure 3.7 Dimensionless coupling constant, $u/q0$,where a nonergodic state $\overline{F} \neq 0$ occurs as a function of the bare phase segregation strength ε_0^2. Results for different strength of the asymmetric interaction $v\phi^3$ are shown. Finite v increases the glassy part of the phase diagram.

Once the correlation functions are determined we can use the fact that the functional $\Phi[G]$ is the same for the local problem as well as the original one and obtain

$$F(m) = \mathcal{F}(m) + \frac{T}{2m}\left(\mathrm{tr}\log G^{-1} - \mathrm{Tr}\log\overline{G}^{-1}\right). \tag{3.111}$$

Here Tr refers to the trace over replicas, but does not include the momentum integration, as opposed to tr which corresponds to a trace with respect to all degrees of freedom. Finally, $\mathcal{F}(m) = -\frac{T}{m}\log\mathcal{Z}(m)$ is the counter part of $F(m)$ for the local problem. Using Eqn. 3.9 it then follows for the configurational entropy

$$\begin{aligned} S_{c,loc} = \log Z(1) - \frac{1}{Z(1)}\int \frac{d\lambda}{\sqrt{2\pi C}} e^{-\frac{\lambda^2}{2C}}\left(\frac{\lambda^2 - C}{2C^2}\right)\left.\frac{\partial C}{\partial m}\right|_{m=1}\Omega(\lambda) \\ - \int \frac{d\lambda}{\sqrt{2\pi C}} e^{-\frac{\lambda^2}{2C}}\Omega(\lambda)\log\Omega(\lambda) \end{aligned} \tag{3.112}$$

with

$$\begin{aligned} \left.\frac{\partial C}{\partial m}\right|_{m\to 1} &= -\frac{(\varepsilon-\kappa)(2\pi(\varepsilon-\kappa)+\kappa(\varepsilon+\kappa))}{q_0\kappa} \\ C &= \frac{\varepsilon^2 - \kappa^2 + 2\pi(\kappa-\varepsilon)}{q_0}. \end{aligned} \tag{3.113}$$

As expected, in the limit $\kappa \to \varepsilon$ without glassy long time correlations, it follows $\mathcal{Z}(1) = \Omega(0)$ as well as $\left.\frac{\partial\mathcal{Z}(m)}{\partial m}\right|_{m\to 1} = \Omega(0)\log\Omega(0)$ and $F(q)$ goes to zero, leading to $S_c(\kappa = \varepsilon) = 0$. The configurational entropy is finite only for nontrivial solutions $\kappa > \varepsilon$. The temperature, T_A, where this happens for the first time is equal to the dynamic transition temperature of the system. The result for $S_c(T)$ also enables us to determine the Kauzmann temperature, $T_\mathrm{K} < T_\mathrm{A}$. In Fig. 3.9, we show the Kauzmann temperature for different $\left|\varepsilon_0^2\right|$. The configurational entropy vanishes like $S_c \propto T - T_\mathrm{K}$.

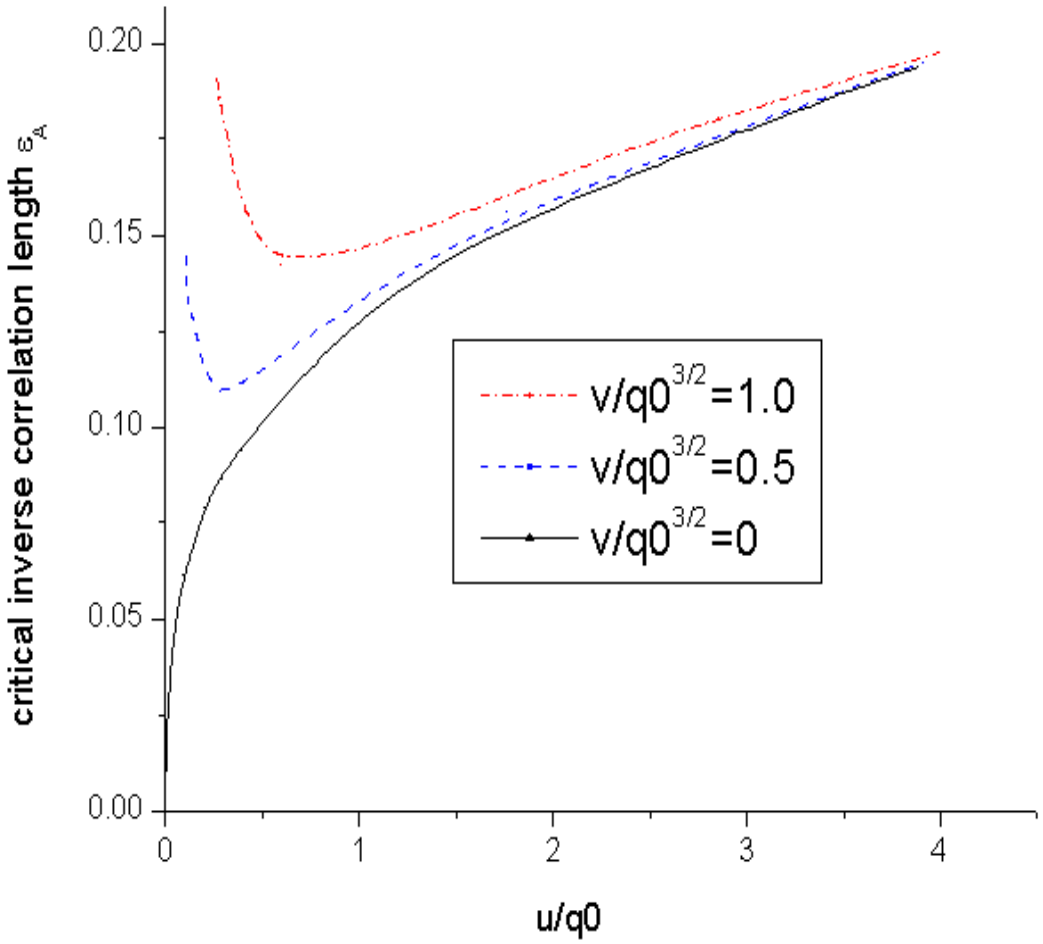

Figure 3.8 Dimensionless inverse correlation length vs coupling constant u/q_0 at the dynamical transition where a nonergodic state with $\overline{F} \neq 0$.

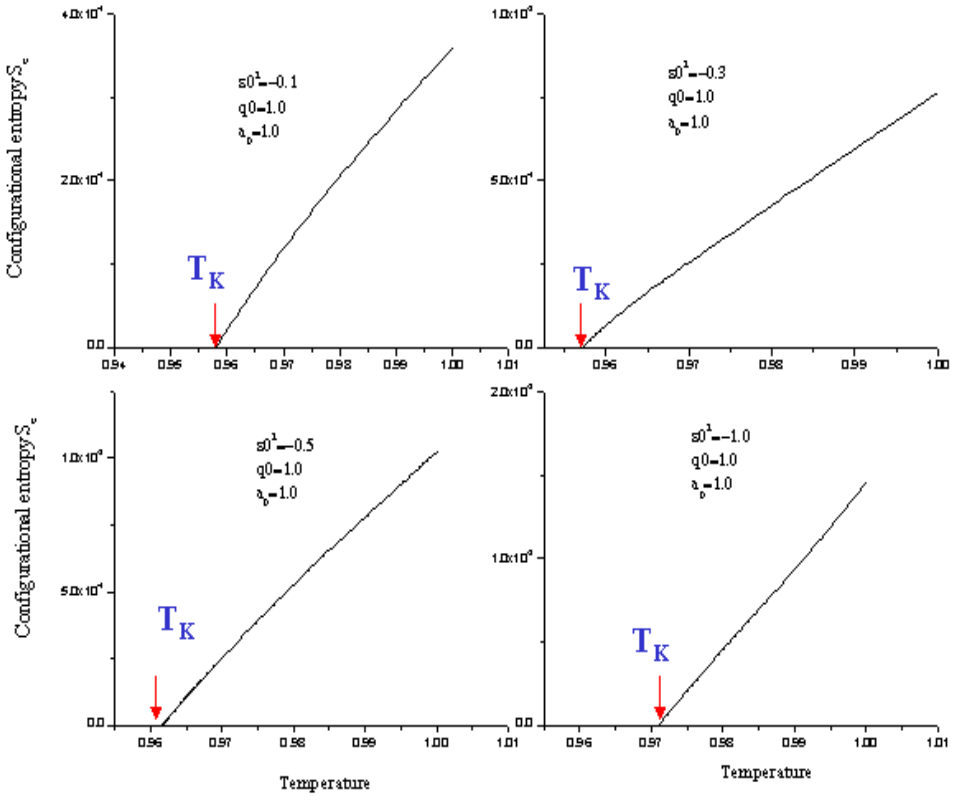

Figure 3.9 Configurational entropy S_c vs. temperature for different bare segregation strength ε_0^2. The configurational entropy vanishes at T_K.

3.4.7 Stability of the solution

An important simplification of our approach resulted from the simple form, Eqn. 3.89, of the correlation function in replica space. All diagonal elements as well as all off diagonal elements are assumed to be identical. Whether this assumption is indeed stable can be addressed by evaluating the eigenvalues of the stability matrix

$$\widehat{H}_{\alpha\beta;\gamma\delta} = \frac{\delta^2 F}{\delta G^{\alpha b}(q)\,\delta G^{\gamma\delta}(q')} \tag{3.114}$$

If there are negative eigenvalues of $\widehat{H}$ our assumption for the replica structure is unstable. Following Ref. (45) we find that the lowest eigenvalue with respect to the replica indices is determined by the lowest eigenvalue of the matrix

$$\widehat{h}_{\mathbf{q},\mathbf{q}'} = \delta\left(\mathbf{q}-\mathbf{q}'\right) K^{-2}(q) + v_0 \tag{3.115}$$

in momentum space, where $v_0 = \frac{\delta^2\Phi}{\delta\overline{G}^{\alpha\beta}\delta\overline{G}^{\alpha\beta}} - 2\frac{\delta^2\Phi}{\delta\overline{G}^{\alpha\beta}\delta\overline{G}^{\alpha\delta}} + \frac{\delta^2\Phi}{\delta\overline{G}^{\alpha\beta}\delta\overline{G}^{\gamma\delta}}$ with distinct α,β,γ and δ. In deriving this result we started from Eqn. 3.50 but used the fact that the functional Φ only depends on the momentum averaged correlation function, such that v_0 becomes momentum independent. Eqn. 3.115 is similar to the Schrödinger equation in momentum space of a single particle with bare Hamiltonian $K^{-2}(q)$ and local potential v_0. The lowest eigenvalue, E, of this problem is given by

$$1 = v_0 \int \frac{d^3q}{(2\pi)^3}\left(K^{-2}(q)+E\right)^{-1}. \tag{3.116}$$

This equation can be analyzed if we find a way to calculate v_0 which is determined by the first derivative of the self energy with respect to the correlation function $\frac{\delta\Sigma_{\alpha\beta}}{\delta\overline{G}_{\gamma\delta}}$. This derivative can be evaluated by following closely Ref. (55). First we add to our local Hamiltonian an additional term $-\sum_{\alpha\beta} U_{\alpha\beta}\phi_a\phi_\beta$ and analyze all correlation functions for finite U. At the end we will take the limit $U\to 0$ and the correlation function has the simple structure Eqn. 3.115. For finite U, the correlation function is determined from the function $\mathcal{Z}[U]$:

$$\overline{G}_{\alpha\beta}[U] = \langle\phi_\alpha\phi_\beta\rangle = -\frac{\delta\log\mathcal{Z}[U]}{\delta U_{\alpha\beta}}. \tag{3.117}$$

The self energy is a functional of only $\overline{G}[U]$ and not of U explicitly such that

$$\frac{\delta\Sigma_{\alpha\beta}}{\delta U_{\gamma\delta}} = \sum_{\mu\nu} \frac{\delta\Sigma_{\alpha\beta}}{\delta\overline{G}_{\mu\nu}} \frac{\delta\overline{G}_{\mu\nu}}{\delta U_{\gamma\delta}}. \tag{3.118}$$

If we furthermore introduce

$$\begin{aligned} L_{\alpha\beta;\gamma\delta} &= \frac{\delta G_{\alpha\gamma}}{\delta U_{\delta\beta}} \\ &= \langle\phi_\alpha\phi_\beta\phi_\gamma\phi_\delta\rangle - \langle\phi_\alpha\phi_\gamma\rangle\langle\phi_\delta\phi_\beta\rangle, \end{aligned} \tag{3.119}$$

which can be evaluated explicitly once $U = 0$, one finds

$$\sum_{\mu\nu} \left(G^{-1}_{\alpha\mu} G^{-1}_{\nu\gamma} - \frac{\delta\Sigma_{\mu\nu}}{\delta\overline{G}_{\alpha\gamma}} \right) L_{\alpha\beta;\gamma\delta} = \delta_{\mu\delta}\delta_{\beta\nu}, \tag{3.120}$$

which determines $\frac{\delta\Sigma_{\mu\nu}}{\delta\overline{G}_{\alpha\gamma}}$ and thus v_0.

Applying this approach to the Brazovskii model we find that the replica structure is marginally stable at the temperature T_A where the glassy state occurs for the first time. Below T_A the replica symmetric ansatz Eqn. 3.115 becomes unstable however it can be made stable if the replica index m does not approach 1 anymore but rather takes a value $m = \frac{T}{T_\mathrm{eff}}$ which defines the effective temperature T_eff of the glass. This is a situation similar to one step replica symmetry breaking with break point given by m. (6)

Stability of the replica symmetric ansatz was only possible because we consistently made the assumption of the dynamical mean field theory. Going beyond the local approach, for example by using cluster DMFT techniques, enables one to study whether or not nonlocal phenomena change the replica structure of the theory.

3.5 SCSA (Self consistent screening approximation) - analytical method

SCSA method developed by Ref. (63) (62) will be discussed in this section. Eqn. 3.36 has a formal similarity to the action of the random field Ising model, obtained within the conventional replica approach, which allows us to use techniques, developed for this model (65). Introducing an N component version of Eqn. 2.13 with field $\varphi = (\varphi_1, ..., \varphi_N)$ and coupling constant, $u = \frac{u_0}{N}$, with fixed u_0 we use a self consistent screening approximation (63), which is exact up to order $1/N$. At the end we perform the limit $N = 1$.

The matrix correlation function, $\mathcal{G}_{\alpha\beta}(\mathbf{q}) = \langle \varphi_a(\mathbf{q})\varphi_b(-\mathbf{q})\rangle$, in replica space with Dyson equation:

$$\mathcal{G}^{-1}(\mathbf{q})\big|_{ab} = \mathcal{G}_0^{-1}(\mathbf{q})\,\delta_{ab} + \Sigma_{ab}(\mathbf{q}) - \frac{g}{m} \tag{3.121}$$

Here, $\mathcal{G}_0(\mathbf{q})$ is the bare propagator. $\Sigma_{\alpha\beta}(\mathbf{q})$ is the self energy in replica space. If the ergodicity of the system is broken by the infinitesimal perturbation, g, the off diagonal element of $\Sigma_{\alpha\beta}(\mathbf{q})$ has nonzero value, which is the signal of the glassy dynamics. On the other hand, if the off diagonal term of $\Sigma_{\alpha\beta}(\mathbf{q})$ is zero, we expect a conventional ergodic dynamics and the system is in its liquid state or may build an ordered solid. However, it turns out that in the present case the off diagonal elements of $\Sigma_{\alpha\beta}(\mathbf{q})$ jump discontinuously from zero to a finite value.

Introducing a matrix $\mathbf{E}$ such that $\mathbf{E}_{ab} = 1$ and the unit matrix $\mathbf{1}$, it is easy to see that the product of any two $m \times m$ matrices with structure

$$\mathbf{A} = a_1\mathbf{1} + a_2\mathbf{E} \tag{3.122}$$

is given by

$$\mathbf{AB} = (a_1b_1)\,\mathbf{1} + (a_1b_2 + a_2b_1 + ma_2b_2)\,\mathbf{E}$$

. This leads to

$$\mathbf{A}^{-1} = \frac{1}{a_1}\mathbf{1} - \frac{a_2}{a_1(a_1 + ma_2)}\mathbf{E} \tag{3.123}$$

for the inverse of $\mathbf{A}$. The self consistent screening approximation is described by the set of Feynman diagrams shown in Fig. 3.10.

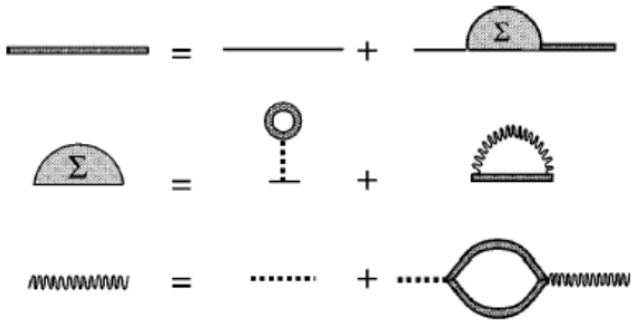

Figure 3.10 Feynman diagrams for SCSA approximation

The self energy is given as

$$\Sigma_{ab}(\mathbf{q}) = \frac{2}{N}\int \frac{d^3p}{(2\pi)^3}\, \mathcal{D}_{ab}(\mathbf{p})\, \mathcal{G}_{ab}(\mathbf{p}+\mathbf{q}) \tag{3.124}$$

where

$$\mathcal{D}(\mathbf{p}) = \left(v_0^{-1} + \Pi(\mathbf{p})\right)^{-1} \tag{3.125}$$

is determined self consistently by the polarization function

$$\Pi_{ab}(\mathbf{p}) = \int \frac{d^3q}{(2\pi)^3} \mathcal{G}_{ab}(\mathbf{q}+\mathbf{p})\, \mathcal{G}_{ba}(\mathbf{q})\,. \tag{3.126}$$

In the above set of equations the p-integration has to be cut-off at $|\mathbf{p}| = \Lambda$ and the temperature, T, and the coupling constant, u_0, occur only in the combination $v_0 = u_0 T$. The Ansatz **??** for the Green's function implies an analogous structure for $\Sigma_{ab}(\mathbf{q})$ and $\Pi_{ab}(\mathbf{q})$ in replica space. Inserting this ansatz into $\Pi_{ab}(\mathbf{p})$ gives

$$\Pi = (\Pi_{\mathcal{G}} - \Pi_{\mathcal{F}})\,\mathbf{1} + \Pi_{\mathcal{F}}\mathbf{E} \tag{3.127}$$

where the diagonal and off-diagonal elements of the polarization function are

$$\Pi_{\mathcal{G}}(\mathbf{p}) = \int \frac{d^3q}{(2\pi)^3} \mathcal{G}(\mathbf{q}+\mathbf{p})\,\mathcal{G}(\mathbf{q})$$
$$\Pi_{\mathcal{F}}(\mathbf{p}) = \int \frac{d^3q}{(2\pi)^3} \mathcal{F}(\mathbf{q}+\mathbf{p})\,\mathcal{F}(\mathbf{q}). \tag{3.128}$$

It is now straightforward to determine $\mathcal{D}_{ab}(\mathbf{p})$ which leads, in the limit $m \to 1$, to

$$\mathcal{D} = (\mathcal{D}_{\mathcal{G}} - \mathcal{D}_{\mathcal{F}})\,\mathbf{1} + \mathcal{D}_{\mathcal{F}}\mathbf{E} \tag{3.129}$$

where

$$\mathcal{D}_{\mathcal{G}}(\mathbf{p}) = \left(v_0^{-1} + \Pi_{\mathcal{G}}(\mathbf{p})\right)^{-1} \tag{3.130}$$

and

$$\mathcal{D}_{\mathcal{F}}(\mathbf{p}) = -\frac{\Pi_{\mathcal{F}}(\mathbf{p})\,\mathcal{D}_{\mathcal{G}}^2(\mathbf{p})}{1 - \Pi_{\mathcal{F}}(\mathbf{p})\,\mathcal{D}_{\mathcal{G}}(\mathbf{p})}. \tag{3.131}$$

Analogously, inserting the above equations into 3.124, we get for the self energies $\Sigma = (\Sigma_{\mathcal{G}} - \Sigma_{\mathcal{F}})\,\mathbf{1} + \Sigma_{\mathcal{F}}\mathbf{E}$ where

$$\Sigma_{\mathcal{G}}(\mathbf{q}) = \frac{2}{N} \int \frac{d^3p}{(2\pi)^3} \mathcal{D}_{\mathcal{G}}(\mathbf{p})\,\mathcal{G}(\mathbf{p}+\mathbf{q}) \tag{3.132}$$

and $\Sigma_{\mathcal{F}}(\mathbf{q}) = \frac{2}{N} \int \frac{d^3p}{(2\pi)^3} \mathcal{D}_{\mathcal{F}}(\mathbf{p})\,\mathcal{F}(\mathbf{p}+\mathbf{q})$.

The self consistent screening approximation is used to calculate the self energy. The key assumption of the analytical approach to the self consistent screening approximation is that the off diagonal self energy $\Sigma_{\mathcal{F}}(\mathbf{q})$ is weakly momentum dependent. We will then calculate $\Sigma_{\mathcal{F}}(q_0)$ at the modulation wave vector q_0.

$$\Sigma_{\mathcal{F}}(\mathbf{q}) \sim \Sigma_{\mathcal{F}}(q_0) \tag{3.133}$$

Due to our assumption that $\Sigma_{\mathcal{F}}$ is weakly dependent on q, we concentrate on $\Sigma_{\mathcal{F}}(q_0)$ at the modulation wave vector. One easily finds that $\Sigma_{\mathcal{F}}(q_0) \leq 0$. A dimensional analysis furthermore shows that $\Sigma_{\mathcal{F}}$ is length^{-2}. This suggests to define a new length scale, λ, via

$$\Sigma_{\mathcal{F}}(q_0) = -\left(\frac{2}{\lambda}\right)^2. \tag{3.134}$$

The length scale λ which determines whether long time correlations are similar or different from instantaneous ones. For the subsequent calculation it is convenient to introduce in addition to the dimensionless parameter ε which gives $\xi^{-1} = \frac{\varepsilon q_0}{2}$ a new dimensionless parameter, κ, defined via

$$\lambda^{-1} = \frac{\sqrt{\kappa^2 - \varepsilon^2} q_0}{2} \tag{3.135}$$

Obviously, in the liquid state, where $\Sigma_{\mathcal{F}} \to 0$, we find $\lambda \to \infty$ and it holds $\kappa = \varepsilon$. In a glassy state $\kappa > \varepsilon$. The correlation function $\mathcal{K} = \mathcal{G} - \mathcal{F}$. Note that $\mathcal{K}$ has the same structure as $\mathcal{G}$ but with $\varepsilon \to \kappa$.

The glassy behavior of the Brazovskii model for ϕ^4 model ($\upsilon = 0$ in Eqn. 3.82) is investigated using SCSA replica approach in local real space. In local real space, the self energy does not depend on the momentum, the Eqn. 3.133 is satisfied automatically and all the physical quantities have only replica index.

$$\Sigma_{ab} = 2 D_{ab} G_{ab}. \tag{3.136}$$

The polarization function is given by the multiplication of the correlation matrix

$$\Pi_{ab} = G_{ab} G_{ba}. \tag{3.137}$$

D is given as

$$D = \left(u_{loc}^{-1} + \Pi\right)^{-1} \tag{3.138}$$

where u_{loc} is defined as $u_{loc} = u a_0^3$. The length scale a_0^3 is q_0^{-3}. The correlation matrix in a replica space is expressed as the replica ansatz as like

$$\begin{aligned} G_{ab} &= \overline{K}\delta_{ab} + \overline{F} \\ \Pi_{ab} &= \left(\overline{K}^2 + 2\overline{KF}\right)\delta_{ab} + \overline{F}^2 \\ &\equiv \Pi_K \delta_{ab} + \Pi_F, \end{aligned} \tag{3.139}$$

where D^{-1} is given as

$$D^{-1} = \left(u_{loc}^{-1} + \Pi_K\right)\delta_{ab} + \Pi_F. \tag{3.140}$$

By the inverse matrix property of Eqn. 3.123 in a replica space, D is given by

$$\begin{aligned} D &= \frac{1}{u_{loc}^{-1} + \Pi_K}\delta_{ab} - \frac{\Pi_F}{\left(u_{loc}^{-1} + \Pi_K\right)\left(u_{loc}^{-1} + \Pi_K + \Pi_F\right)} \\ &\equiv D_K\delta_{ab} + D_F \end{aligned} \tag{3.141}$$

where

$$\begin{aligned} D_K &= \frac{1}{u_{loc}^{-1} + \Pi_K} \\ D_F &= -\frac{\Pi_F D_K^2}{1 + \Pi_F D_K}. \end{aligned} \tag{3.142}$$

The local diagonal self energy and the local off diagonal self energy are given as

$$\begin{aligned} \Sigma_{ab} &= 2\left(D_K\delta_{ab} + D_F\right)\left(K\delta_{ab} + F\right) \\ &= 2\left(D_K K + D_K F + D_F K\right)\delta_{ab} - 2D_F F \\ &\equiv \Sigma_K\delta_{ab} + \Sigma_F \end{aligned} \tag{3.143}$$

where

$$\begin{aligned} \Sigma_F &= 2D_F F \\ \Sigma_K &= 2\left(D_K K + D_K F + D_F K\right). \end{aligned} \tag{3.144}$$

From Eqn. 3.92 and Dyson equation, ε and κ have the relation with the local self energies as follows;

$$\begin{aligned} \kappa^2 q_0^2 &= \varepsilon_0^2 q_0^2 - q_0^3\Sigma_K \\ \varepsilon^2 q_0^2 &= \varepsilon_0^2 q_0^2 - q_0^3\left(\Sigma_K - \Sigma_F\right) \\ \kappa^2 q_0^2 &= \varepsilon^2 q_0^2 + q_0^3\Sigma_F. \end{aligned} \tag{3.145}$$

By some algebra, the off diagonal self energy, the signal of the glassy dynamics, is given by

$$\begin{aligned} \Sigma_F &= 2D_F F \\ &= 2\frac{\Pi_F D_K^2}{1 + \Pi_F D_K}F \\ &= \left(\frac{1}{\varepsilon} - \frac{1}{\kappa}\right)\frac{4\pi}{q_0}\frac{\frac{\left(1-\frac{\varepsilon}{\kappa}\right)^2}{1+\varepsilon^2 a^{-1}}}{a^{-1} + \frac{1}{\varepsilon^2} - \left(\frac{1}{\varepsilon} - \frac{1}{\kappa}\right)^2} \end{aligned} \tag{3.146}$$

where $a^{-1} = u^{-1}\left(\frac{2\pi}{q_0}\right)^2$. From the relation of Eqn. 3.134, the self consistent equation for a local off diagonal self energy Σ_F is given by

$$\kappa^2 - \varepsilon^2 = 4\pi\left(\frac{1}{\varepsilon} - \frac{1}{\kappa}\right)\frac{\varepsilon^2\frac{\left(1-\frac{\varepsilon}{\kappa}\right)^2}{1+\varepsilon^2 a^{-1}}}{\varepsilon^2 a^{-1} + 1 - \left(1-\frac{\varepsilon}{\kappa}\right)^2}. \tag{3.147}$$

The numerical and analytical calculation for the glassy behavior of Brazovskii model (ϕ^4) are plotted in Fig. 3.11.For small coupling constant u/q_0, the SCSA approach is quite consistent with numerical one. However, as the coupling constant u/q_0 increases, the SCSA prediction for glassiness shows a deviation from the numerical result.

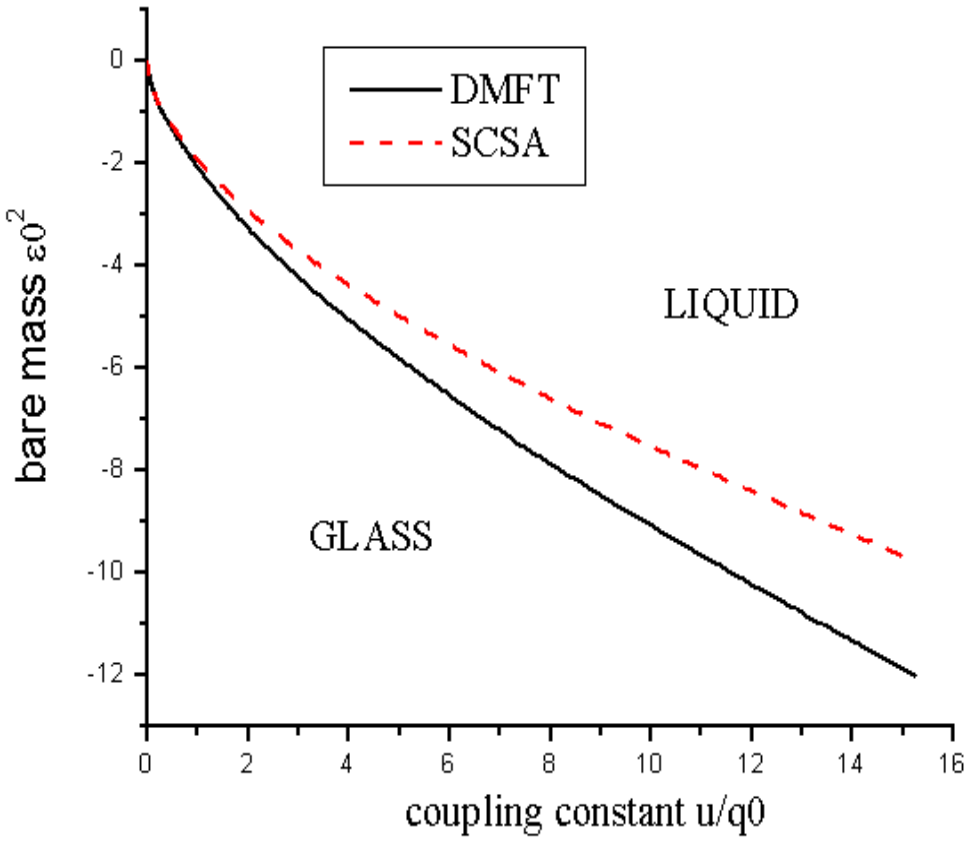

Figure 3.11 The glassy behavior for Brazovskii model by two different approaches

CHAPTER 4. NONEQUILIBRIUM PHYSICS OF MICROEMULSIONS AND BLOCKCOPOLYMERS

In this chapter, we will discuss the nonequilibrium physics of a microemulsion and block copolymer. The glassy behavior of a microemulsion is supported by small angle neutron scattering and dynamical light scattering. (20) (76) The density correlation function of the droplets shows a slowing down with nonexponetial KWW(Kohlrausch-Williams-Watts) decay. (77) The diffusion of droplets becomes dynamical self arrest due to an entrapment in cages formed by environment under certain conditions. (77) We analyze the glassy behavior of a microemulsion with a SCSA replica approach discussed in chapter 3. The boundary of the glassy state in a microemulsion is obtained by determining the dependence of the correlation length ξ and the modulation length l_m as a function of t, f, and r_s/a. Since the glass occurs for a fairly moderate correlation length, we can ignore effects due to critical fluctuations (relevant as $\xi \to \infty$) and use our results for ξ and l_m of the Hartree analysis to determine the boundary to the microemulsion glass state. This leads to the following implicit equation for the onset temperature of glassiness $T_A = t_A T_c^0$:

$$f = \frac{\left(1 + B\left(t_A, \frac{r_s}{a}\right) f\right)^2}{\frac{r_s}{a} t_A} \tag{4.1}$$

where $B(t,x) = \frac{6^{1/3}\pi^{8/3}t^3}{x(t-1)^2}$. The glass temperature for a microemulsion is derived in Appendix D. The solution of this equation for different r_s gives the boundary of the microemulsion glass shown in Fig. 4.1. Examples for the temperature dependence of ξ and l_m for $f > f^*$ and $f < f^*$ are shown in Fig. 4.2.

Since the frustrating potential is of finite range, a finite critical strength of the frustration, $\sim f^*$, must be reached to form a microemulsion glass. The larger the amphiphilic molecule and

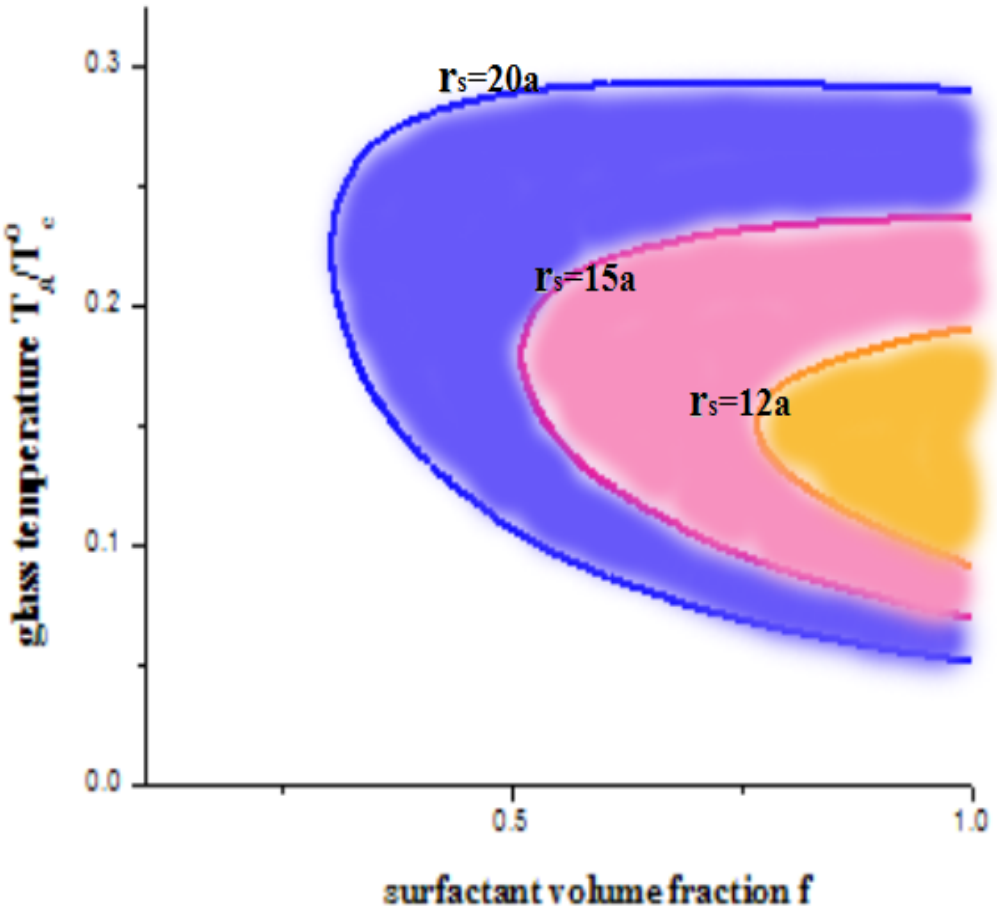

Figure 4.1 The emergence of a microemulsion glass for different ratio of r_s/a.

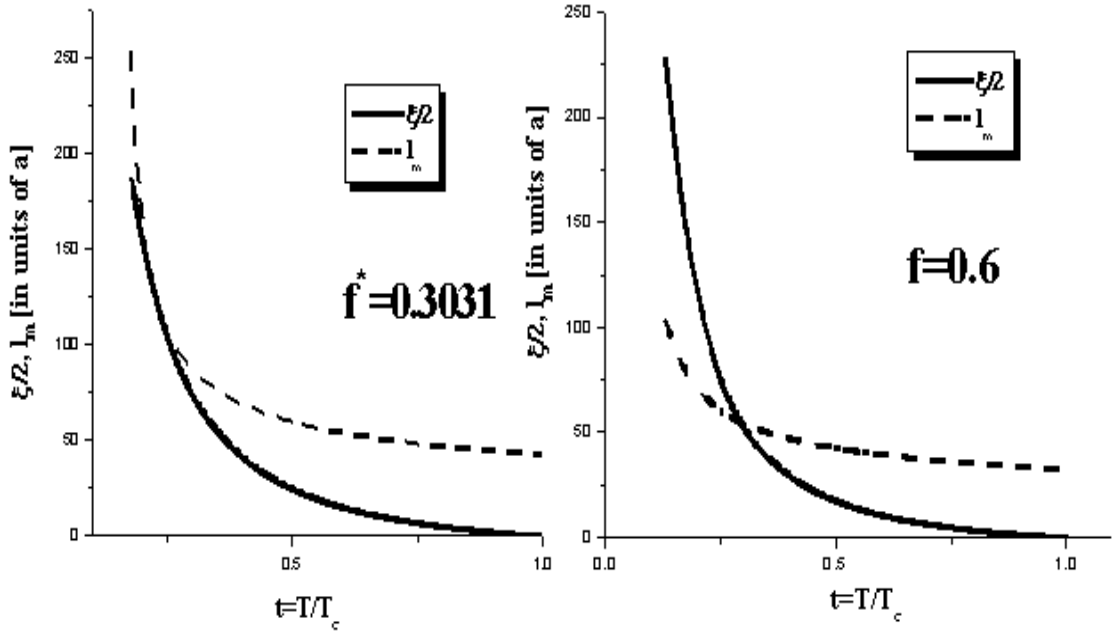

Figure 4.2 The ratio of $\xi/2$ to l_m for different surfactant volume fraction. At $f = 0.3$, $\xi/2 \sim l_m$, at which the glassy behavior sets in.

the larger its volume fraction, the more pronounced is the glass state. Yet, the sizes of the oil and water regions have to be much larger than the size of their interfaces, i.e., $l_m \gg r_s$. In the proximity of the glass transition we find $\frac{l_m}{r_s} = \frac{2\pi}{\sqrt{6}}(\sqrt{\frac{r_s}{a}t\,f} - 1)^{-1/2}$. Provided that $r_s \ll 54.45a$ (a value much larger than the critical value of r_s for glassiness) we indeed find that $l_m \gg r_s$.

The glassy state of our theory is self generated, i.e., it is due to the frustrated nature of the interactions of the system. One way to test our theory is to deliberately "lift" this frustration. For example, we expect that if some disorder is imposed in the surfactant chain length, the glass formation might be reduced. In fact, glassiness will disappear if we add a certain amount of short chain amphiphiles to a system with long chain surfactants. Since the effective mean square root length of the surfactant molecule is then given by (25) $r_{\rm s} = \left(\sum_i x_i r_{{\rm s},i}^2\right)^{1/2}$, with x_i being the mole fraction of a surfactant with length $r_{{\rm s},i}$, $r_{\rm s}$ can easily become smaller than the critical value $r_{\rm s}^*$. Another way of testing our theory is to compare the transitions on the high-T and low-T side of the glass state for given f. As shown in Fig.3, we find that the low-T transition has a larger modulation length. Thus, using $S_c \propto l_m^{-3}$, (62), it has a smaller configurational entropy compared to the high-T side of the transition, an effect which can be observed by measuring the specific heat anomaly at the vitrification. At the same time, along the glass transition curve $\xi/l_m \simeq 2$. Thus, the position of a small angle neutron scattering (SANS) peak should be shifted along the transition curve, whereas the peak-width ratio should stay essentially unchanged. The phase diagrams of a microemulsion for different r_s/a values are plotted in Fig. 4.3 and Fig. 4.4 respectively.

When we increase the ratio of r_s/a, the microemulsion glass region is expanded, which is due to the increase of the frustration by increasing the length of the surfactant in the system as mentioned in Chapter 2. Fig. 4.3 and Fig. 4.4 show the role of frustration in forming glass in microemulsion. These results are based on the φ_4 model, since we consider the same amount of oil and water molecules. The different amount of water and oil molecules requires to add the symmetry breaking φ_3 term in our model Hamiltonian 2.13, which will estimate more broad microemulsion region from the result of Fig.3.8.

We analyzed the glassy behavior of lamellar phase for $f = 0.5$. The cubic and quartic terms,

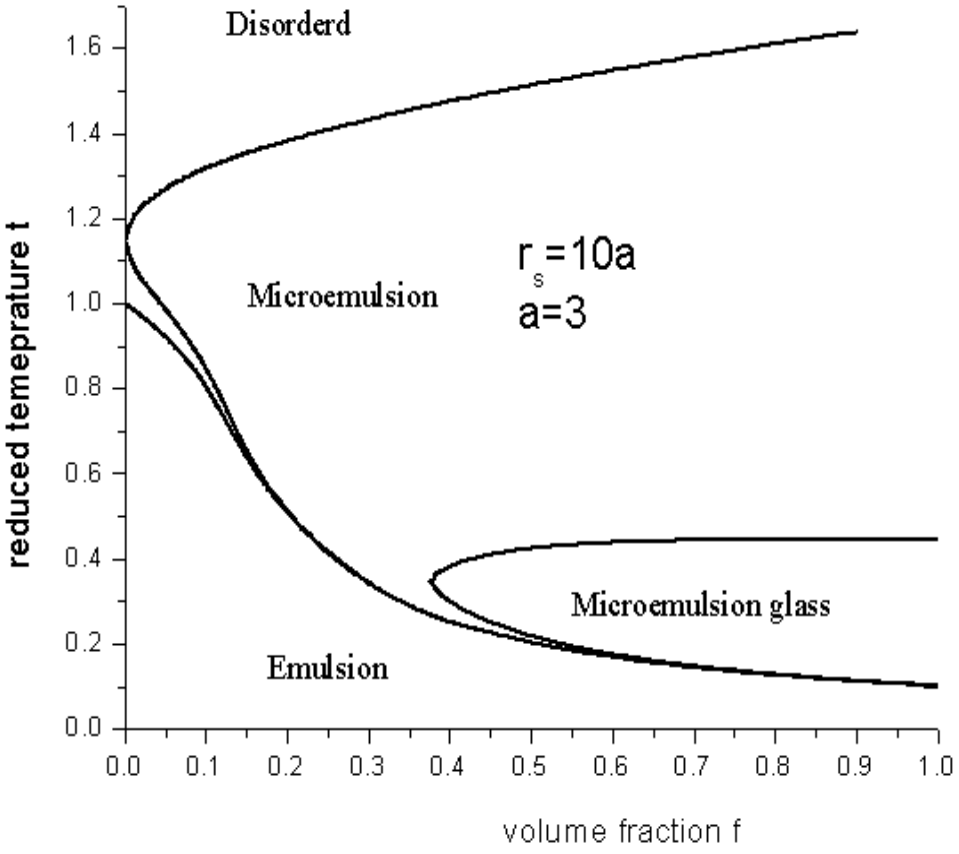

Figure 4.3 The phase diagram of a microemulsion with $r_s/a = 10$

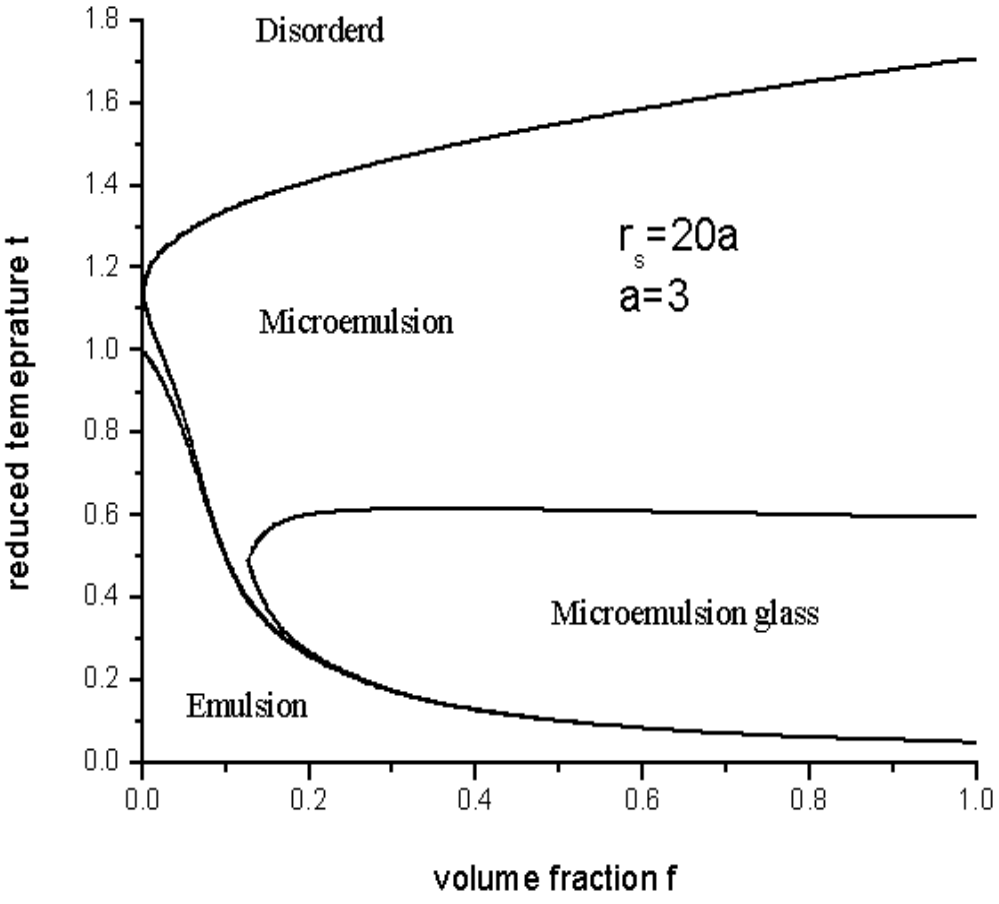

Figure 4.4 The phase diagram of a microemulsion with $r_s/a = 20$

$\Gamma_3(\mathbf{q}_1, \mathbf{q}_2, \mathbf{q}_3)$ and $\Gamma_4(\mathbf{q}_1, \mathbf{q}_2, \mathbf{q}_3, \mathbf{q}_4)$ are given by $\Gamma_3(q_0)$ and $\Gamma(0,0)$ in a weak segregation limit respectively.

From the self consistent solution for fixed f, S, q_0, we can determine the critical ε_0^2 value which indicates that the glassiness sets in. We find there is only one solution for a critical point and no solution for a liquid phase and two non trivial solutions for a glass phase. Once ε_0 is determined, the critical Flory-Hugggins parameter can be obtained from the relation of $\varepsilon_0^2 = \dfrac{F^* - 2\chi S}{F^{**}x^{*2}}$ for the glass transition of the diblock copolymer. In Fig. 4.5, $(\chi S)_A$ is plotted versus the volume fraction f for $S = 1026$. And $(\chi S)_A$ is compared to spinodal line $(\chi S)_{spinodal}$ and mean field solution of Leibler, $(\chi S)_{MF}$. Since the perturbation theory breaks down below $S = 10^4$, only the mean field calculation result is shown in Fig. 4.5.

In Fig. 4.6, $(\chi S)_A$ for $S = 10^4$ and $(\chi S)_A$ for $S = 1026$ are plotted versus the volume fraction f for $S = 1026$. Fig. 4.6 shows that the $(\chi S)_A$ value for $S = 10^4$ becomes more closer to the MST line by increasing the chain length of block copolymer.

The Flory-Huggins parameter χ can be expressed as $\frac{A}{T} + B$. A, B is constant and T is absolute temperature. From this, the glass transition temperature can be plotted as a function of the chain length of block copolymer approximately.($\chi \sim \frac{1}{T}$). Fig. 4.7 shows the glass transition temperature of block copolymer for $f = 0.5$ versus the chain length. The glass transition temperature increases as the chain length of polymer increases. This is quite consistent with the free volume theory. The chain ends introduce incremental amounts of the free volume over the end segments, which increase the glass temperature as the chain length increases. (83).

However, comparing our theoretical calculation with experimental data, we should consider the stiffness of polymeric chains. Since the restriction of a rotation by a stiff chain gives a rise to an entropy decrease, we expect the stiffness of polymer chains changes the magnitude of vertex functions. In the case of homopolymer, for example, only by attaching a bulky side chain to a homopolymer backbone chain, the stiffness increases, which elevates a glass transition temperature. (84) This implies the glass temperature of diblock copolymers would have a strong dependence on the stiffness of polymer chains as like homopolymer chain. The

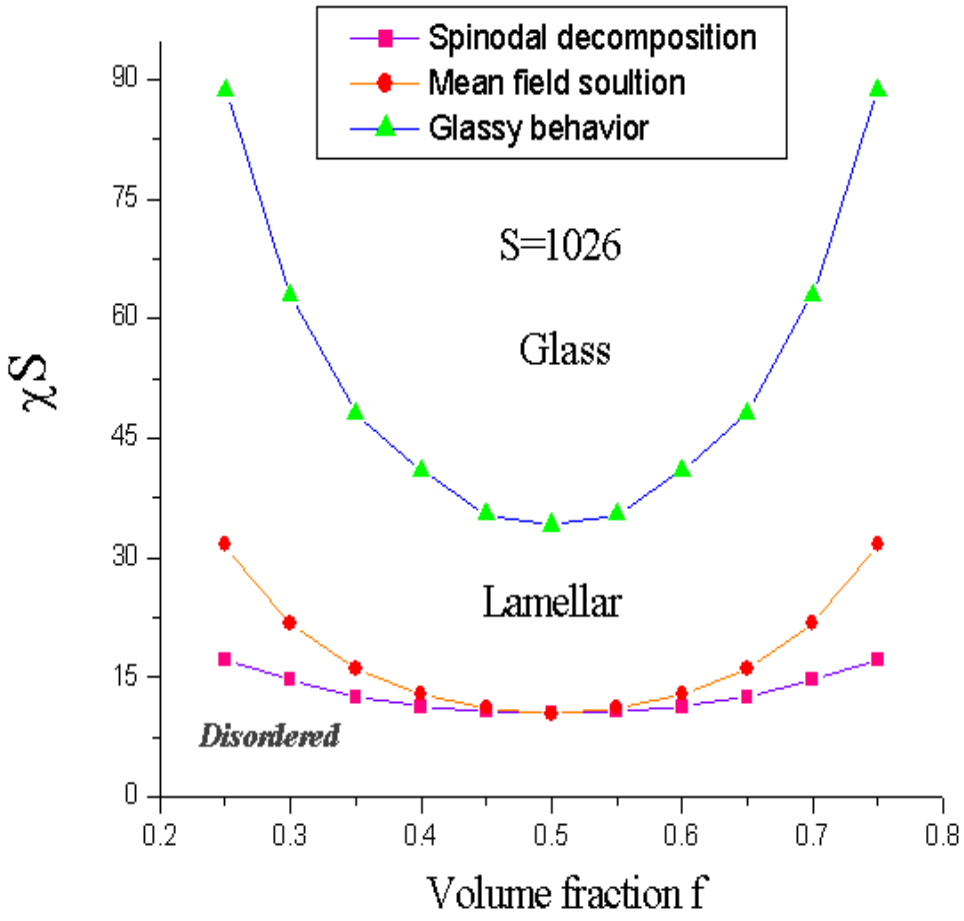

Figure 4.5 The phase diagram of lamellar and glass phase for $S = 1026$ and $f = 0.5$

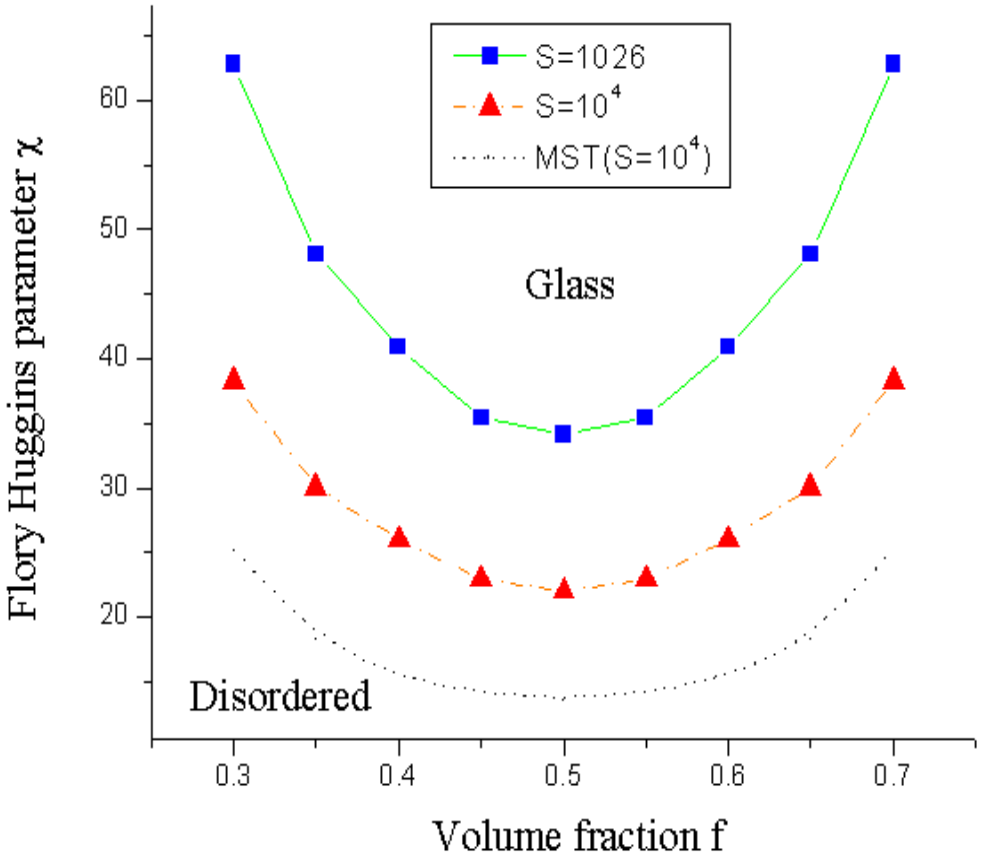

Figure 4.6 The phase diagram of lamellar and glass phase for $S = 1026$ and $S = 10^4$

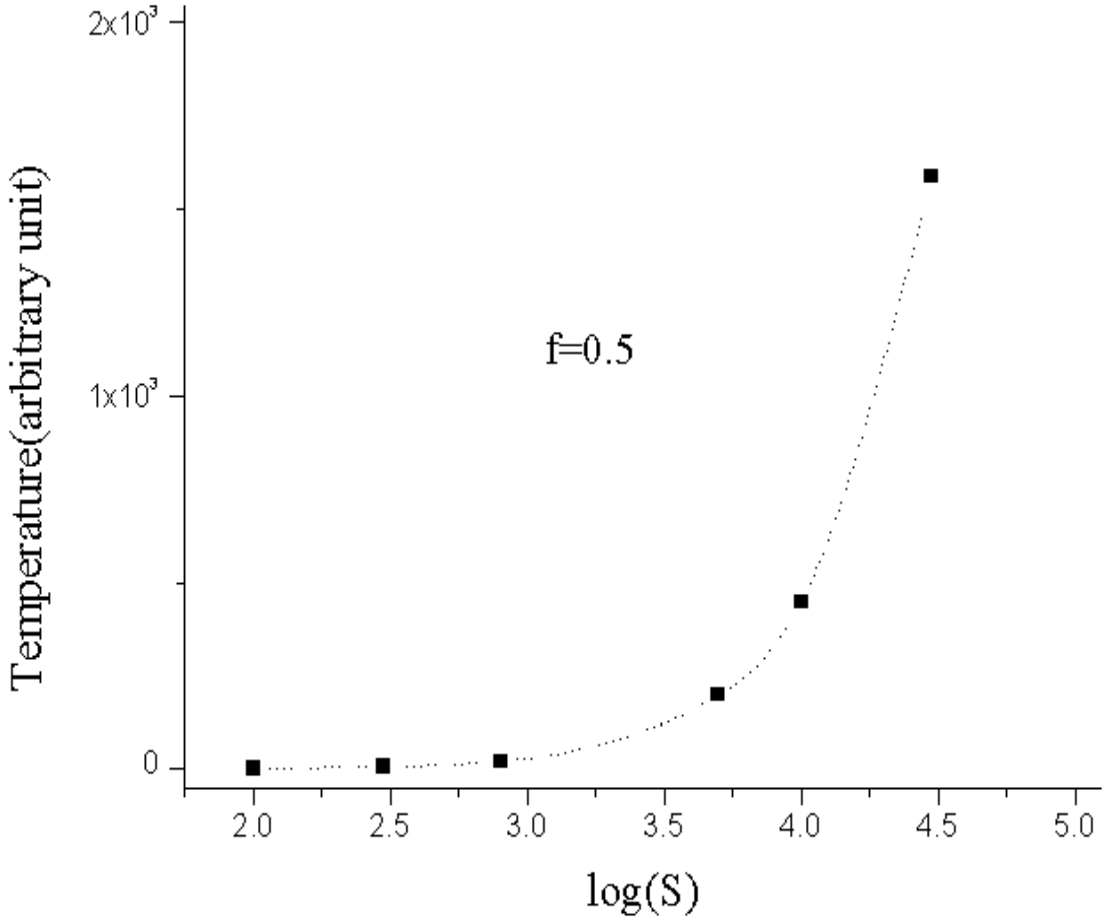

Figure 4.7 The glass transition temperature versus degree of polymerization. The temperature has an arbitrary unit.

theoretical calculation of $(\chi S)_A$ for a different stiffness of polymer chains is required for the comparison with experimental data.

Fig. 4.8 shows an inverse maximum scattering intensity $I^{-1}(q_0)$ ($\sim\varepsilon^2 q_0^2$) versus 1/temperature ($\chi \sim \frac{1}{T}$) for $f = 0.5$, $S = 1026$ in a diblock copolymer.

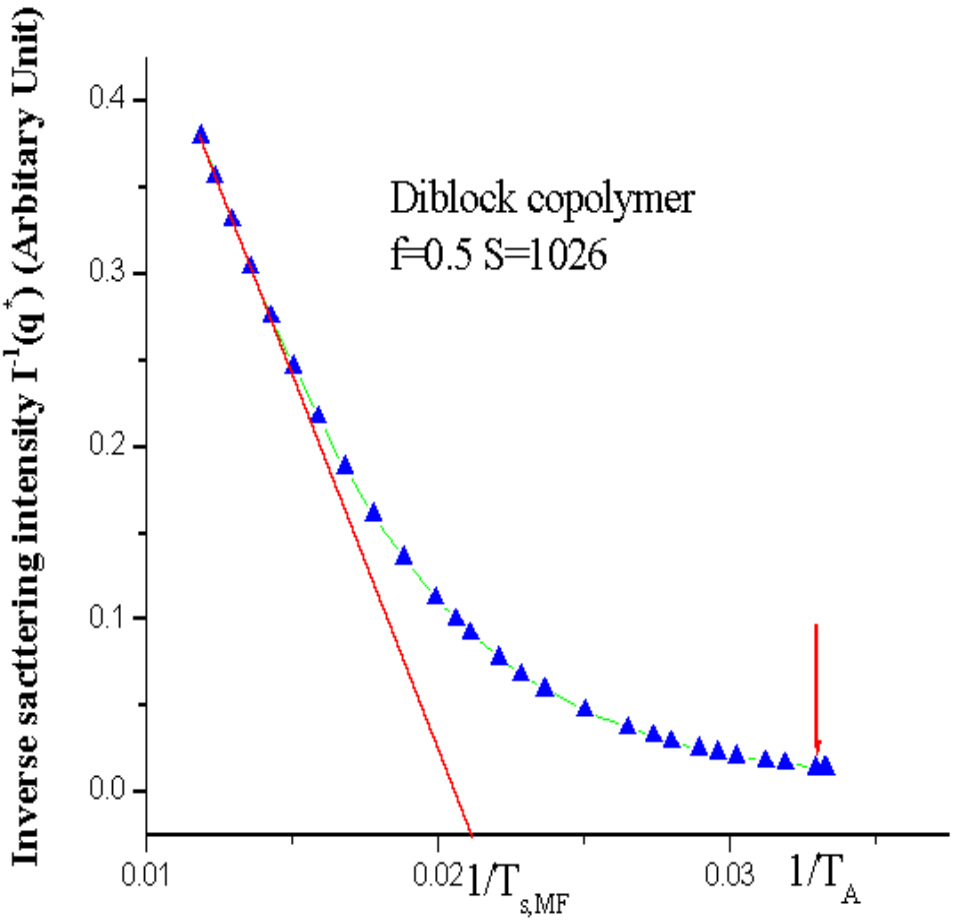

Figure 4.8 Inverse scattering intensity versus 1/temperature for $f = 0.5$, $S = 1026$

The linearity in a graph determines the temperature $1/T_{MF}$, at which ordering sets in. The nonlinearity shows the emergence of fluctuation effect as the temperature approaches to

T_{ODT}. (78) Fig. 4.9 shows the schematic inverse maximum scattering intensity for the order-disorder transition and glass-disorder transition for lamellar phase. Despite of the controversies, the small gap in the inverse scattering intensity at T_{ODT} is verified by some experimental groups. (79) (80) (81) This schematic picture reminds us the thermodynamic behavior of the supercooled liquid and the crystal.

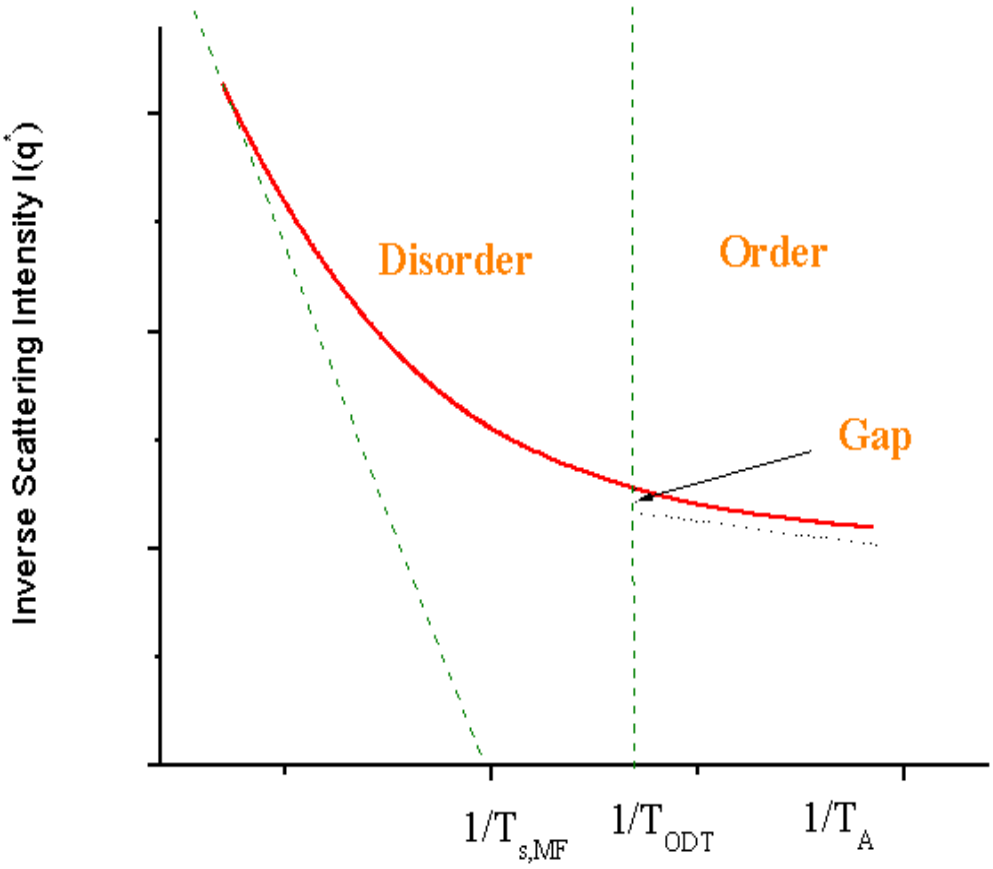

Figure 4.9 Schematic picture for inverse scattering for order-disorder transition(experiment) and glass-disorder transition(calculation)

Fig. 4.10 shows the configurations in a real space for disorder and glassy state from Fourier

transformation of the correlation function $G(q)$ and $F(q)$ by the clipped random wave analysis. (10)

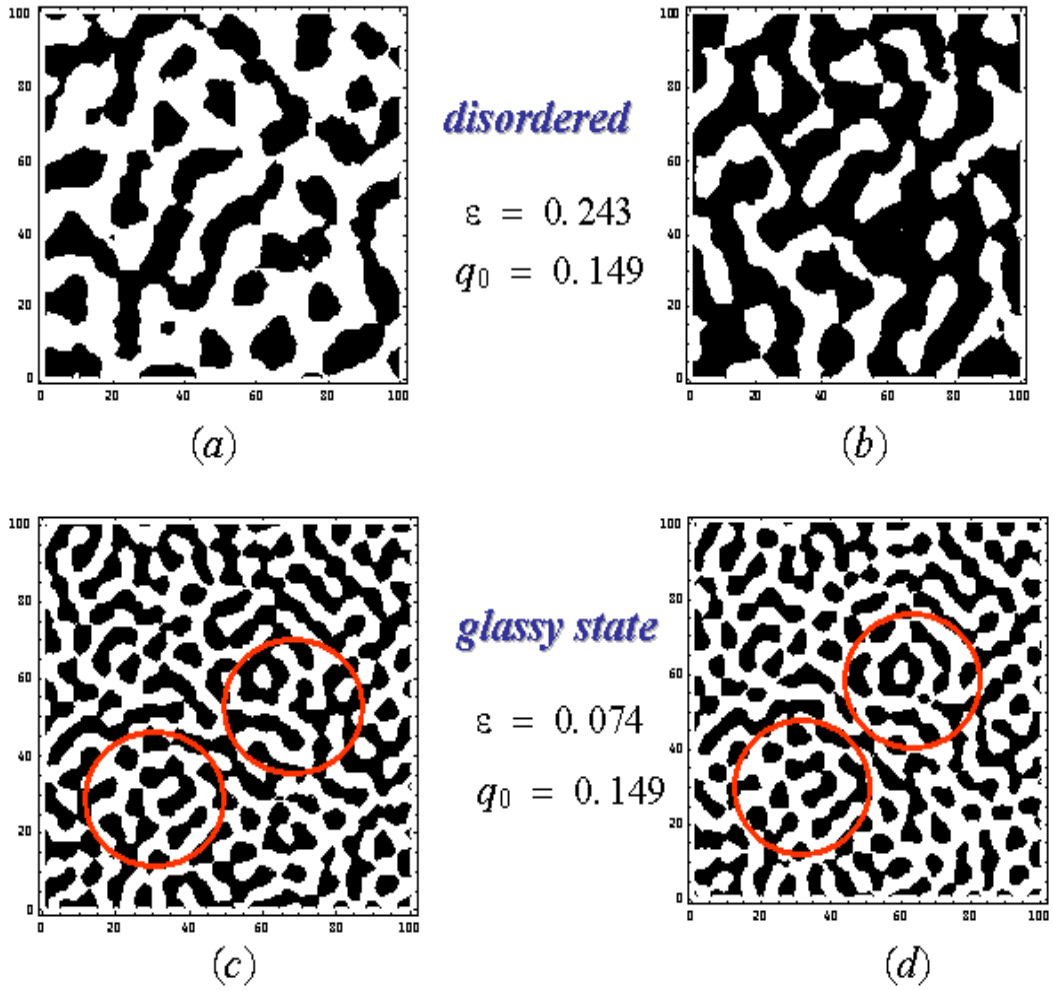

Figure 4.10 The visualization of the configurations of A block and B block in disordered state and glassy state.

The method for the visualization is explained in Appendix C. The white part corresponds to A block and the black part to B block. (a) in Fig. 4.10 shows a certain configuration in disordered state at $t = t_1$. (b) shows the configuration in disordered state at $t = t_2$ with $t = t_2 > t = t_1$. We find there is no correlation between (a) and (b) as like liquid state.

However, there is a strong correlation in (c) and (d) configurations in glassy state. The configurations within circles in Fig. 4.10 are conserved as time elapses at lab time scale. In the glassy state far below T_{ODT}, two configurations show the memory effect due to a slow dynamics of block copolymer.

In Fig. 4.11 we plotted critical Flory-Huggins parameter for the gelation versus the interaction strength Q.As we increase the interaction strength Q, the χ_A decreases to zero sharply. At certain value of Q, the χ_A becomes negative. In negative χ_A, the aggregation happens not only between the end segments of A blocks but also between the middle block (B block). The repulsive excluded volume interaction between polymeric chains and the attractive interaction at the end segments generates an additional frustration within triblock copolymer chains, which makes aggregation process easier.

In the calculation of the gelation, two different configurations are considered: loop structure and no loop structure. When the interaction energy V_P is given as

$$V_P = -\sum_{n_1,\cdots,n_p}\sum_{s_1,\cdots,s_p} U(\mathbf{R}_{n_1,s_1},\cdots,\mathbf{R}_{n_p,s_p}), \tag{4.2}$$

the architecture of bridge or loop is not allowed. Our result shows χ_A without loop or bridge structure for the gelation is larger than the χ_A of the loop structure. This implies the aggregation with the bridge or loop structure comes before the fully extended network structure when the temperature is decreased. Fig. 4.12 shows a schematic gelation process as a function of the temperature. This is quite consistent with the solid/liquid transition of the acrylic triblock copolymers (19). In our theory, the basic difference between the gelation and glassiness depends on the presence of the configurations such as loop or bridge in the interaction.

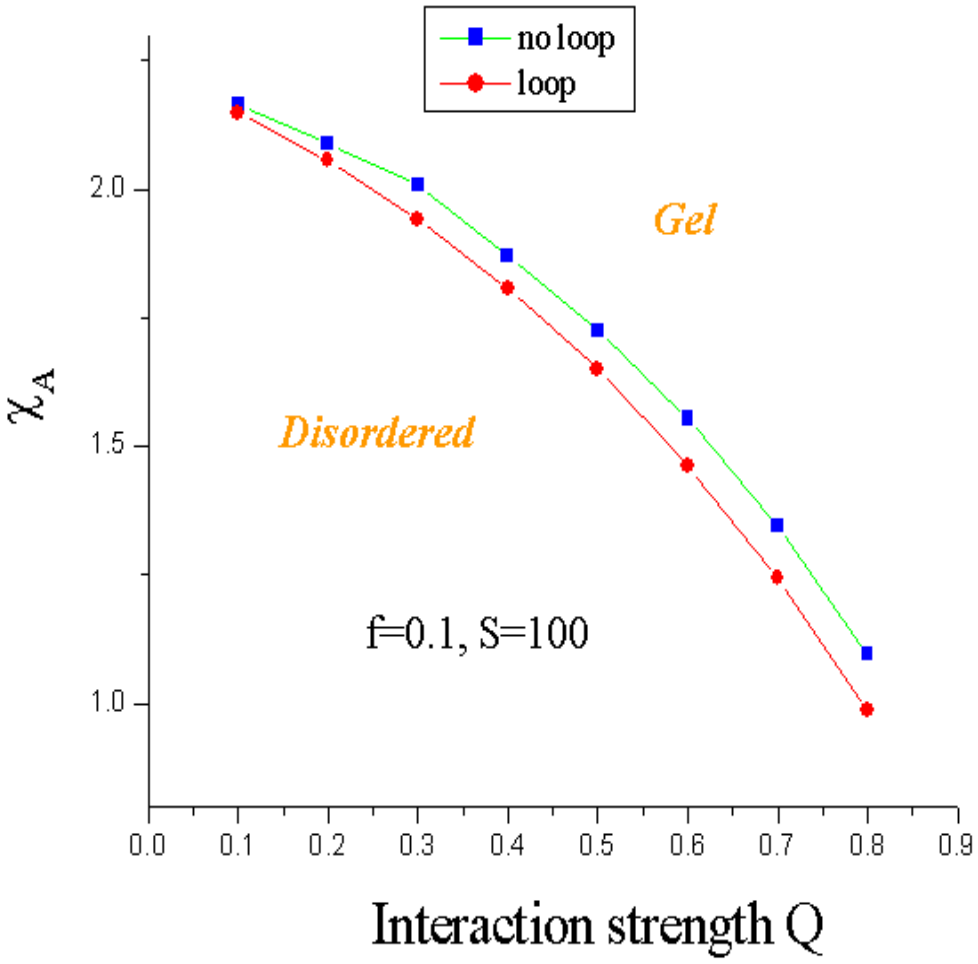

Figure 4.11 The critical Flory Huggins parameter of the gelation for loop structure and no loop structure at $M = 4$.

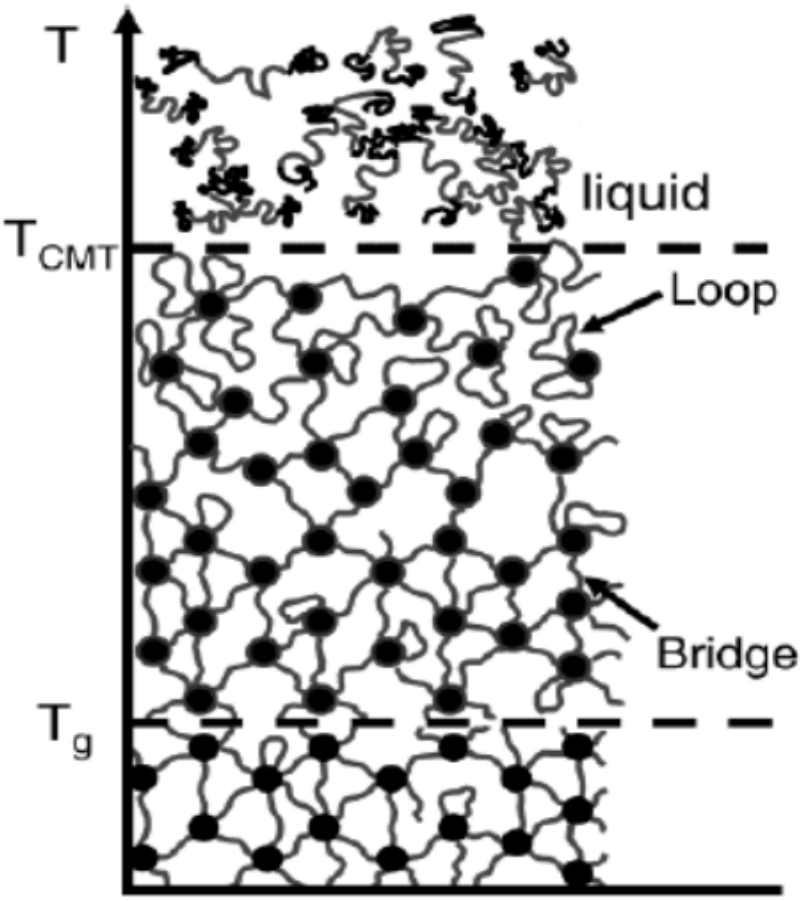

Figure 4.12 The schematic picture of gel configuration according to the temperature change (19)

CHAPTER 5. SUMMARY AND DISCUSSION

The main purpose of this work is to investigate the glassy behavior of microemulsions and block copolymers. The origin of glassy behavior in microemulsions and block copolymers is frustration due to a competition between short-range interaction and long range interaction. According to the charge frustrated Ising model, the competition between ferromganetic interaction and antiferromagnetic interaction is the origin of frustration in microemulsions. The competition between entropic effects and stoichiometric constraints responsible for the formation of micelles in microemulsions can lead to the emergence of a self generated glassy behavior in these systems. In the block copolymer, the competition between the repulsive short range interaction between monomers in polymer chains and the long range interaction by chemical bonds can lead to the emergence of a self generated glassy behavior. The criteria for the fluctuation induced first order transition and our microemulsion and block copolymer glasses are essentially the same. Both are a consequence of the large phase space of low energy excitations (14) (62) (all states with momenta $\mathbf{q}$ which fulfill $|\mathbf{q}| = q_m$) and are of at the most a moderate supercooling of the liquid state is required. This is strongly supported by the observation in Ref. (14) that the metastable states which are first to appear at a fluctuation induced first order transition are the ones build by a superposition of large amplitude waves of wavenumber q_m, but with random orientations and phases, i.e. just the ones which form the metastable states of our microemulsion and block copolymer glass. (38)

In a microemulsion, we showed that there is a critical volume fraction to achieve the glassy behavior which depends solely on $\frac{r_s}{a}$. Owing to the smaller energy densities at the larger length scales relevant to them, nonlinearity is easier to achieve in the laboratory for microemulsion glasses than the usual structural glasses. In fact, the mechanical properties

of the microemulsion glass proposed here are likely much closer to soft materials (72) (73) (74) such as gels and pastes than to a rigid window glass. It is intriguing that in several copolymer systems a "stiff gel" was found in a region of volume fraction - temperature phase diagram similar to the one where we find our microemulsion glass (67). Despite these different mechanical properties, the universality class of the microemulsion glasses is identical to the one which is believed to apply to structural glasses (68) (69) (70) (71), a conclusion which is also supported by the results of Refs. (72) (73).

In block copolymer, we showed that $(\chi S)_A$ is larger than $(\chi S)_{MF}$ for the symmetric diblock copolymer, which means the temperature T_A is lower than T_{MF}. This is evident in the inverse scattering intensity versus 1/temperature picture. The glass-disorder transition temperature for the symmetric diblock copolymer is lower than the T_{ODT}. Also, the glass transition temperature increases with the increase of the chain length, which is consistent with the traditional free volume theory. However, for the qualitative comparison with the experimental data, the dependence of higher vertex terms on the stiffness of the polymeric chains should be considered. The higher vertex terms, the entropic terms, are sensitive to the chain stiffness. Numerical method enables us to deal with the glassy behavior of asymmetric polymer chains ($f \neq 0.5$) as well as symmetric case. The asymmetric case of block copolymer is applied to the gelation, especially with telechelic structure. In the gelation of the symmetric ABA triblock copolymer with the hydrophobic ends groups, there exists an additional frustration by the competition between the repulsive interaction between polymeric chains and the attractive interactions at the end groups. (34) The increase of the interaction Q, the additional frustration, leads to the easier gelation process. Basically, the gelation and glassy behavior are treated in the same manner: same criterion for the self arrest from the solution of the self equation for $\overline{F}$. Only the main difference between the gel state and glassy state is whether the bridge or loop are involved in the association or not. For the qualitative comparison with the experimental data, more careful rheology analysis about elasticity in the gel and glassy states is required.

Based on the recent development in the theory of strongly interacting electron systems we developed a dynamic mean field theory for self generated glasses. The key assumption of our

approach, which applies to physical systems with short range higher order virial coefficients, is that glass formation is the consequence of predominantly local correlations. It is then possible to map the problem onto a purely local theory with same interaction and with a Gaussian part of the energy which is determined self consistently. A complete numerical approach did not make any assumption with respect to the momentum dependence of the self energy. The approach is a comparatively simple first step to investigate the glass problem and can easily be applied to multi component systems : the gelation of triblock copolymer in a solution. Most importantly, recent developments in the cluster DMFT approach allow to generalize this theory to include non-local effects and to investigate the role of dynamic heterogeneity, droplet and mosaic formation etc. This is an aspect no other existing mean field theory of the glass transition seems to have.

APPENDIX A. CALCULATION OF THE HIGHER ORDER VERTEX FUNCTIONS

A.1 Three point correlation function in triblock copolymers

Three point correlation function in triblock copolymer is given as

$$G^{(3)}_{ijk}(\mathbf{q}_1,\mathbf{q}_2,\mathbf{q}_3)=\frac{1}{N}\sum_{I=1}^{N}\sum_{J=1}^{N}\sum_{K=1}^{N}\theta_I^{(i)}\theta_J^{(j)}\theta_K^{(k)}P_{IJK}(\mathbf{q}_1,\mathbf{q}_2,\mathbf{q}_3) \tag{A.1}$$

with $\mathbf{q}_1+\mathbf{q}_2+\mathbf{q}_3=0$ and $|\mathbf{q}_1|=|\mathbf{q}_2|=|\mathbf{q}_3|=q_0$.$P_{IJK}(\mathbf{q}_1,\mathbf{q}_2,\mathbf{q}_3)$ is Fourier transform of $P_{IJK}(\mathbf{r}_1,\mathbf{r}_2,\mathbf{r}_3)$, which is the probability that the same chain has the monomer I,J,K at the position $\mathbf{r}_1,\mathbf{r}_2,\mathbf{r}_3$.$P_{IJK}(\mathbf{r}_1,\mathbf{r}_2,\mathbf{r}_3)$ is expressed in terms of the pair correlation function $P_{IJ}(\mathbf{r}_1,\mathbf{r})P_{JK}(\mathbf{r}_2,\mathbf{r}_3)$. For example, when the sequence of monomer is arranged as $I<J<K$, $P_{IJK}(\mathbf{r}_1,\mathbf{r}_2,\mathbf{r}_3)=P_{IJ}(\mathbf{r}_1,\mathbf{r})P_{JK}(\mathbf{r}_2,\mathbf{r}_3)$.The Fourier transform of $P_{IJK}(\mathbf{r}_1,\mathbf{r}_2,\mathbf{r}_3)$ is given by $P_{IJ}(\mathbf{q}_1)P_{JK}(\mathbf{q}_3)$ with $P_{IJ}(\mathbf{q}_1)=\exp(-\frac{x^2}{N}|I-J|)$.

For example, G_{2BB}

$$\begin{aligned}G_{2BB}&=\frac{2}{N}\int_{(1-g)N}^{N}\int_{fN}^{(1-g)N}\int_{fN}^{j}\exp[-\frac{x^2}{N}(j-i)]\exp[-\frac{x^2}{N}(k-j)]didjdk \qquad (A.2)\\ &=\frac{2N^2}{x^6}[-e^{-x^2}(-e^{fx^2}+e^{(1-g)x^2}-e^{fx^2}x^2+fe^{fx^2}x^2+ge^{fx^2}x^2)+\\ &e^{-(1-g)x^2}(-e^{fx^2}+e^{(1-g)x^2}-e^{fx^2}x^2+fe^{fx^2}x^2+ge^{fx^2}x^2)],\end{aligned}$$

where $x^2=q^2R^2$.When we set $g\to 0$ and $g\to f$,we obtain three point correlations function for a diblock copolymer and a symmetric ABA triblock copolymer. The whole building blocks

for a calculation of a third order vertex function $\Gamma^{(3)}$ are given as

$$
\begin{aligned}
G_{AAA} &= G_{111} + G_{112} + G_{121} + G_{122} + G_{211} + G_{212} + G_{221} + G_{222} \\
G_{AAB} &= G_{11B} + G_{22B} + G_{12B} + G_{21B} \\
G_{ABA} &= G_{1B1} + G_{2B2} + G_{1B2} + G_{2B1} \\
G_{ABB} &= G_{1BB} + G_{2BB} \\
G_{BAA} &= G_{B11} + G_{B22} + G_{B12} + G_{B21} \\
G_{BBA} &= G_{BB1} + G_{BB2} \\
G_{BAB} &= G_{B1B} + G_{B2B} \\
& G_{BBB}. \qquad \text{(A.1)}
\end{aligned}
$$

A.2 Four point correlation function in asymmetric triblock copolymers

When we calculate $\Gamma^{(4)}$ term, we consider two angle dependence in momentum space for weak segregation limit. For example, $\Gamma^{(4)}(q_0, q_0)$ is define the angle dependence as like

$$\begin{aligned} |\mathbf{q}_1 + \mathbf{q}_2|^2 &= q_0^2 = |\mathbf{q}_3 + \mathbf{q}_4|^2 \\ |\mathbf{q}_1 + \mathbf{q}_4|^2 &= q_0^2 = |\mathbf{q}_2 + \mathbf{q}_3|^2 \\ |\mathbf{q}_1 + \mathbf{q}_3|^2 &= 2q_0^2 = |\mathbf{q}_2 + \mathbf{q}_3|^2 . \end{aligned} \tag{A.3}$$

$$\begin{aligned} G_{BBB1} = \frac{2}{N} \int_{fN}^{(1-g)N} \int_{fN}^{k} \int_{fN}^{j} \int_{0}^{fN} \{ & \exp[-\frac{x^2}{N}(i-l)] \exp[-\frac{2x^2}{N}(j-i) \exp[-\frac{x^2}{N}(k-j)] \\ & + \exp[-\frac{x^2}{N}(i-l)] \exp[-\frac{x^2}{N}(j-i) \exp[-\frac{x^2}{N}(k-j)] + \\ & \exp[-\frac{x^2}{N}(i-l)] \exp[-\frac{2x^2}{N}(j-i) \exp[-\frac{x^2}{N}(k-j)]\} dl di dj dk. \end{aligned} \tag{A.4}$$

$$G^{(4)}_{ijkl}(\mathbf{q}_1, \mathbf{q}_2, \mathbf{q}_3, \mathbf{q}_4) = \frac{1}{N} \sum_{I=1}^{N} \sum_{J=1}^{N} \sum_{K=1}^{N} \theta_I^{(i)} \theta_J^{(j)} \theta_K^{(k)} \theta_L^{(l)} P_{IJK}(\mathbf{q}_1, \mathbf{q}_2, \mathbf{q}_3, \mathbf{q}_4). \tag{A.5}$$

The 16 building blocks for a fourth order vertex function $\Gamma^{(4)}$ are give as

$$
\begin{aligned}
G_{AAAA} &= G_{1111} + G_{1112} + G_{1121} + G_{1211} + G_{1122} + G_{1221} + G_{1212} + G_{1222} \\
&\quad + G_{2221} + G_{2212} + G_{2122} + G_{2211} + G_{2112} + G_{2121} + G_{2111} + G_{2222} \\
G_{BBBA} &= G_{BBB1} + G_{BBB2} \\
G_{BBAB} &= G_{BB1B} + G_{BB2B} \\
G_{BABB} &= G_{B1BB} + G_{B2BB} \\
G_{ABBB} &= G_{1BBB} + G_{2BBB} \\
G_{AABB} &= G_{11BB} + G_{22BB} + G_{12BB} + G_{21BB} \\
G_{BBAA} &= G_{BB11} + G_{BB22} + G_{BB12} + G_{BB21} \\
G_{ABBA} &= G_{1BB1} + G_{2BB2} + G_{1BB2} + G_{2BB1} \\
G_{BAAB} &= G_{B11B} + G_{B22B} + G_{B12B} + G_{B21B} \\
G_{BABA} &= G_{B1B1} + G_{B2B2} + G_{B1B2} + G_{B2B1} \\
G_{ABAB} &= G_{1B1B} + G_{2B2B} + G_{1B2B} + G_{2B1B} \\
G_{AAAB} &= G_{111B} + G_{222B} + G_{112B} + G_{121B} + G_{122B} + G_{211B} + G_{212B} + G_{221B} \\
G_{AABA} &= G_{11B1} + G_{22B2} + G_{12B2} + G_{12B1} + G_{21B1} + G_{21B2} + G_{22B1} + G_{22B2} \\
G_{ABAA} &= G_{1B11} + G_{2B22} + G_{1B22} + G_{2B11} + G_{2B12} + G_{1B22} + G_{1B21} + G_{2B22} \\
G_{BAAA} &= G_{B111} + G_{B222} + G_{B112} + G_{B121} + G_{B221} + G_{B212} + G_{B122} + G_{B222} \\
&\quad G_{BBBB}. \qquad \text{(A.2)}
\end{aligned}
$$

The higher order vertex functions $\Gamma_3(\mathbf{q}_1, \mathbf{q}_2, \mathbf{q}_3)$ and $\Gamma_4(\mathbf{q}_1, \mathbf{q}_2, \mathbf{q}_3, \mathbf{q}_4)$ can be expanded near a critical point and only one characteristic length scale q_0^{-1} exists.(30)

APPENDIX B. THE ASSOCIATING INTERACTION ENERGY V_3 and V_4

In this appendix we derive the form of the three and four body interaction causing the associated interaction between end segments. We express V_3 in terms of these collective coordinates. We assume that the three body and four body interaction as

$$\begin{aligned} U(\mathbf{R},\mathbf{R},\mathbf{R}'') &= u(\mathbf{R}-\mathbf{R}')u(\mathbf{R}-\mathbf{R}'') \\ U(\mathbf{R},\mathbf{R}',\mathbf{R}'',\mathbf{R}''') &= u(\mathbf{R}-\mathbf{R}')u(\mathbf{R}-\mathbf{R}'')u(\mathbf{R}-\mathbf{R}''') \end{aligned} \tag{B.1}$$

and the finite range potential $u(\mathbf{r})$ can be characterized by a strength

$$Q^{1/2} = \int d^3 r u(\mathbf{r}). \tag{B.2}$$

In case, we obtain $u(\mathbf{0})$ at some point. This is understood as $u(\mathbf{0}) = Q^{1/2}\delta(\mathbf{0}) = Q^{1/2}a_0^{-3}$, where a_0 is a typical length scale.

$$\begin{aligned} V_3 &= -\sum_{n_1,\cdots,n_3}\sum_{s_1,\cdots,s_3} U(\mathbf{R}_{n_1,s_1},\mathbf{R}_{n_2,s_2},\mathbf{R}_{n_3,s_3})\textstyle\prod_{i,j}(1-\delta_{n_i,n_j}\delta_{\widehat{s}_i,\widehat{s}_j}) \\ &= -\sum_{n_1,\cdots,n_3}\sum_{s_1,\cdots,s_3} U(\mathbf{R}_{n_1,s_1},\mathbf{R}_{n_2,s_2},\mathbf{R}_{n_3,s_3}) \\ &+ 3\sum_{n_1,n_3}\sum_{s_1,\cdots,s_3} U(\mathbf{R}_{n_1,s_1},\mathbf{R}_{n_1,s_2},\mathbf{R}_{n_3,s_3})\delta_{\widehat{s}_1,\widehat{s}_2} \\ &- 2\sum_{n_1}\sum_{s_1,\cdots,s_3} U(\mathbf{R}_{n_1,s_1},\mathbf{R}_{n_1,s_2},\mathbf{R}_{n_3,s_3})\delta_{\widehat{s}_1,\widehat{s}_2}\delta_{\widehat{s}_2,\widehat{s}_3}, \end{aligned} \tag{B.3}$$

where we used that

$$\begin{aligned} (1-\delta_{1,2})(1-\delta_{1,3})(1-\delta_{2,3}) &= 1-\delta_{1,2}-\delta_{1,3}-\delta_{2,3}+\delta_{1,3}\delta_{2,3} \\ &+ \delta_{1,2}\delta_{2,3}+\delta_{1,2}\delta_{1,3}-\delta_{1,2}\delta_{1,3}\delta_{2,3} \\ &= 1-\delta_{1,2}-\delta_{1,3}-\delta_{2,3}+2\delta_{1,3}\delta_{2,3} \end{aligned} \tag{B.4}$$

with $\delta_{i,j} = \delta_{n_i,n_j}\delta_{\widehat{s}_i,\widehat{s}_j}$.Also, the total end segment particle density $\rho_e(\mathbf{r})$ is given as

$$\rho_e(\mathbf{r}) = \sum_{n,s}'' \delta\left(\mathbf{r} - \mathbf{R}_{n,s}\right). \tag{B.5}$$

We can thus write

$$\begin{aligned} I_1 &= -\sum_{n_1,\cdots,n_3}\sum_{s_1,\cdots,s_3} U(\mathbf{R}_{n_1,s_1},\mathbf{R}_{n_2,s_2},\mathbf{R}_{n_3,s_3}) \\ &= -\int d^3r d^3r' d^3r'' \rho_e(\mathbf{r})\rho_e(\mathbf{r}')\rho_e(\mathbf{r}'')u(\mathbf{r}-\mathbf{r}')u(\mathbf{r}-\mathbf{r}'') \\ &= -Q\int d^3r \rho_e(\mathbf{r})^3 \end{aligned} \tag{B.6}$$

as well as

$$\begin{aligned} I_2 &= 3\sum_{n_1,n_3}\sum_{s_1,\cdots,s_3} U(\mathbf{R}_{n_1,s_1},\mathbf{R}_{n_1,s_2},\mathbf{R}_{n_3,s_3})\delta_{\widehat{s}_1,\widehat{s}_2} \\ &= 3\sum_{n_1,n_3}\sum_{s_3}\left(\sum_{s_1,s_2=1}^{fS} U(\mathbf{R}_{n_1,s_1},\mathbf{R}_{n_1,s_1},\mathbf{R}_{n_3,s_3}) + \sum_{s_1,s_2=S-fS}^{S} U(\mathbf{R}_{n_1,s_1},\mathbf{R}_{n_1,s_1},\mathbf{R}_{n_3,s_3})\right) \\ &= 6fSu(\mathbf{0})\sum_{n_1,n_3}\sum_{s_1,s_3} u(\mathbf{R}_{n_1,s_1} - \mathbf{R}_{n_3,s_3}) \\ &= 6fSu(\mathbf{0})\int d^3r d^3r' \rho_e(\mathbf{r})\rho_e(\mathbf{r}')u(\mathbf{r}-\mathbf{r}') \\ &= 6fSQa_0^{-3}\int d^3r \rho_e(\mathbf{r})^2. \end{aligned} \tag{B.7}$$

I_2 term describe the "bridge form".

$$\begin{aligned} I_3 &= -2\sum_{n_1}\sum_{s_1,\cdots,s_3} U(\mathbf{R}_{n_1,s_1},\mathbf{R}_{n_1,s_2},\mathbf{R}_{n_1,s_3})\delta_{\widehat{s}_1,\widehat{s}_2}\delta_{\widehat{s}_2,\widehat{s}_3} \\ &= -2\sum_{n_1}\left(\sum_{s_1,s_2,s_3=1}^{fS} U(\mathbf{R}_{n_1,s_1},\mathbf{R}_{n_1,s_2},\mathbf{R}_{n_1,s_3}) + \sum_{s_1,s_2,s_3=S-fS}^{S} U(\mathbf{R}_{n_1,s_1},\mathbf{R}_{n_1,s_2},\mathbf{R}_{n_1,s_3})\right) \\ &= -2u(\mathbf{0})^2(2fS)^3\sum_{n_1} u(\mathbf{R}_{n_1,\widehat{s}_1} - \mathbf{R}_{n_1,\widehat{s}_1})u(\mathbf{R}_{n_1,\widehat{s}_1} - \mathbf{R}_{n_1,\widehat{s}_1}) \\ &= -2Qa_0^{-6}(2fS)^3 N. \end{aligned} \tag{B.8}$$

It then follows the result

$$V_3 = -Q\int d^3r \rho_e(\mathbf{r})^3 + 6fSQa_0^{-3}\int d^3r \rho_e(\mathbf{r})^2 + const. \tag{B.9}$$

In a similar way, the four point associating interaction term V_4 is calculated as

$$\begin{aligned}
V_4 &= -\sum_{n_1,\cdots,n_4}\sum_{\widehat{s}_1,\cdots,\widehat{s}_4} U(\mathbf{R}_{n_1,\widehat{s}_1},\mathbf{R}_{n_2,\widehat{s}_2},\mathbf{R}_{n_3,\widehat{s}_3},\mathbf{R}_{n_4,\widehat{s}_4})\textstyle\prod_{i,j(i>j)}(1-\delta_{n_i,n_j}\delta_{\widehat{s}_i,\widehat{s}_j}) \\
&= -\sum_{n_1,\cdots,n_4}\sum_{\widehat{s}_1,\cdots,\widehat{s}_4} U(\mathbf{R}_{n_1,\widehat{s}_1},\mathbf{R}_{n_2,\widehat{s}_2},\mathbf{R}_{n_3,\widehat{s}_3},\mathbf{R}_{n_4,\widehat{s}_4}) \\
&+ 6\sum_{n_1,n_3,n_4}\sum_{\widehat{s}_1,\cdots,\widehat{s}_4} U(\mathbf{R}_{n_1,\widehat{s}_1},\mathbf{R}_{n_1,\widehat{s}_2},\mathbf{R}_{n_3,\widehat{s}_3},\mathbf{R}_{n_4,\widehat{s}_4})\delta_{\widehat{s}_1,\widehat{s}_2} \\
&- 15\sum_{n_1,n_4}\sum_{\widehat{s}_1,\cdots,\widehat{s}_4} U(\mathbf{R}_{n_1,\widehat{s}_1},\mathbf{R}_{n_1,\widehat{s}_2},\mathbf{R}_{n_1,\widehat{s}_3},\mathbf{R}_{n_4,\widehat{s}_4})\delta_{\widehat{s}_1,\widehat{s}_2}\delta_{\widehat{s}_1,\widehat{s}_3} \\
&+ 20\sum_{n_1}\sum_{\widehat{s}_1,\cdots,\widehat{s}_4} U(\mathbf{R}_{n_1,\widehat{s}_1},\mathbf{R}_{n_1,\widehat{s}_2},\mathbf{R}_{n_1,\widehat{s}_3},\mathbf{R}_{n_1,\widehat{s}_4})\delta_{\widehat{s}_1,\widehat{s}_2}\delta_{\widehat{s}_1,\widehat{s}_3}\delta_{\widehat{s}_1,\widehat{s}_4}+\cdots,
\end{aligned} \tag{B.10}$$

where we used that

$$\begin{aligned}
&(1-\delta_{1,2})(1-\delta_{1,3})(1-\delta_{1,4})(1-\delta_{2,3})(1-\delta_{2,4})(1-\delta_{3,4}) \\
&= 1-6\delta_{1,2}+15\delta_{1,2}\delta_{1,3}-20\delta_{1,2}\delta_{1,3}\delta_{1,4}+\cdots
\end{aligned} \tag{B.11}$$

with $\delta_{i,j}=\delta_{n_i,n_j}\delta_{\widehat{s}_i,\widehat{s}_j}$. We can thus write

$$\begin{aligned}
J_1 &= -\sum_{n_1,\cdots,n_4}\sum_{\widehat{s}_1,\cdots,\widehat{s}_4} U(\mathbf{R}_{n_1,\widehat{s}_1},\mathbf{R}_{n_2,\widehat{s}_2},\mathbf{R}_{n_3,\widehat{s}_3},\mathbf{R}_{n_4,\widehat{s}_4}) \\
&= -\int d^3r d^3r' d^3r'' d^3r''' \rho_e(\mathbf{r})\rho_e(\mathbf{r}')\rho_e(\mathbf{r}'')\rho_e(\mathbf{r}''')u(\mathbf{r}-\mathbf{r}')u(\mathbf{r}-\mathbf{r}'')u(\mathbf{r}-\mathbf{r}''') \\
&= -Q^{3/2}\int d^3r\rho_e(\mathbf{r})^4
\end{aligned} \tag{B.12}$$

as well as

$$\begin{aligned}
J_2 &= 6\sum_{n_1,n_3,n_4}\sum_{s_1,\cdots,s_4}'' U(\mathbf{R}_{n_1,s_1},\mathbf{R}_{n_1,s_2},\mathbf{R}_{n_3,s_3},\mathbf{R}_{n_4,s_4})\delta_{\widehat{s}_1,\widehat{s}_2} \\
&= 12u(\mathbf{0})fS\sum_{n_1,n_3,n_4}\sum_{s_1,s_3,s_4}'' u(\mathbf{R}_{n_1,\widehat{s}_1}-\mathbf{R}_{n_3,\widehat{s}_3})u(\mathbf{R}_{n_1,\widehat{s}_1}-\mathbf{R}_{n_4,\widehat{s}_4}) \\
&= 12u(\mathbf{0})fS\int d^3r d^3r' d^3r'' \rho_e(\mathbf{r})\rho_e(\mathbf{r}')\rho_e(\mathbf{r}'')u(\mathbf{r}-\mathbf{r}')u(\mathbf{r}-\mathbf{r}'') \\
&= 12Q^{3/2}a_0^{-3}fS\int d^3r\rho_e(\mathbf{r})^3.
\end{aligned} \tag{B.13}$$

$$
\begin{aligned}
J_3 &= -12 \sum_{n_1,n_4} {\sum_{s_1,\cdots,s_4}}'' U(\mathbf{R}_{n_1,s_1,}\mathbf{R}_{n_1,s_2,}\mathbf{R}_{n_1,s_3},\mathbf{R}_{n_4,s_4})\delta_{\widehat{s}_1,\widehat{s}_2}\delta_{\widehat{s}_1,\widehat{s}_3} \\
&= -12u(\mathbf{0})^2\,(2fS)^2 \sum_{n_1,n_4}\sum_{s_1,s_4} u(\mathbf{R}_{n_1,s_1}-\mathbf{R}_{n_4,s_4}) \\
&= -48f^2S^2Q^{3/2}a_0^{-6}\int d^3r d^3r'\rho_e(\mathbf{r})\rho_e(\mathbf{r}')u(\mathbf{r}-\mathbf{r}') \\
&= -48f^2S^2Q^{3/2}a_0^{-6}\int d^3r\rho_e(\mathbf{r})^2. \qquad \text{(B.14)}
\end{aligned}
$$

J_3 term describe the "backfolding".

$$
\begin{aligned}
J_3' &= -3 \sum_{n_1,n_3} \sum_{s_1,\cdots,s_4} U(\mathbf{R}_{n_1,s_1,}\mathbf{R}_{n_1,s_2,}\mathbf{R}_{n_3,s_3},\mathbf{R}_{n_3,s_4})\delta_{\widehat{s}_1,\widehat{s}_2}\delta_{\widehat{s}_3,\widehat{s}_4} \\
&= -3u(\mathbf{0})^2\,(2fS)^2 \sum_{n_1,n_3}\sum_{s_1,s_3} u(\mathbf{R}_{n_1,s_1}-\mathbf{R}_{n_3,s_3}) \\
&= -12f^2S^2Q^{3/2}a_0^{-6}\int d^3r d^3r'\rho_e(\mathbf{r})\rho_e(\mathbf{r}')u(\mathbf{r}-\mathbf{r}') \\
&= -12f^2S^2Q^{3/2}a_0^{-6}\int d^3r\rho_e(\mathbf{r})^2. \qquad \text{(B.15)}
\end{aligned}
$$

The remaining terms only contribute to constant terms, then the result follows

$$
V_4 = -Q^{3/2}\int d^3r\rho_e(\mathbf{r})^4 + 12Q^{3/2}fSa_0^{-3}\int d^3r\rho_e(\mathbf{r})^3 - 60Q^{3/2}f^2S^2a_0^{-6}\int d^3r\rho_e(\mathbf{r})^2 + const \qquad \text{(B.16)}
$$

APPENDIX C. VISUALIZATION OF THE CORRELATION FUNCTIONS

C.1 Visualization of instantaneous configurations

If one wants to visualize a configuration $\phi(\mathbf{r})$ of a field with correlation function in momentum space

$$G_k = \langle \phi_{\mathbf{k}} \phi_{-\mathbf{k}} \rangle , \tag{C.1}$$

one can use the following procedure: Introduce a set of uncorrelated random numbers $\xi_{\mathbf{k}}$ with correlation function

$$\langle \xi_{\mathbf{k}} \xi_{\mathbf{k}'} \rangle = \delta_{\mathbf{k}+\mathbf{k}'} \tag{C.2}$$

and then the configuration

$$\phi_{\mathbf{k}} = \sqrt{G_{\mathbf{k}}} \xi_{\mathbf{k}} \tag{C.3}$$

can be averaged to

$$\langle \phi_{\mathbf{k}} \phi_{\mathbf{k}'} \rangle = \sqrt{G_{\mathbf{k}} G_{\mathbf{k}'}} \langle \xi_{\mathbf{k}} \xi_{\mathbf{k}'} \rangle = \delta_{\mathbf{k}+\mathbf{k}'} G_{\mathbf{k}} \tag{C.4}$$

as desired. The Fourier transformation, $\phi(\mathbf{r})$, of $\phi_{\mathbf{k}}$ is then a real space configuration which, after averaging over all possible random numbers $\xi_{\mathbf{k}}$ is correlated according to $G_{\mathbf{k}}$.

A useful random number for a situation without broken symmetry is

$$\xi_{\mathbf{k}} = A_{\mathbf{k}} \exp\left(i 2\pi \eta_{\mathbf{k}}\right) \tag{C.5}$$

where $A_{\mathbf{k}}$ and $\eta_{\mathbf{k}}$ random numbers between $[0, 1]$ which are statistically independend for different $\mathbf{k}$-values.

C.2 Visualization with memory between distinct configurations

Generalizing the approach of the previous section one can introduce m different uncorrelated random numbers $\xi^j_{\mathbf{k}}$, $j = 1, ..., m$ with $\left\langle \xi^j_{\mathbf{k}} \xi^{j'}_{-\mathbf{k}} \right\rangle = \delta_{jj'}$, which generate m distinct configurations $\phi^i_{\mathbf{k}}$ via

$$\phi^i_{\mathbf{k}} = \sum_{j=1}^{m} R^{ij}_{\mathbf{k}} \xi^j_{\mathbf{k}}. \tag{C.6}$$

We require that the correlation of a configuration with itself is

$$G_{\mathbf{k}} = \left\langle \phi^i_{\mathbf{k}} \phi^i_{-\mathbf{k}} \right\rangle, \tag{C.7}$$

whereas for all $i \neq i'$ holds that

$$F_{\mathbf{k}} = \left\langle \phi^i_{\mathbf{k}} \phi^{i'}_{-\mathbf{k}} \right\rangle. \tag{C.8}$$

Inserting the above expression for $\phi^i_{\mathbf{k}}$ yields

$$\begin{aligned} G_{\mathbf{k}} &= \sum_{j,j'} R^{ij}_{\mathbf{k}} R^{ij'}_{\mathbf{k}} \left\langle \xi^j_{\mathbf{k}} \xi^{j'}_{-\mathbf{k}} \right\rangle = \sum_{j} \left(R^{ij}_{\mathbf{k}} \right)^2 \\ F_{\mathbf{k}} &= \sum_{j,j'} R^{ij}_{\mathbf{k}} R^{i'j'}_{\mathbf{k}} \left\langle \xi^j_{\mathbf{k}} \xi^{j'}_{-\mathbf{k}} \right\rangle = \sum_{j} R^{ij}_{\mathbf{k}} R^{i'j}_{\mathbf{k}} \end{aligned} \tag{C.9}$$

Next we assume that the $m \times m$-matrix $R^{ij}_{\mathbf{k}}$ has equal diagonal and off diagonal elements, i.e.

$$R^{ij}_{\mathbf{k}} = \begin{cases} a_{\mathbf{k}} & \text{if } i = j \\ b_{\mathbf{k}} & \text{if } i \neq j \end{cases}. \tag{C.10}$$

Inserting this ansatz gives

$$\begin{aligned} G_{\mathbf{k}} &= a^2_{\mathbf{k}} + (m-1)\, b^2_{\mathbf{k}} \\ F_{\mathbf{k}} &= 2 a_{\mathbf{k}} b_{\mathbf{k}} + (m-2)\, b^2_{\mathbf{k}}, \end{aligned} \tag{C.11}$$

which implies $G_{\mathbf{k}} - F_{\mathbf{k}} = (a_{\mathbf{k}} - b_{\mathbf{k}})^2$. It follows

$$\begin{aligned} a_{\mathbf{k}} &= \frac{\sqrt{G_{\mathbf{k}} + (m-1)\, F_{\mathbf{k}}} + (m-1)\sqrt{G_{\mathbf{k}} - F_{\mathbf{k}}}}{m} \\ b_{\mathbf{k}} &= \frac{\sqrt{G_{\mathbf{k}} + (m-1)\, F_{\mathbf{k}}} - \sqrt{G_{\mathbf{k}} - F_{\mathbf{k}}}}{m}. \end{aligned} \tag{C.12}$$

Obviously, if $F_{\mathbf{k}} = 0$, it follows $a_{\mathbf{k}} = \sqrt{G_{\mathbf{k}}}$ and $b_{\mathbf{k}} = 0$. For the plot routine I used $m = 2$.

APPENDIX D. CALCULATION OF THE GLASS TRANSITION TEMPERATURE IN MICROEMULSIONS

In this appendix we the off diagonal self energy in replica space, $\Sigma_{\mathcal{F}}$ by SCSA approximation. We start from the correlation function

$$G(q) = \frac{q_m^2 + q_D^2}{\left(q^2 - q_m^2\right)^2 + \varepsilon^2 q_m^4}. \tag{D.1}$$

The polarization function $\Pi_G(q)$ is given as

$$\begin{aligned}\Pi_G(q) = & \int \frac{d^3p}{8\pi^3} G(\mathbf{p})\, G(\mathbf{p}+\mathbf{q}) \\ & = \frac{1}{16q\varepsilon^2}\left(1 + \left(\frac{q_D}{q_m}\right)^2\right)^2 \text{ for } q_m < q < 2q_m.\end{aligned}$$

An analogous calculation for the off diagonal polarization function $\Pi_{\mathcal{F}}(q)$ can be calculated.

$$\int \frac{d^3p}{8\pi^3} K(\mathbf{p})\, K(\mathbf{p}+\mathbf{q}) \simeq \frac{1}{16q\Delta^2}\left(1 + \left(\frac{q_D}{q_m}\right)^2\right)^2 \text{ for } q_m < q < 2q_m$$

where Δ is defined as

$$\Delta \equiv \left[\kappa^2 + \left(\frac{q_D}{q_m}\right)^2 (\kappa^2 - \varepsilon^2)\right]^{1/2}. \tag{D.2}$$

Then,

$$\int \frac{d^3p}{8\pi^3} G(\mathbf{p})\, K(\mathbf{p}+\mathbf{q}) \simeq \frac{1}{16q\Delta}\left(1 + \left(\frac{q_D}{q_m}\right)^2\right)^2 \text{ for } q_m < q < 2q_m$$

For $q_m < q < 2q_m$, we can use the approximate expressions

$$\begin{aligned}\Pi_G(q) &= \frac{1}{16q\varepsilon^2}\left(1 + \left(\frac{q_D}{q_m}\right)^2\right)^2 \\ \Pi_F(q) &= \frac{1}{16q}\left(\frac{1}{\varepsilon} - \frac{1}{\Delta}\right)^2 \left(1 + \left(\frac{q_D}{q_m}\right)^2\right)^2,\end{aligned}$$

which gives

$$D_G(q) = \frac{16 q_m a}{1 + \frac{q_m a}{q\varepsilon^2}\left(1 + \left(\frac{q_D}{q_m}\right)^2\right)^2}$$

with dimensionless number $a = \frac{v_0}{16 q_m} \lesssim 1$. The product $D_G(q)\Pi_F(q)$ becomes momentum independent,

$$D_G(q)\Pi_F(q) \simeq \left(1 - \frac{\varepsilon}{\Delta}\right)^2$$

and $D_F(q)$ is given as

$$\begin{aligned} D_F(q) &= \left[\frac{-D_G(q)\,\Pi_F(q)}{1 - D_G(q)\,\Pi_F(q)}\right] D_G(q) \\ &\simeq \left[\frac{-\left(1 - \frac{\varepsilon}{\Delta}\right)^2}{1 - \left(1 - \frac{\varepsilon}{\Delta}\right)^2}\right] D_G(q). \end{aligned}$$

The off diagonal self energy Σ_F is given by

$$\Sigma_F(\mathbf{q}) = \int \frac{d^3p}{8\pi^3} D_F(\mathbf{q}+\mathbf{p}) F(\mathbf{p}). \tag{D.3}$$

From our assumption of weak momentum dependence of the off diagonal self energy, $\Sigma_F(\mathbf{q})$ can be approximated as

$$\begin{aligned} \Sigma_F(q_m) &\simeq \int_0^2 t dt\; D_F(q_m t) \int \frac{p^2 dp}{4\pi^2}(p) \\ &\simeq D_F(q_m) \int \frac{p^2 dp}{4\pi^2}(p) \end{aligned} \tag{D.4}$$

where $t = \sqrt{2(1+\cos\theta)}$. Using $\int \frac{q^2 dq}{4\pi^2} F(p) = \frac{q_m}{8\pi}\left(\frac{1}{\varepsilon} - \frac{1}{\Delta}\right)\left(1 + \left(\frac{q_D}{q_m}\right)^2\right)$, the off diagonal self energy $\Sigma_F(\mathbf{q})$ is given as

$$\Sigma_F(q_m) = -\frac{8 q_m^2 \varepsilon^2}{\pi} \frac{\left(1 - \frac{\varepsilon}{\Delta}\right)^2}{1 - \left(1 - \frac{\varepsilon}{\Delta}\right)^2} \left(\frac{1}{\varepsilon} - \frac{1}{\Delta}\right) \frac{1}{1 + \left(\frac{q_D}{q_m}\right)^2}. \tag{D.5}$$

When $q_D \to 0$, $\Sigma_F(q_m)$ becomes consistent with the result by Ref. (82) The self consistent equation for the off diagonal self energy in SCSA approximation is given by

$$\frac{8\varepsilon^2}{\pi} \frac{\left(1 - \frac{\varepsilon}{\Delta}\right)^2}{1 - \left(1 - \frac{\varepsilon}{\Delta}\right)^2} \left(\frac{1}{\varepsilon} - \frac{1}{\Delta}\right) \frac{1}{1 + \left(\frac{q_D}{q_m}\right)^2} = (\kappa^2 - \varepsilon^2). \tag{D.6}$$

Within mean field approximation, the temperature dependence of r is determined by

$$r = r_0 + u_0 T \int \frac{d^3q}{8\pi^3} G(q). \tag{D.7}$$

For the case without frustration, $Q = 0$, the usual critical temperature $T_c^0 = \frac{2\pi^2|r_0|}{u\Lambda}$ results from the requirement $r\left(T_c^0\right) = 0$. Λ is momentum cut-off. For finite Q,

$$r(T) = r_0 + \frac{u_0 T}{2\pi^2}\left(\frac{\pi q_m}{2\varepsilon}\left(1 + \left(\frac{q_D}{q_m}\right)^2\right) + \Lambda\right). \tag{D.8}$$

For the glass transition region, $r(T) \sim q_D^2 - 2\sqrt{Q}$, Eqn. D.8 is given as

$$\frac{T}{T_C^0}\left(\frac{\pi\sqrt{Q}}{2\varepsilon\left(\sqrt{Q} - q_D^2\right)^{1/2}} + 1\right) = 1, \tag{D.9}$$

where we used $q_m^2 + q_D^2 = \sqrt{Q}$ and set $\Lambda = 1$. If ε_A is obtained from the nontrivial solution of the Eqn. D.5, the glass temperature is given as

$$T_A = \frac{2\varepsilon_A\left(\sqrt{Q} - q_D^2\right)^{1/2} T_C^0}{\pi\sqrt{Q} + 2\varepsilon_A\left(\sqrt{Q} - q_D^2\right)^{1/2}}. \tag{D.10}$$

From the relation of Eqn. 2.14, T_A is plotted as a function of $f, t, r_s/a$.

BIBLIOGRAPHY

[1] W. Kauzmann, Chem. Rev. **43**, 219 (1948)

[2] E. Leutheusser, Phys. Rev. A **29**, 2765 (1984)

[3] K. Binder, J. Baschnagel, W. Kob, and W. Paul, cond-mat/0202337, xxx.lanl.gov, (Date accessed : 10 March 2005)

[4] W. Götze, J. Sjögren, Rep. Prog. Phys. **55**, 214 (1992)

[5] M. Grousson, V. Krakoviack, G. Tarjus, and P. Viot, Phys. Rev. E **66**, 026126 (2002)

[6] R. Monnason, Phys. Rev. Lett. **75**, 2875 (1995)

[7] M. Mézard and G. Parisi, Phys. Rev. Lett. **82**, 747 (1999)

[8] P. G. deGennes and C. Taupin, J. Phys. Chem. **86**, 2294 (1982)

[9] E. Sheu, S. Chen, J. S. Huang, and J. C. Sung, Phys. Rev. A **39**, 5867 (1989)

[10] D. Choy and S. Chen, Phys. Rev. E **61**, 4148 (2000)

[11] H. Gang, A. H. Krall, H. Z. Cummins, and D. A. Weitz, Phys. Rev. E **59**, 715 (1999)

[12] L. Leibler, Macromolecules **13**, 1602 (1980).

[13] G. H. Fredrikson and E. Helfand, J. Chem. Phys. **87**, 697 (1987)

[14] S. A. Brazovskii, Zh. Exp. Teor. Fiz. **68**, 175(1975) [Sov. Phys. JEPT **41**, 85 (2975)].

[15] B. Stühn, J. Polym. Sci. Polym. Phys. **30**, 1013 (1992)

[16] F. S. Bates, J. H. Rosedale, and G. H. Fredrikson, J. Chem. Phys. **92**, 6255 (1990)

[17] H. Lindner, G. Scherf, and O. Glatter, Phys. Rev. E **67**, 061402 (2003)

[18] K. Mortensen, K. Almdal, R. Kleppinger, N. Mischenko, and H. Reynaers, Physica B **1025**, 241 (1998)

[19] P. L. Drazal and K. R. Shull, Macromolecules **36**, 2000 (2003)

[20] M. Kotlarchyk, S. H. Chen, J. S. Huang, and M. W. Kim, Phys. Rev. A **29**, 2054 (1984)

[21] G. J. Tiddy, Phys.Rep. **57**, 1 (1980)

[22] F. H. Stillinger, J. Chem. Phys. **78**, 4654 (1983)

[23] H. J. Woo, C. Carraro, and D. Chandler, Phys. Rev. E **52**, 6497 (1995)

[24] D. Wu, D. Chandler and B. Smith, J. Phys. Chem. **96**, 4077 (1992)

[25] H. J. Woo, C. Carraro, and D. Chandler, Phys. Rev. E **53**, R41 (1996)

[26] S. Chitanvis, Phys. Rev. E **57**, 1921 (1998)

[27] K. H. Fischer and J. A. Hertz, *Spin Glasses*, (Cambridge University Press, Cambridge, 1991)

[28] V. Dotsenko, *An Introduction to the theory of spin glasses and neural network*, (World Scientific, Singapore, 1994)

[29] N. Hadjichristidis, S. Pispas and G. A. Floudas, *Block copolymers*, (A John wiley Sons, Inc., New Jersey, 2003)

[30] T. Ohta and K. Kawasaki, Macromolecules **19**, 2621(1986)

[31] H. K. Tsao, J. Y. Chen, and Y. J. Sheng, Macromolecules **36**, 5863(2003)

[32] Y. B. Raviv, T. M. Snyder, and Z. G. Wang, Langmuir **20**, 7860(2004)

[33] A. G. Ajaz, Rubber Chem. Tschnol. **68**, 481(1995)

[34] P. Goldbart, Private communication, (Date : 1 July 2002)

[35] M. Peskin and D. V. Schroeder, *An Introduction to Quantum Field Theory*, (Perseus Books, Cambridge, 1995)

[36] I. W. Hamley, *The physics of block copolymers*,(Oxford University Press, New York, 1998)

[37] A. M. Mayes and O. Cruz, J. Chem. Phys. **91**, 7228 (1989)

[38] G. H. Fredrikson and K. Binder, J. Chem. Phys. **91**, 7265 (1989)

[39] P. Papon, J. Leblond and P. H. E. Meijer, *The physics of phase transitions*, (Springer-Verlag, Berlin, 2002)

[40] Y. Wang, W. L. Mattice and D. H. Napper, Macromolecules **25**, 4073 (1992)

[41] E. Raspaud, D. Lairez, M. Adam, and J. P. Carton, Macromolecules **27**, 2956 (1994)

[42] K. C. Tam, R. D. Jenkins, M. A. Winnik, and D. R. Bassette, Macromolecules, **31**, 4149 (1998)

[43] S. F. Edwards and P. W. Anderson, J. Phys. F:Metal Phys. **5**, 965 (1975)

[44] S. Kirkpatrick and D. Sherrington, Phys. Rev. B **17**, 4384 (1978)

[45] J. R. L. de Alameida and D. J. Thouless, J. Phys. A **11**, 983 (1978)

[46] G. Parisi, J. Phys. A:Math. Gen. **13** L115, (1980)

[47] M. Mézard, G. Parisi, N. Sourlas, G. Toulouse, and M. Virasoro, J. Physique **45** 843, (1984)

[48] C. De Dominicis and I. Kondor, Phys. Rev. B **27** 606,(1983)

[49] M. Mézard, G. Parisi, and M. A. Virasoro, *Spin glass theory and beyond* (World Scientific, Singapore, 1987)

[50] G. Kortliar and D. Vollhardt, *Physics Today*, March (2004)

[51] D. Vollhardt, *Correlated electron system*, (World Scientific, Singapore, 1993)

[52] A. Georges, G. Kortliar, W. Krauth, and M. J. Rosenberg, Rev. Mod. Phys. **68**, 13 (1996)

[53] W. Metzner and D. Vollhardt, Phy. Rev. Lett. **62**, 324, (1989)

[54] E. Müller-Hartmann, Z. Phys. B **74**, 507, (1989)

[55] G. Baym and L. P. Kadanoff, Phys. Rev **124**, 287 (1961)

[56] G. Baym, Phys. Rev **127**, 1391 (1962)

[57] M. W. Deem and D. Chandler, Phys. Rev. E **49**, 4268 (1994)

[58] S. Wu, H. Westfahl Jr., J. Schmalian, and P. G. Wolynes, Chem. Phys. Lett. **359**, 1 (2002)

[59] V. J. Emery and S. A. Kivelson, Physica **209 C**, 597 (1993)

[60] T. Kirkpatrick and D. Thirumalai, J. Phys. A Math. Gen. **22**, L49 (1989)

[61] J. Schmalian and P. G. Wolynes, Phys. Rev. Lett. **85**, 836 (2000)

[62] H. Westfahl Jr., J. Schmalian, and P. G. Wolynes, Phys. Rev. B **64**, 174203 (2001)

[63] A. J. Bray, Phys. Rev. Lett. **32**, 1413 (1974)

[64] A replica symmetric ansatz in the approach used here corresponds to one step replica symmetry breaking in the conventional replica approach.

[65] M. Mézard and A. P. Young, Europhys. Lett. **18**, 653 (1992)

[66] M. P. Kennett and C. Chamon, Phys. Rev. Lett. **86**, 1622 (2001)

[67] O. Glatter, G. Scherf, K. Schillen, and W. Brown, Macromolecules **27**, 6046 (1994)

[68] T. R. Kirkpatrick and P. G. Wolynes, Phys. Rev. A **35**, 3072 (1987)

[69] T. R. Kirkpatrick and P. G. Wolynes, Phys. Rev. B **36**, 8552 (1987)

[70] T. R. Kirkpatrick and D.Thirumalai, and P. G. Wolynes, Phys. Rev. A **40**, 1045 (1989)

[71] T. R. Kirkpatrick and D. Thirumalai, Phys. Rev. Lett. **58**, 2091 (1987)

[72] M. Cloitre, R. Borrega, and L. Leibler, Phys. Rev. Lett. **85**, 4819 (2000).

[73] P. Sollich, F. Lequeux, P. Hébraud, and M. E. Cates, Phys. Rev. Lett. **78**, 2020 (1997)

[74] T. G. Mason, J. Bibette, and D. A. Weitz, Phys. Rev. Lett. **75**, 2051 (1995)

[75] P. C. Hohenberg and J. B. Swift, Phys. Rev. E **52**, 1828 (1995)

[76] S. Magazu, D. Majolino, F. Mallamace, and N. Micali, Phys. Rev. A **40**, 2643(1989)

[77] D. Majolino, F. Mallamace, and S. Venuto, Phys. Rev. A **42**, 7330 (1990)

[78] N. Sakamoto and T. Hashimoto, Macromolecules **28**, 6825 (1995)

[79] B. Stuhn, R. Mutter, and T. Albrecht, Europhys. Lett. **18**, 427 (1992)

[80] T. Hashimoto, T. Ogawa, and C. D. Han, J. Phys. Soc. Jpn. **63**, 2206 (1994)

[81] T. Wolff, C. Burger, and W. Ruland, Macromolecules **26**, 1707 (1993)

[82] H. Westfahl Jr., J. Schmalian, and P. G. Wolynes, Phys. Rev. B **68**, 134203 (2003)

[83] K. O'Driscoll and R. A. Sanayei, Macromolecules **24**, 4479 (1991)

[84] U. Eisele, *Introduction to Polymer Physics*, (Springer-Verlag, Berlin 1990)

ACKNOWLEDGEMENTS